

1

Introduction

1.1 Scope

Emulsions are systems in which at least one immiscible liquid is dispersed into another in the form of droplets^{1,2} (Fig. 1.1). In everyday life, emulsions have numerous applications, such as in inks, paints, coatings, latex preparation, cosmetics and foods. In foods, emulsions play an important role in the formulation of water-based products containing oils or fats or the other way around. Examples of food emulsions are dairy products, desserts, sauces, mayonaises, margarine etc.

Emulsions are intrinsically unstable systems and tend to demix into the liquids of which it consists by a number of mechanisms (section 1.2). Control of the instability of emulsions is therefore highly desired in order to tune appearance, shelf-life and rheological properties of food emulsions. Because food systems usually contain a large variety of ingredients, control of emulsion stability is complex and still mainly based on experience, and a trial-and-error approach. Fundamental scientific effort is required to improve control.

The work described in this thesis concentrates on the application of polysaccharides in emulsions. Polysaccharides are often used as stabilisers or thickening agents in food systems.^{3,4} Polysaccharides can thicken the aqueous phase of emulsions, which retards destabilisation processes. However, under some conditions polysaccharides induce destabilisation of emulsions.⁵ (section 1.3). This destabilisation leads to separation of a serum layer from the emulsion. Because of these opposite effects, effective application of polysaccharides as emulsion thickeners requires in-depth knowledge on colloidal interactions, flocculation and creaming processes, and structure formation as a result of flocculation.

1.2 Oil-in-water emulsions

1.2.1 Emulsion instability

Oil and water, two major food components, are immiscible, but they can be dispersed into another in the form of small droplets (diameter ~ 0.1 - $10 \mu\text{m}$). In order to form such small droplets, a large amount of oil-water interface must be formed (Fig. 1.1A,B). Because of the existence of a surface tension between oil and water, the formation of a large amount of

surface requires a large energy input.^{2,6} For the same reason, the surface tends to decrease when the energy input is stopped. Ultimately, this leads to a complete separation into oil and water, which proceeds by a number of mechanisms. An emulsion can be kinetically stabilised by inhibiting or retarding one or more of these mechanisms.

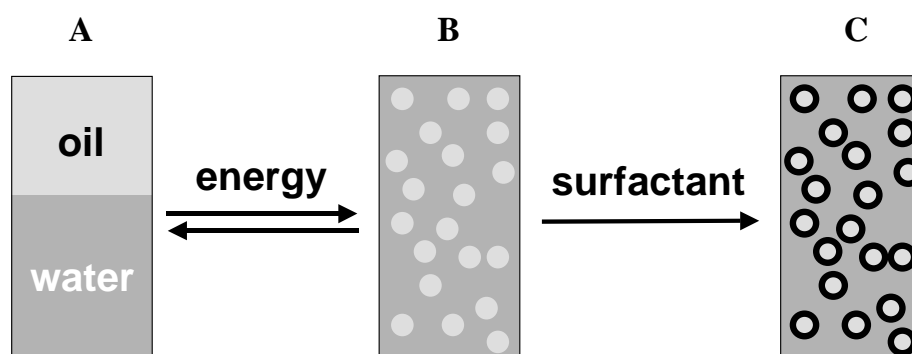


Fig. 1.1 Sketch of oil and water forming an emulsion. Addition of sufficient emulsifier to cover the oil/water interface can stabilise the emulsion.

Because emulsion droplets attract each other, e.g., due to Van der Waals forces, they tend to stick to each other when they encounter, which is here denoted as flocculation.⁷ When the film between the emulsion droplets breaks the droplets will merge, hereby reducing the total surface of the two droplets, which is denoted as coalescence.⁷ Emulsions can be stabilised against these mechanisms by an emulsifier (e.g. a surfactant or a protein) that adsorbs to the oil-water interface (Fig. 1.1C). Once adsorbed to the interface, the emulsifier causes steric and/or electrostatic repulsion between the droplets, which prevents flocculation and coalescence.

Another important instability mechanism in emulsions, apart from flocculation and coalescence is creaming. In this process, emulsion droplets move to the top of a container, because oil usually has a lower density than water. This process can be retarded, e.g., by increasing the viscosity of the aqueous phase.

1.2.2 Emulsions stabilised by globular proteins

Globular proteins form a special class of biological emulsifiers and because of their nutritional value they are often applied in foods. Proteins are polyampholitic molecules, composed of linear chains of amino-acids bound by peptide bonds.⁸ Proteins usually carry ionizable groups, giving rise to an electric charge density, which depends on pH and the presence of salts. The molecular structure of globular proteins is usually highly organised

into α -helices and β -sheets and sometimes stabilised by intramolecular disulphide bonds. Such a molecular structure usually gives rise to the formation of gelled layers on interfaces,^{9,10} leading to irreversible adsorption.¹¹

Because of their surface-activity and their good water solubility remote from their isoelectric point (I.E.P.), globular proteins easily adsorb to the oil-water interface.¹² Moreover, the repulsive gelled layer they form around the oil droplets offers protection against flocculation and coalescence.

In this thesis, sunflower oil-in-water emulsions are described that are stabilised by the milk protein β -lactoglobulin (β -lg), the main component of whey protein and a well described globular protein.¹³ It is well soluble above and below its I.E.P. (4.5 - 5.1).^{7,13} At pH-values above and below their I.E.P. and at moderate salt concentrations (up to 100 mM), emulsions stabilised by β -lg are stable against flocculation. At pH-values near the I.E.P. or upon addition of multivalent ions (e.g. Ca^{2+}), flocculation is promoted. β -Lg-stabilised emulsions are stable against coalescence at rest and under centrifugational forces,¹⁴ provided that sufficient protein ($\sim 2 \text{ mg}\cdot\text{m}^{-2}$) is available to cover the total oil-water interface.¹⁵ However, emulsions in which the protein layers are connected, e.g., in highly concentrated or flocculated emulsions, are sensitive to coalescence when they are forced to flow.¹⁶ Under the circumstances described in this thesis, coalescence can be neglected.^{17,18}

1.3 Polysaccharides in emulsions

Polysaccharides are biological macromolecules that mostly originate from a botanical, algal or microbial source.¹⁹ These macromolecules consist of linear or branched chains of various monosaccharides, and their total molecular weights range from 10^4 to 10^8 Da.¹⁹ Polysaccharides behave as flexible freely jointed or compact chains with coil sizes, usually ranging between 10 and 200 nm.⁷ Because of their large molecular weight, polysaccharides give a substantial viscosity increase in solution, especially in the regime where chain overlap leads to entanglements.⁷ This feature makes them well suited as thickening agents. When added to oil-in-water emulsions, polysaccharides will not only induce a viscosity increase, but they can also induce flocculation of the emulsion droplets in two distinct ways as described below.

1.3.1 Depletion-flocculation

If a polysaccharide does not adsorb at (protein coated) emulsion droplets, the centres of mass of the polysaccharide molecules cannot approach the droplet surface closer than a distance of about their radius of gyration, r_g (Fig. 1.2). As a consequence, the concentration of polysaccharide segments in a region around the droplet is lower than in the bulk solution. This depletion effect gives rise to an osmotic pressure difference between the depleted zones and the bulk solution. When two depleted zones overlap, this pressure difference induces an attractive force between the oil droplets.²⁰ The interaction energy is given by the product of the osmotic pressure, P_{OSM} , and the overlap volume, $V_{overlap}$. These factors are related to respectively the polysaccharide concentration and the sizes of the droplets and the polysaccharide.²¹

When the attraction is sufficiently strong to overcome the entropy of the emulsion droplets, i.e. above a minimum polysaccharide concentration, the droplets flocculate.²²

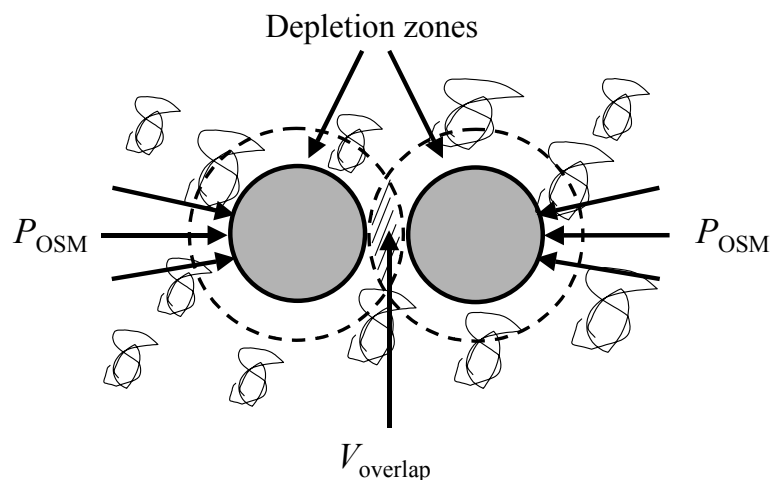


Fig. 1.2 Sketch of the depletion mechanism in between two emulsion droplets in a solution of non-adsorbing polysaccharides.

1.3.2 Bridging-flocculation

If a polysaccharide adsorbs to the oil droplets or to the protein layers around the oil droplets, the polysaccharide can interconnect two or more emulsion droplets (Fig. 1.3). Because the polysaccharide acts as a bridge between the droplets this mechanism is denoted as bridging-flocculation.⁵

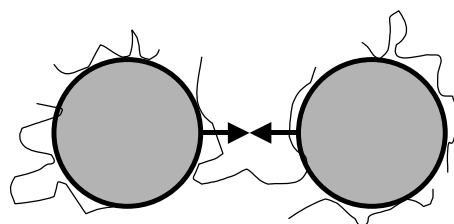


Fig. 1.3 Sketch of the bridging mechanism between two emulsion droplets in a solution of adsorbing polysaccharides.

As a function of the polysaccharide concentration, the effectiveness of the bridging-interaction shows a maximum at an effective surface coverage of 0.5.²³ At this condition the product of the numbers of sites covered and uncovered with polysaccharide on the droplet interface shows a maximum. The polysaccharide concentration at this optimum is usually smaller than the concentration above which depletion occurs.

1.4 Creaming and flocculation

Creaming and flocculation are the main instability mechanisms in emulsions that are stabilised by β -lg and to which polysaccharides are added. When both mechanisms occur at the same time, the interplay between them can lead to different types of demixing of emulsions. Which type occurs is dependent on the relative rates of creaming and flocculation (Fig. 1.4). Three main types of demixing can be distinguished.

- I. If the creaming rate is much higher than the flocculation rate, the oil droplets rise separately to the top of a container, where they form a dense creamed layer of emulsion droplets.
- II. If the flocculation rate and the creaming rate are of the same order of magnitude, small flocs are formed, which cream faster than single droplets. As a consequence, this situation leads to accelerated creaming.
- III. If the flocculation rate is much larger than the creaming rate, a network of emulsion droplets can be formed. Such a system is denoted as an emulsion gel. However, gravity still exerts a compressive pressure on the droplet network. When this pressure is greater than the maximum stress the gel can withstand,^{24,25} the network will be compressed and separates a serum layer.

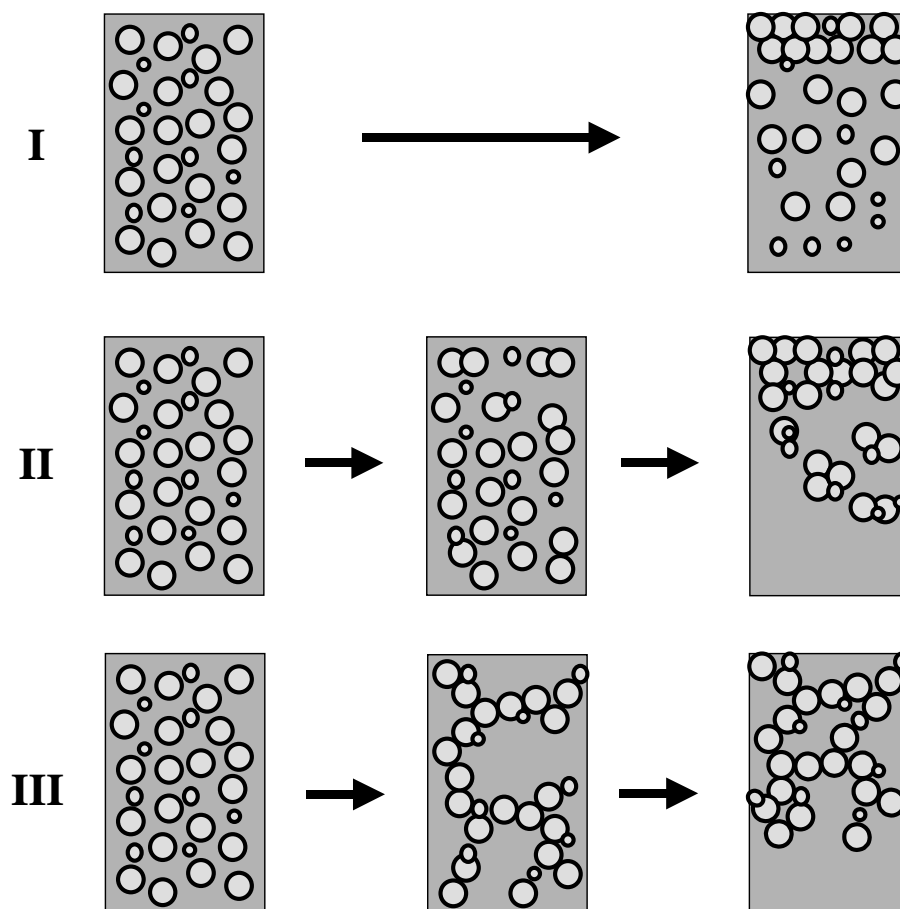


Fig. 1.4 Sketch of the interplay between flocculation and creaming. I) creaming rate \gg flocculation rate: creaming; II) creaming rate \approx flocculation rate: accelerated creaming; III) creaming rate \ll flocculation rate: network formation.

1.5 Objective

The objective of this thesis is to relate droplet-droplet interactions arising from polysaccharide addition and resulting microstructure formation to rheological properties and gravity-induced demixing of protein-stabilised oil-in-water emulsions. Hereto, the emulsion structure (-formation) and rheology has been investigated at the mesoscopic level by confocal scanning laser microscopy (CSLM) and diffusing wave spectroscopy (DWS). At the macroscopic level, the main techniques used to characterise the mechanical properties and demixing behaviour are classical rheology and turbidimetry.

1.6 Outline of this thesis

In the first part of this thesis, the effects of droplet-droplet interactions and aqueous phase rheology on microstructure formation and demixing will be discussed. The central model system is a protein-stabilised emulsion in which depletion-flocculation is induced by dextran. The effect of depletion-flocculation on emulsion-microstructure and demixing is explained on the basis of the Smoluchowski theory, combined with fractal growth and Stokes' law of sedimentation.

Chapter 2 describes the effect of an excess amount of protein in the aqueous phase, which is often present in food systems. Protein was found to kinetically suppress the flocculation process, hereby suppressing network formation and accelerating creaming.

In chapter 3, a combination was made of a long-range depletion interaction with short-range electrostatic interactions by using Ca^{2+} ions. This combination is discussed in terms of microstructure formation and network strengthening, with regard to retardation of serum separation.

Emulsions applied in sweetened foods often contain large amounts of sucrose. In chapter 4, it is shown how sucrose affects rheology and demixing of depletion-flocculated emulsions.

In the second part of the thesis, the effects of depletion- and bridging-flocculation are compared in terms of network microstructure, rheology and stability against demixing.

Chapter 5 shows that the prevailing flocculation mechanism (depletion or bridging) can be tuned by setting the electrostatic interactions between the polysaccharide and the adsorbed protein layer. In addition, differences in the processes of demixing between bridging- and depletion-flocculated emulsions are discussed.

In chapter 6, a detailed (micro-) rheological study is presented of the scaling behaviour of the emulsion network elasticity with oil content for depletion- and bridging-flocculated emulsions. In addition, demixing behaviour is discussed and the occurrence of delayed demixing in depletion-flocculated emulsions is described as a function of polysaccharide concentration, oil content and density difference between the oil and the aqueous phase.

References

- (1) Sherman P. *Emulsion Science* **1968**, Academic Press, London.
- (2) Becher P. *Emulsions: Theory and Practice* **1965**, American Chemical Society, New York.
- (3) Phillips G. O. and Williams, P. A. *Handbook of hydrocolloids* **2000**, Woodhead publishing ltd., Cambridge.
- (4) Williams P. A. and Phillips G. O. *Gums and stabilisers for the food industry* **2002**, Royal Society of Chemistry, Cambridge.
- (5) Dickinson E. *Food Hydrocolloids* **2003**, *17*, 25-39.
- (6) Lyklema L. *Fundamentals of Interface and Colloid Science* **1995**, Academic Press, London.
- (7) Walstra P. *Physical Chemistry of Foods* **2003**, Marcel Dekker, Inc., New York.
- (8) Belitz H.-D. *Food Chemistry* **1987**, Springer Verlag, Berlin.
- (9) Prins A. *Coll. Surf. A* **1999**, *149*, 467-473.
- (10) Martin A. H.; Grolle K.; Bos M. A.; Cohen Stuart M. A.; van Vliet T. *J. Coll. Int. Sci.* **2002**, *254*, 175-183.
- (11) Schwenke K.D. in *Proteins at liquid interfaces*, Möbius D., Miller R., Eds. Elsevier, Amsterdam **1998**; Chapter 1.
- (12) P. E. A. Smulders, *Formation and stability of emulsions made with proteins and peptides*, **2001**, Thesis, Wageningen University
- (13) McKenzie H. A. *Milk proteins: chemistry and molecular biology* **1971**, Academic Press, London.
- (14) van Aken G. A.; Zoet F. D. *Langmuir* **2000**, *16*, 7131-7138.
- (15) Hunt J. A.; Dalgleish D. A. *Food Hydrocolloids* **1994**, *8*, 175-187.
- (16) van Aken G. A. *Langmuir* **2002**, *18*, 2549-2556.
- (17) van Aken G. A.; van Vliet T. *Langmuir* **2002**, *20*, 7364-7370.
- (18) van Aken G. A.; Blijdenstein T. B. J.; Hotrum N. E. *Curr. Op. Coll. Int. Sci.* **2003**, *8*, 369-377.
- (19) Glicksman, M. *Food Hydrocolloids* **1982**, CRC Press, Boca Raton.
- (20) Asakura S.; Oosawa F. *J. Chem. Phys.* **1954**, *22*, 1255-1256.
- (21) Vrij A. *Pure Appl. Chem.* **1976**, *48*, 471-483.
- (22) Tuinier R.; de Kruif C. G. *J. Coll. Int. Sci.* **1999**, *218*, 201-210.
- (23) Healy T.; La Mer V. K. *J. Coll. Sci.* **1964**, *19*, 323-332.
- (24) Buscall R.; White L. R. *Journal of the Chemical Society Faraday Transactions. 1. Physical Chemistry* **1987**, *83*, 873-891.
- (25) van Vliet, T and Walstra, P. *Food Colloids* Bee, R. D., Richmond, P., and Mingins, J. Eds, The Royal Society of Chemistry, Cambridge **1989**, 206-217.

2

Suppression of depletion-flocculation in oil-in-water emulsions: A kinetic effect of β -lactoglobulin*

Abstract

This paper reports on creaming and flocculation in 10 wt % oil-in-water emulsions, stabilised by β -lactoglobulin (β -lg) and flocculated by dextran. Dextran and an additional amount of β -lg were added at various concentrations after emulsion formation. A substantial effect of the β -lg concentration was observed. At higher β -lg concentrations, a larger dextran concentration was required to induce network formation. This effect was explained by a retardation of the flocculation process at larger β -lg concentrations, shown by diffusing wave spectroscopy (DWS). This retardation was caused by the unexpectedly high apparent viscosity at low shear-rates of mixed solutions of β -lg and dextran.

2.1 Introduction

Creaming is an important cause of product decay in food emulsions.¹ This process can be slowed by addition of thickening agents. Such an addition has two effects. Firstly, it retards creaming by increasing the viscosity at high concentrations, but for a non-gelling polysaccharide this is usually a small effect. Secondly, it induces droplet flocculation, often caused by depletion forces.² Flocculation may lead to an increase of the creaming rate,^{3,4} which is employed in some processes, for example accelerated separation of cream from milk or to remove colloidal particles from waste-water.

Stabilisation of the emulsions by a non-gelling polysaccharide occurs if the flocculation rate is larger than the creaming rate. The flocs may grow until they overlap and form a space-filling network before creaming occurs.⁵ In this way emulsions are thickened and become relatively stable against creaming for a certain time, the so-called *delay time*.^{6,7} After this delay time the emulsion separates serum, due to rearrangements in the droplet network.

De Hek and Vrij⁸ derived a thermodynamic expression for the position of the spinodal demixing line, which defines the onset of depletion-flocculation. Tuinier and de Kruij⁹ showed that this model reasonably predicts the minimum concentration of an exocellular polysaccharide needed for depletion-flocculation in whey protein stabilised oil-in-water emulsions. In their work, the protein concentration was chosen relatively low (below 1 wt %), in order to minimise effects of protein in the aqueous phase. In food emulsions, however, protein concentrations in the aqueous phase are often higher (up to a few wt %) and may affect the creaming and flocculation of the oil droplets. A suppression of droplet flocculation was reported at increasing β -lg concentration before homogenisation, which was ascribed to polymerisation of adsorbed protein.¹⁰ Flocculation can also be influenced by thermodynamic incompatibility of protein and polysaccharides in the aqueous phase.¹¹⁻¹³ Reiffers Magnani et al.¹⁴ showed that this incompatibility occurs in oil-in-water emulsions after centrifugation, however, at protein and polysaccharide concentrations much higher than usually applied in food systems.

In a previous study¹⁵ we demonstrated for three different polysaccharides that whey protein isolate (WPI) affects depletion-flocculation. It occurred at concentrations of protein and

polysaccharide where incompatibility is not expected and at that time it was argued that it might be caused by minor components in WPI.

In this work we used purified β -lg and compared results with those obtained for WPI. The polysaccharide used in this study was dextran. The approach was to study flocculation and creaming independently. Creaming was monitored macroscopically by turbidimetry and flocculation was monitored at a colloidal level by Diffusing Wave Spectroscopy (DWS). It is shown that addition of protein retards flocculation by an increase in the low-shear viscosity of the aqueous phase. This result opens a new possibility to tune the interplay between flocculation and creaming by adjusting the protein concentration.

2.2 Materials and methods

2.2.1 Materials

β -Lactoglobulin was purified from bovine milk¹⁶ and had a protein content of 92.5 wt %. WPI (Bipro, Davisco International) contained 71% β -lactoglobulin, 12% α -lactalbumin, 5% bovine serum albumin, 5% immunoglobulins, 2% salt, 1% lactose and 4% moisture. Dextran (isolated from *Leuconostoc*; $M_w = 2 \times 10^6$ Da) was obtained from Sigma Chemicals (St. Louis, USA). The conductivity of a 0.8% dextran solution in distilled water was measured as 14.6 μ S/cm. NaCl (p. a.) and thiomersal (97 %) were obtained from Merck (Shuchardt, Germany). Sunflower oil (Reddy, Vandemoortele, the Netherlands) was purchased from a local retailer.

2.2.2 Characterisation of dextran

The polysaccharide dextran described in this paper contains 95% 1,6-linked D-anhydroglucose units. The remaining sugar residues are 1,3-linked and form short branches.¹⁷ Its radius of gyration, $r_g = 32$ nm, was determined via the intrinsic viscosity $[\eta] = 0.095$ l/g. Viscosities were measured by capillary viscometry or at higher c_{ps} , by using a Bohlin VOR rheometer (see below).

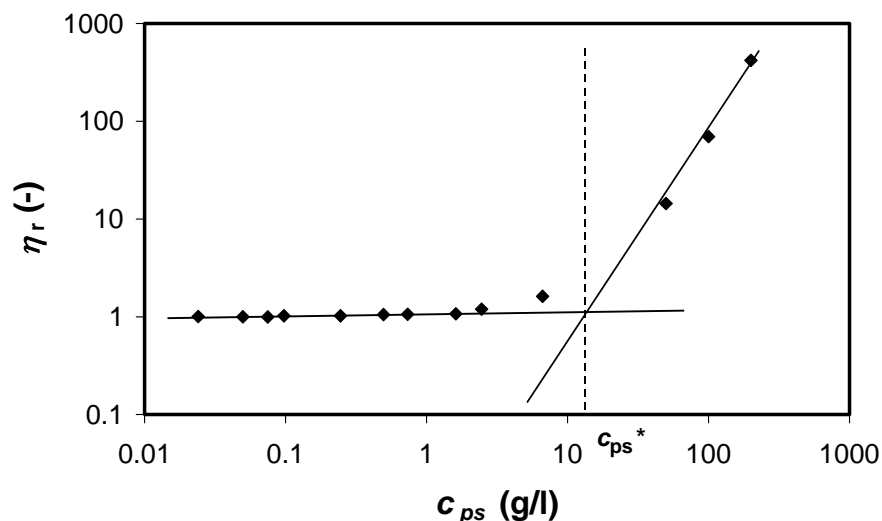


Fig. 2.1 Relative viscosity of aqueous dextran solutions as a function of the dextran concentration c_{ps} . The curve shows a point of interception at c_{ps}^* .

Fig. 2.1 shows the viscosity as a function of c_{ps} in 0.1 M NaCl. Roughly linear dependence was observed at both sides of the inflection point. This point corresponds to c_{ps}^* and is situated at 14 g/l, which agrees with the value calculated from the intrinsic viscosity.

2.2.3 Sample preparation

Protein solutions (β -lg or WPI) were prepared by adding protein powder to the required amount of NaCl solution and by gentle stirring overnight, avoiding incorporation of air. The pH varied between 6.6 and 6.8. The NaCl concentration was kept at 0.10 M and the solutions contained 0.02 wt % thiomersal to inhibit microbial growth.

Stock emulsions contained 40 wt % sunflower oil and 1 wt % protein. Pre-emulsions were prepared by mixing oil into a protein solution using an Ultra Turrax (Polytron, Switzerland). This pre-emulsion was homogenised by 10 passes through a Delta Lab-scale homogeniser operating at a pressure of 50 bar. The droplet size distribution and the volume-over-surface-averaged droplet diameter, d_{32} , were determined using a laser diffraction apparatus (Coulter LS 230, Miami, USA).

A dextran solution was prepared by adding dextran to 0.10 M NaCl solution and stirring “au bain marie” in boiling water for 4 hours.

Emulsion samples containing 10 wt % oil and various amounts of protein and dextran were prepared by mixing various amounts of dextran solution, protein solution and salt solution

with the stock emulsion. This way the droplet size distribution and the NaCl concentration of the emulsions were kept constant in all samples.

2.2.4 Creaming measurements

Creaming of emulsions was measured in two ways. In the first, we measured the backscattering intensity of incident laser light along the height of an optical glass tube,¹⁸ using a Turbiscan MA 2000 apparatus (Ramonville St. Agne, France). This profile gives a qualitative indication of the distribution of the oil droplets along the height of the tube, since the backscattering intensity varies with the volume fraction of oil. Emulsion samples were brought into these tubes using an automatic pipette and then stored at 25 °C. At different times after bringing the sample into the tube, the backscattering profile was measured.

In the second way, the volume fractions of oil in the serum layers were determined. Homogeneous emulsions were brought into a separating funnel and left to cream for twenty hours. After this time the serum layer was collected and its weight, w_s , was determined. Subsequently, the serum was mixed by gently shaking and the weight of the oil in this layer was determined via an oil extraction method.¹⁹ The average volume fraction of oil in the serum, ϕ_s , was calculated from the oil concentrations in the serum and the weight of the serum layer.

2.2.5 Protein adsorption measurements

The surface concentration of protein, Γ , was determined by the depletion method.²⁰ Serum was separated from the oil droplets by centrifugation at 10,000 g for 40 minutes. The concentration of protein in the serum phase was determined using a Thermoquest C.E. Instruments, NA 2100 Protein analyser (Milan, Italy).

2.2.6 Diffusing wave spectroscopy (DWS)

DWS measurements were carried out in a transmission geometry^{21,22} using a He/Ne laser ($\lambda = 633$ nm) and a cuvette with an inner width, L , of 1.98 mm. The transmitted and scattered light was focussed by a lens into a single mode fibre, attached to a photomultiplier (ALV, SO-SIPD, Langen/Hessen, Germany). The signal was analysed by a correlator board (ALV, flex-5000, Langen/Hessen, Germany), which calculated the intensity autocorrelation function, $g_2(t)$, from the transmitted light over a period of one

minute. Within this period, enough fluctuations had occurred to obtain an adequate time average. The decay time, $\tau_{1/2}$, is defined as the time at which $g_2(t) - 1$ had decayed to half of its initial value. Larger values of $\tau_{1/2}$ are indicative for a lower mobility of the oil droplets.

The mean square displacement $\langle \Delta r^2(t) \rangle$ as a function of time was calculated numerically using eq. 2.1.²²

$$g_2(t) - 1 = \beta \left(\frac{L/l^* \sqrt{k_0^2 \langle \Delta r^2(t) \rangle}}{\sinh[L/l^* \sqrt{k_0^2 \langle \Delta r^2(t) \rangle}]} \right)^2 \quad (2.1)$$

In this equation, β is an instrumental factor and l^* the distance above which the light is randomly scattered. The wavevector, k_0 , equals $2\pi/\lambda$ where λ is the wavelength of the laser light in vacuum.

2.2.7 Viscometry

The viscosity of very dilute dextran solutions ($c_{ps} < 0.25$ wt %) was determined using an Ubbelohde viscometer.

Strain-rate-controlled shear viscometry was carried out using a Bohlin VOR Rheometer (Huntingdon, UK) at 25 °C using a concentric cylinder geometry (C 25) with a gap of 2.5 mm. A shear rate, $\dot{\gamma}$, was applied to the sample by rotating the outer cylinder. The torsion exerted on the inner cylinder was measured by a 0.315 g torsion bar, connected to an electromagnetic transducer.

Stress-controlled shear measurements were carried out using a constant stress parallel plate rheometer, suited for very low shear stresses.²³

2.3 Results

2.3.1 Creaming behaviour

Fig. 2.2 shows the droplet size distribution of the emulsion. From this distribution we calculated d_{32} to be 1.0 μm . Creaming profiles of 10 wt % oil-in-water emulsions were measured at varying concentrations of protein and polysaccharides.

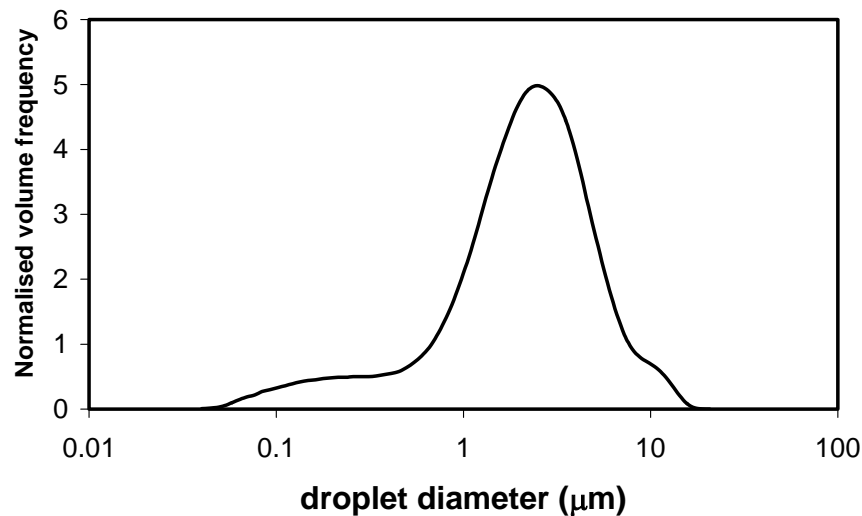


Fig. 2.2 Droplet size distribution of the stock emulsion.

Fig. 2.3A shows a typical backscattering profile for creaming of individual droplets. The droplets accumulated at the top of the sample, forming a creamed layer which could be recognised by its larger backscattering. The gradual increase of the backscattering along the height of the serum layer was caused by the polydispersity of the emulsion. According to Stokes' law,²⁴ the velocity of an isolated particle in a homogeneous medium is equal to $\Delta\rho d_e^2 g / 18\eta$, where $\Delta\rho$ is the density difference between oil and the aqueous phase, d_e is the droplet diameter, g is the gravitational acceleration and η the viscosity of the medium. Hence, large droplets cream faster than the smaller ones.

Fig. 2.3B shows a typical backscattering profile for creaming of a flocculated emulsion. Initially, a creamed layer was formed by accumulation of single droplets and flocs at the top of the sample. Later a serum layer was formed, separated by a sharp boundary which quickly moved upward. The sharpness of this boundary indicates the presence of a weak network of emulsion droplets.⁷

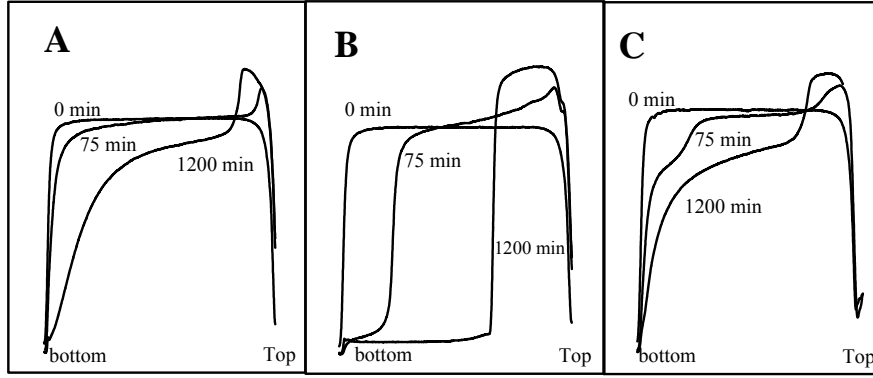


Fig. 2.3 Typical creaming profiles of polydisperse emulsions (10 wt % oil-in-water) at different times. **A**: non-flocculating emulsion ($c_{ps} = 0$ wt %, $c_p = 0.2$ wt %); **B**: flocculating emulsion ($c_{ps} = 0.36$ wt %, $c_p = 0.2$ wt %); **C**: flocculating emulsion ($c_{ps} = 0.36$ wt %, $c_p = 3$ wt %).

The time required to form a flocculated emulsion network was estimated from the kinetics of fast flocculation.²⁵ From this theory the increase of the average number of oil droplets per floc, $\langle N_{\text{floc}}(t) \rangle$, can be obtained which is given by

$$\langle N_{\text{floc}}(t) \rangle = 1 + \frac{t}{\tau_s}. \quad (2.2)$$

Here $\tau_s = 1/(4\pi D d_e n_0)$ is the time at which the total number of particles has decreased to half its initial value n_0 . The diffusion coefficient D equals $k_B T / 3\pi\eta d_e$ for spheres, where k_B is the Boltzmann constant and T the absolute temperature. Assuming fractal structure of the flocs, the effective volume fraction (defined as the volume fraction of oil and water enclosed by the flocs) of the flocculated emulsion, ϕ_{eff} can be expressed as a function of $\langle N_{\text{floc}}(t) \rangle$ and D_f , the fractal dimension of the floc, which is a number between 1 and 3.²⁶

$$\phi_{\text{eff}}(t) = \phi_e \left(1 + \frac{t}{\tau_s} \right)^{\frac{3}{D_f} - 1} \quad (2.3)$$

When ϕ_{eff} has reached unity, the flocs must overlap and a space-filling network is formed. Combination of eq. 2.3 and the Stokes equation yields an expression for the creaming rate as a function of time in a flocculating system:

$$v_{\text{eff}}(t) = \frac{\langle N_{\text{floc}}(t) \rangle^{1-\frac{1}{D_f}} \Delta\rho d_e^2 g}{18\eta} \cdot (1 - \phi_{\text{eff}}(t))^n. \quad (2.4)$$

Here the term $(1 - \phi_{\text{eff}}(t))^n$ accounts for mutual hindrance of the oil droplets and n is an empirical exponent, which is often taken to be 4.65 at $\phi < 0.5$.²⁷ For flocs we may to good approximation replace d_e and ρ_{oil} by the floc diameter and density.²⁶ Fig. 2.4 shows calculated values of $\phi_{\text{eff}}(t)$ and $v_{\text{eff}}(t)$ as a function of time, calculated for the emulsion system described below. Here, the fractal dimension was chosen 2.3, which was experimentally found for other kinds of particle gels.²⁶ Initially, v_{eff} increases due to an increase of $\langle N_{\text{floc}}(t) \rangle$ with time, but due to increasing ϕ_{eff} it finally drops to zero. For a 10 wt % oil-in-water emulsion, the time required for formation of a network is about 1 hour. Since the creaming velocity of single droplets decreased to zero, the upward movement of the phase boundary must have been caused by gravity driven collapse of the network of oil droplets.

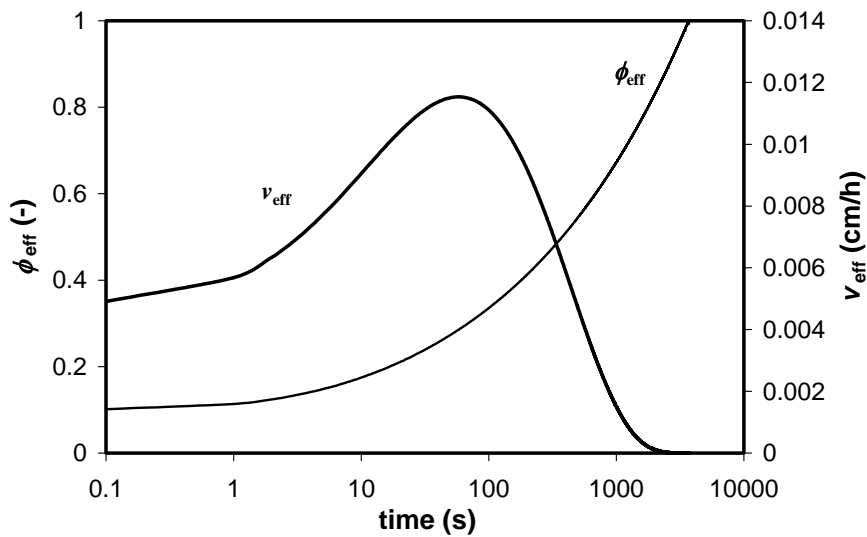


Fig. 2.4 Evolution of ϕ_{eff} and v_{eff} as a function of time, according to fractal growth of the flocs for an emulsion, with $\phi_e = 0.1$, $d_e = 1 \mu\text{m}$, $T = 298 \text{ K}$, $D_f = 2.3$, $\Delta\rho = 80 \text{ kg/m}^3$ and $\eta = 2 \text{ mPa}\cdot\text{s}$. After about 1 hour the flocs overlap.

At larger protein concentrations (c_p) we observed a different evolution of backscattering profiles (Fig. 2.3C). Firstly, the sharp boundary described in situation B reduced to a shoulder in the backscattering profile along the height of the sample. Secondly, a larger backscattering intensity in the serum layer was observed than at low c_p (Fig. 2.3B), which was related to a larger ϕ_s . Measured values of ϕ_s at a constant dextran concentration of 0.24 wt % and increasing c_p confirm this increase of ϕ_s (see Table 2.1). Table 2.1 also shows that the weight of the creamed layers decreased with c_p , showing that less oil had moved to the creamed layer after 20 h.

Table 2.1 Weights of the serum and the cream layers (w_s and w_c resp.), and the volume fraction of oil ϕ_s in the serum layers for 10 wt % oil-in-water emulsions at different protein concentrations after 20 hours of creaming.

c_p [% w/w]	w_s [g]	w_c [g]	ϕ_s [-]
0.23	15.7	4.10	0.0017
0.93	17.3	2.50	0.0040
2.76	17.8	1.94	0.0050
5.52	17.8	2.05	0.0052

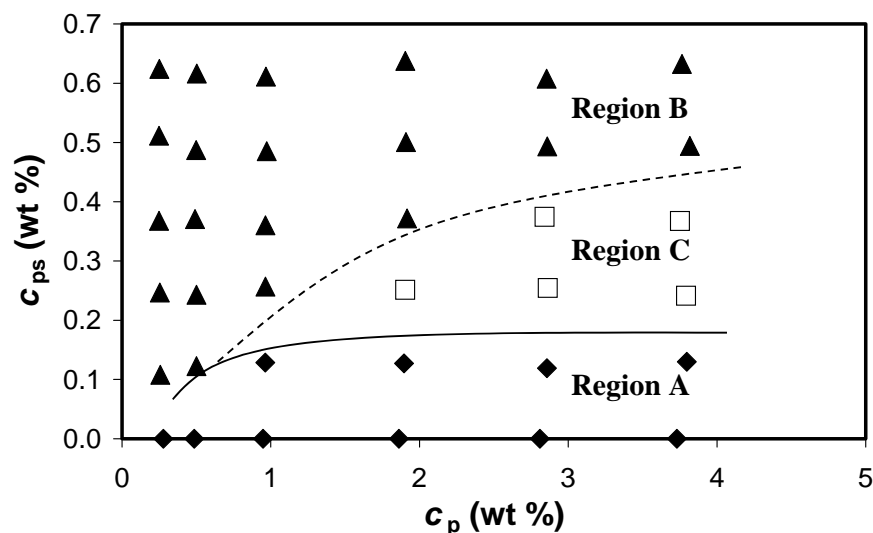


Fig. 2.5 Stability diagram of 10 wt % oil-in-water emulsions, containing dextran and β -lg. Different symbols correspond to the different situations shown in Fig. 2.4. \blacklozenge A, non-flocculating emulsion; \blacktriangle B, flocculating emulsion; \square C, flocculating emulsion. Lines are drawn to guide the eye.

The observations of the creaming behaviour as a function of β -lg and dextran concentration are summarised in a stability diagram (Fig. 2.5). In the diagram, c_p refers to the overall protein concentration in the emulsion, i.e. in solution and adsorbed on the oil droplets. At low c_p (< 1 wt %), the regions corresponding to situation A and B border at $c_{pf} = 0.1$ wt %. This value should correspond to the critical concentration for polymer-induced depletion-flocculation. This critical value of c_{pf} can be calculated following the approach of de Hek and Vrij.⁸ The volume fraction of oil at the boundary of spinodal demixing, ϕ_e^{sp} , is given by

$$\phi_e^{sp} = \frac{V_e}{-4\pi \int_0^\infty r^2 \left[1 - \exp\left(-\frac{U_T(r)}{k_B T}\right) \right] dr}, \quad (2.5)$$

where V_e is the volume of an oil droplet, k_B the Boltzmann constant, T is the absolute temperature and $U_T(r)$ the interaction potential between a pair of oil droplets at their centre to centre distance r . The total interaction potential consists of a number of contributions: $U_T(r) = U_{VdW}(r) + U_e(r) + U_{dep}(r) + U_{HC}(r)$. The Van der Waals attraction $U_{VdW}(r)$ between the oil droplets is equal to $-d_e A/24(r - d_e + \Delta)$, where A is the Hamaker constant and Δ a correction for the thickness of the protein layer. Electrostatic screening and retardation effects were not taken into account. The electrostatic repulsion $U_e(r)$ equals $\pi \epsilon d_e \psi_0^2 \ln(1 + \exp(-\kappa(r - d_e)))$, where ϵ is the dielectric constant of water, ψ_0 the wall potential of the protein layer around the oil droplet, which is assumed to be constant, and κ the reciprocal Debye length which approximately equals $3.29 \times \sqrt{I} \text{ nm}^{-1}$ at 25 °C (I is the ionic strength of the aqueous phase).²⁸

The depletion interaction potential $U_{dep}(r)$ is then given by²⁹

$$U_{dep}(r) = -\frac{c_{ps} RT}{6M} \cdot \pi (d_e + d_{ps})^3 \left[1 - \frac{3r}{2(d_e + d_{ps})} + \frac{r^3}{2(d_e + d_{ps})^3} \right] \quad (2.6)$$

for $d_e \leq r \leq (d_e + d_{ps})$.

Here we approximate the oil droplets by hard spheres with diameter d_e and volume fraction ϕ_e and the polysaccharide molecules by smaller spheres with diameter d_{ps} . In eq. 2.6, c_{ps} is the polysaccharide concentration, R the gas constant, T the absolute temperature and M is the molecular mass of the polysaccharide. In our calculations, d_{ps} is taken two times the radius of gyration, r_g , of the polysaccharide. Finally, hard core steric repulsion ($U_{HC}(r)$) was assumed.

The ζ potential of the oil droplets was measured -24 mV in 0.1 M NaCl, using a Zetasizer2000 (Malvern instruments, Southborough, UK). For the Hamaker constant we took 4×10^{-21} J,²⁸ and for Δ the diameter of a β -lg molecule of 3 nm was taken.³⁰ We found reasonable agreement between the measured and the calculated values of c_{pf} at low c_p for dextran and two other polysaccharides (see Table 2.2). If only depletion interaction was taken into account, c_{pf} was overestimated.

Table 2.2 Measured and calculated values for c_{pf} in emulsions, containing different polysaccharides. $\varepsilon = 6.9 \times 10^{-10}$ C \cdot V $^{-1}$ m $^{-1}$, $\zeta = -24$ mV, $\kappa^{-1} = 1$ nm, $A = 4 \times 10^{-21}$ J, $\Delta = 3$ nm, $d_e = 1$ μ m and $d_{ps} = 64$ nm.

polysaccharide	measured c_{pf} [% w/w]	calculated c_{pf} with $U_{tot}(r)$ [% w/w]	calculated c_{pf} with $U_{dep}(r)$ [% w/w]
dextran	0.1	0.1	0.5
EPS	0.01 ¹	0.01	0.03
galactomannan	0.03 ²	0.05	0.09

^a taken from Tuinier, 1999; ^b taken from Blijdenstein et al., 2002.

If c_p was increased, the transition was split up by the presence of region C in which a shoulder in the backscattering profiles was observed. Region B was only reached at polysaccharide concentrations that are larger than expected on the basis of spinodal decomposition. To find an explanation for the presence of region C in between region A and B at higher protein concentrations, we investigated the effect of protein on a) the critical polysaccharide where flocculation starts, b) the surface concentration of adsorbed protein and c) the kinetics of flocculation. These will be discussed in the following sections.

2.3.2 Effect of protein on c_{pf}

The presence of protein would induce a second depleted layer of the size of the radius of the protein molecules. However, because of their small radius (~ 2 nm) the protein molecules do not make a significant contribution to $U_{dep}(r)$. This is in agreement with the experimental results, because the border between region A and C at high protein concentrations starts at a value of c_{ps} , similar to the border between region A and B.

2.3.3 A change in surface concentration of adsorbed protein

Suppression of flocculation by β -lg was reported before,¹⁰ but at lower protein concentrations. These authors hypothesised that sticking of lumps of non-dissolved protein onto the adsorbed protein layer suppresses flocculation of oil droplets. In order to test their hypothesis we performed protein adsorption measurements for emulsions containing various concentrations of WPI or β -lg, added after emulsification.

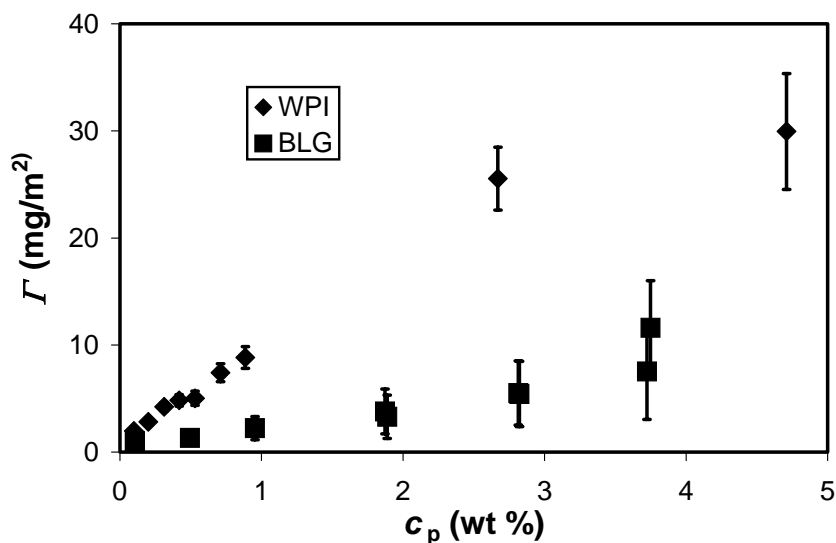


Fig. 2.6 Adsorption isotherms of protein at the surface of oil droplets as a function of the total protein content in 10 wt % oil-in-water emulsions.

The surface concentrations, Γ , as a function of protein concentration are shown in Fig. 2.6. If no protein was added after emulsification, Γ was approximately 2 mg/m^2 for both WPI and β -lg, which is in good agreement with surface concentrations found before.³¹⁻³³ The adsorbed amounts of WPI increased strongly when extra protein was added. This may be caused by multi-layer adsorption, but also by small protein aggregates sticking to the adsorbed protein layer. Solutions of WPI always remained slightly turbid which indicates

the presence of these aggregates which were probably formed during spray drying of WPI. For β -lg, which gives clear solutions, no significant increase of Γ was observed.

Although a strong increase in Γ was found only on addition of WPI to emulsions, the effect of extra protein in the continuous phase on flocculation and creaming was similar for WPI and β -lg. This shows that the latter effect is not due to a change in Γ .

2.3.4 A change in flocculation kinetics

We investigated the kinetics of flocculation using DWS. The mobility of the oil droplets was monitored in time in the absence and presence of dextran. In the absence of dextran, $\tau_{1/2}$ of the emulsions did not change significantly in time at any protein concentration studied (Fig. 2.7). When c_p was increased, $\tau_{1/2}$ increased and this increase corresponds well with the expected increase of the relative viscosity, calculated using the Krieger-Dougherty equation.³⁴ For the calculation we again approximated β -lg as hard spheres with a diameter of 3 nm, suspended in water together with 10 wt % oil droplets. For the volume fraction of closest packing we took 0.75.

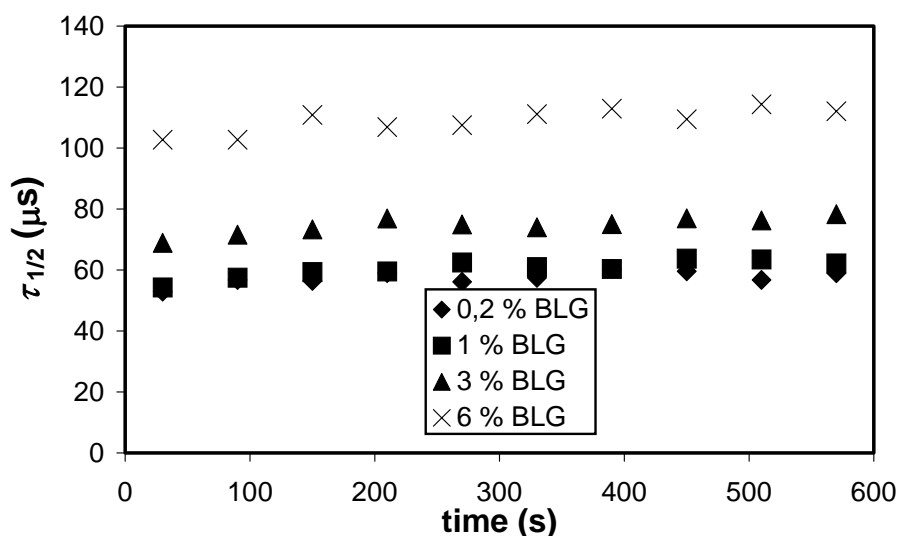


Fig. 2.7 Decay times of intensity autocorrelation functions plotted against time, for 10 wt % oil-in-water emulsions, at various β -lg concentrations.

In the presence of 0.24 wt % dextran, which is just above c_{pf} , the initial values of $\tau_{1/2}$ were higher than without dextran (Fig. 2.8), which could be caused by two factors. Firstly, dextran increased the viscosity, lowering the mobility of the oil droplets. Secondly, the flocculation process already occurred during the recording of the first autocorrelation function. Fig. 2.8 also shows that the increase of $\tau_{1/2}$ in time is very small at 6 wt % β -lg, which suggests that protein retards the flocculation process.

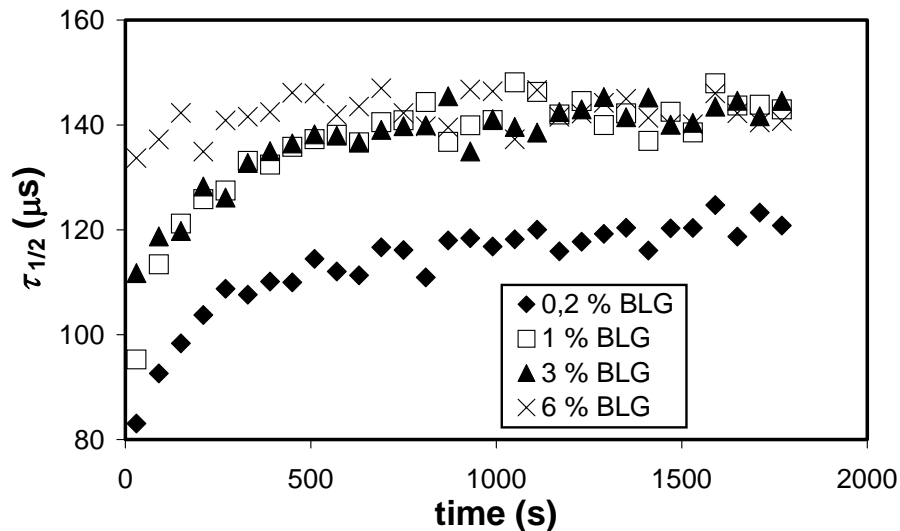


Fig. 2.8 Decay times of intensity autocorrelation functions plotted against time, for 10 wt % oil-in-water emulsions containing 0.24 wt % dextran at various protein concentrations.

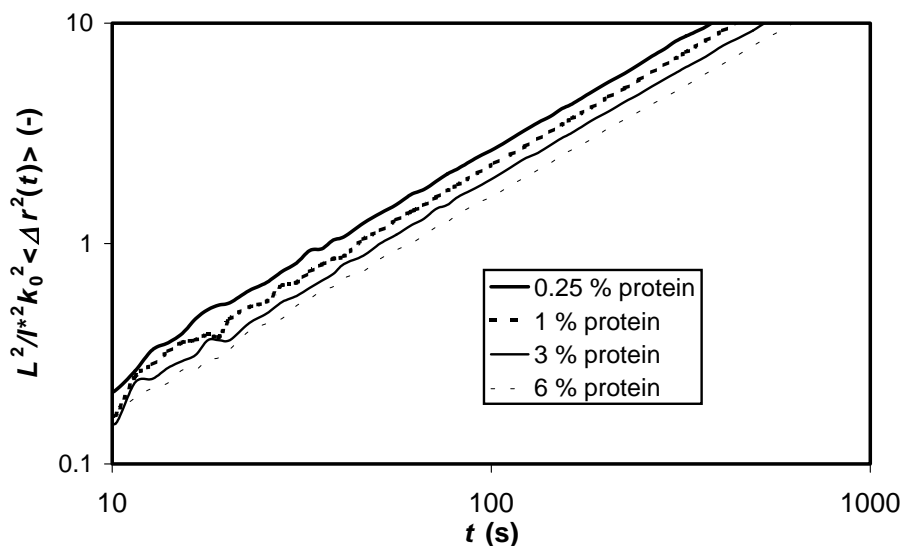


Fig. 2.9 Mean square displacement plotted as a function of time of oil droplets in a medium, containing 0.24 wt % dextran and various concentrations of protein.

The autocorrelation functions measured within the first minute after mixing were inverted for different protein concentrations at 0.25 wt % dextran using eq. 2.1. Since l^* is unknown, we plotted $L^2/l^{*2}k_0^2\langle\Delta r^2(t)\rangle$ (which is proportional to $\langle\Delta r^2(t)\rangle$) as a function of time in Fig. 2.9. All curves had a slope of 1 on a double logarithmic scale, indicating that the movement of the oil droplets was Brownian within the time scales of the measurement. When the protein concentration was increased, the lines shifted to lower displacement, due to the higher viscosity.

2.3.5 Rheology of mixed solutions of protein and dextran

The previous sections have shown that the effect of added protein seems to be related to a change in the flocculation kinetics, caused by a viscosity increase in the aqueous phase. Therefore the rheological behaviour of the aqueous phase was studied by strain-rate controlled viscometry. Fig. 2.10 shows that a 1 wt % dextran solution has a viscosity of approximately 2 mPa·s, independent of $\dot{\gamma}$. An aqueous solution of 10 wt % WPI was shear-thinning, but the increase in the apparent viscosity, η_{app} , with decreasing $\dot{\gamma}$ remained relatively small. However, mixed solutions of WPI and dextran were strongly shear thinning and η_{app} at low shear-rate was much higher. The apparent viscosities were approximately equal for a 1 and 6 wt % WPI solution at $c_{ps} = 1$ wt %, showing that mainly the presence of a small amount of protein affects the viscosity of a dextran solution and this effect does not become stronger at higher c_p .

A similar effect was found for mixed solutions of β -lg and dextran by stress controlled measurements at low shear stresses (Fig. 2.11). In the mixed solutions, η_{app} was large at low shear-rate, comparable to mixed solutions of WPI and dextran. A yield stress could not be detected within the applied range of shear stresses ($2 \times 10^{-5} - 10^{-2}$ Pa).

At present, we cannot give a good explanation for the large increase of η_{app} at low shear-rates. We believe that this increase is due to weak interactions between β -lg and dextran. At concentrations used in this study, the interaction is too weak to induce phase separation by depletion.³⁵ Incompatibility between WPI and dextran occurs at higher concentrations (above 10 wt % WPI + 5 wt % dextran), as shown by Syrbe et al.³⁶ CSLM-images showed no signs of phase separation or complex coacervation in the aqueous phase in a solution of 5 wt % WPI + 5 wt % dextran (results not shown). Also surface tension measurements³⁷ did not give indications for complex formation of β -lg with dextran. Perhaps the viscosity increase is due to specific interactions between β -lg and dextran which are too weak to

lead to incompatibility or complex formation and therefore do not lead to phase separation or a change in surface. A molecular study on these interactions is however outside the scope of this paper.

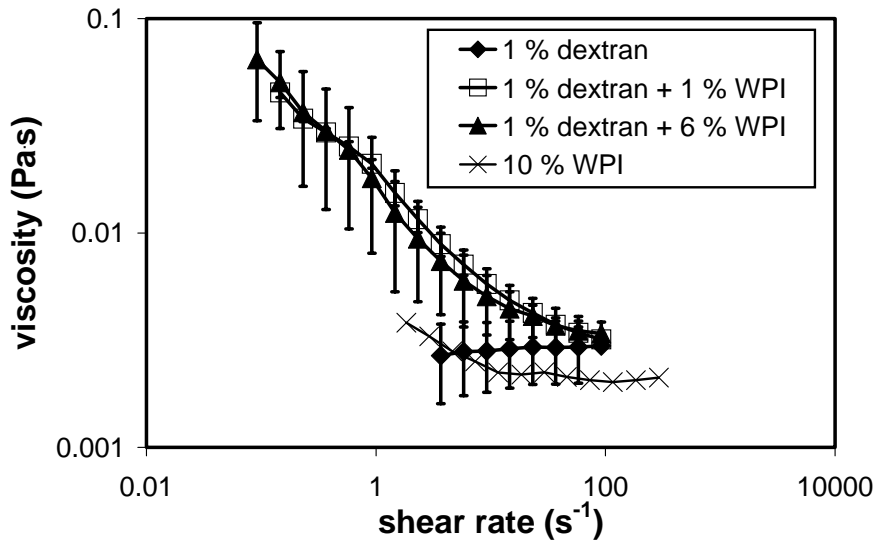


Fig. 2.10 Apparent viscosity of aqueous solutions of dextran, WPI and mixtures of these in 0.1 M NaCl as a function of the shear rate.

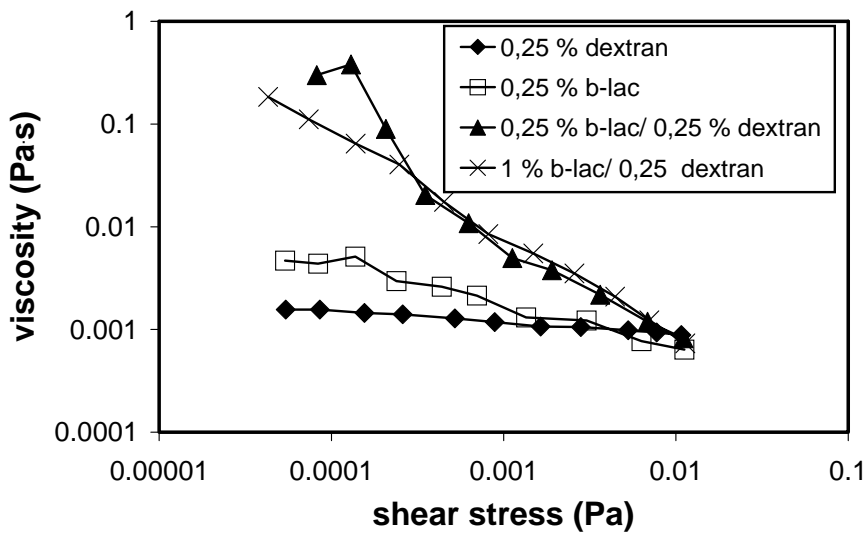


Fig. 2.11 Apparent viscosity of aqueous solutions of dextran, β -lg and mixtures of these in 0.1 M NaCl as a function of the shear stress.

Nevertheless, the large increase of the low-shear viscosity on addition of protein to dextran solutions must have a large effect on droplet flocculation and creaming, as will be argued below.

The rate of perikinetic flocculation of the oil droplets will be determined by η_{app} at low shear-rate. According to eq. 2.3, higher η -values lead to a slower increase of ϕ_{eff} during flocculation and for $\eta = 200 \text{ mPa}\cdot\text{s}$ and $d_e = 1 \text{ }\mu\text{m}$, ϕ_{eff} will reach overlap after about 1 day, instead of 1 hour. This retardation of the flocculation process at high c_p is in qualitative agreement with the DWS results (Fig. 2.9). Because the flocculation rate is now much slower than the creaming rate, small flocs will disappear from the solution and the unflocculated oil droplets will stay in the serum phase. These remaining droplets will be mainly the smaller droplets because $U_{\text{dep}}(r)$ is smaller for these droplets (eq. 2.6). The rising flocs exert a higher upward pressure on the aqueous phase and consequently experience a lower viscosity of the solution and therefore cream relatively quickly. This explains the shoulder in the observed backscattering profiles (Fig. 2.3C) formed by fast creaming of small flocs consisting of larger droplets. Smaller single droplets remain in the serum layer, which is in agreement with the larger oil concentrations measured in the serum layer (see Table 2.1).

At larger c_{ps} , more droplets will participate in flocculation and it may be argued that the rheology will become dominated more by dextran, which behaves Newtonian. Therefore at sufficiently high dextran concentration a network will again be formed as shown by a transition from region C to region B in the stability diagram (Fig. 2.5).

2.4 Conclusion

Creaming and flocculation were studied in emulsions, stabilised by WPI or β -lg. The polysaccharide concentration above which flocculation of the emulsions occurs was well predicted by spinodal demixing theory if the interaction between the droplets includes Van der Waals, electrostatic, and depletion interactions. Above this polysaccharide concentration, a sharp boundary between a serum and an emulsion phase was observed which moves upward. However, the observed creaming behaviour of these emulsions was influenced strongly by the presence of an excess amount of protein in the continuous phase. At increasing excess protein concentration, a shoulder was observed in the

backscattering profiles instead of a sharp phase boundary and more droplets stayed behind in the serum layer at high protein concentration.

The different creaming behaviour was shown to be caused by a change in the kinetics of flocculation. It was demonstrated by monitoring the flocculation process using DWS, that addition of protein retards the flocculation rate. This retardation is caused by a strong increase of the apparent low-shear-rate viscosity in mixed solutions of β -lg and dextran. The cause of this increase is not yet understood and remains a topic for further research, but it has a strong effect on the macroscopic creaming process in emulsions. At larger protein concentrations, the high apparent viscosity at low shear-rate retards the kinetics of flocculation but creaming of large droplets and flocs is determined by a lower apparent viscosity. This explains why no sharp phase boundary is observed at higher protein concentrations.

This effect of protein addition has implications for the use of polysaccharides as thickening agents. At large bulk protein concentration, more polysaccharide must be added to induce sufficient flocculation, in order to thicken an emulsion by formation of a droplet network.

Acknowledgement

The authors thank Fadel Aljawaheri for measuring the ζ potential of the oil droplets

References

- (1) Syrbe A.; Bauer W. J.; Klostermeyer N. *Int. Dairy J.* **1998**, *8*, 179-193.
- (2) Robins M. M. *Curr. Op. Coll. Int. Sci.* **2000**, *5*, 265-272.
- (3) Cao Y. H.; Dickinson E.; Wedlock D. J. *Food Hydrocolloids* **1990**, *4*, 185-195.
- (4) Demetriades K.; McClements D. J. *J. Agric. Food Chem.* **1998**, *46*, 3929-3935.
- (5) Poon W. C. K.; Haw M. D. *Adv. Coll. Int. Sci.* **1997**, *73*, 71-126.
- (6) Manoj P.; Watson A. D.; Hibberd D.; Fillery-Travis A.; Robins M. M. *J. Coll. Int. Sci.* **2000**, *228*, 200-206.
- (7) Manoj P.; Fillery-Travis A.; Watson A. D.; Hibberd D.; Robins M. M. *J. Coll. Int. Sci.* **1998**, *207*, 283-293.
- (8) de Hek H.; Vrij A. *J. Coll. Int. Sci.* **1981**, *84*, 409-422.
- (9) Tuinier R.; de Kruif C. G. *J. Coll. Int. Sci.* **1999**, *218*, 201-210.
- (10) Dimitrova T. D.; Gurkov T. D.; Vassileva N.; Campbell B.; Borwankar R. P. *J. Coll. Int. Sci.* **2000**, *230*, 254-267.
- (11) Tolstoguzov V.B. in *Functional properties of food macromolecules*, Mitchell J.R., Ledward D.A., Eds. Elsevier Applied Science, London **1986**; Chapter 9.

- (12) Grinberg V. A.; Tolstoguzov V. B. *Food Hydrocolloids* **1997**, *11*, 145-158.
- (13) Doublier J. L.; Garnier C.; Renard D.; Sanchez C. *Curr. Op. Coll. Int. Sci.* **2000**, *5*, 202-214.
- (14) Reiffers-Magnani C. K.; Cuq J. L.; Watzke H. J. *Food Hydrocolloids* **2000**, *14*, 521-530.
- (15) Blijdenstein T. B. J., van der Linden E., van Vliet T, and van Aken G. A. *Gums and stabilisers for the food industry II* Williams, P. A. and Phillips, G. O. Eds, Royal Society of Chemistry **2002**, 256-262.
- (16) de Jongh H. H. J.; Gröneveld T.; de Groot J. *J. Dairy Sci.* **2001**, *84*, 562-571.
- (17) Van Cleve J. W.; Schaefer W. C.; Rist C. E. *J. Am. Chem. Soc.* **1956**, *78*, 4435-4438.
- (18) Mengual O.; Meunier G.; Cayré I.; Puech K.; Snabre P. *Coll. Surf. A* **1999**, *152*, 111-123.
- (19) de Jong C.; Badings H. T. *J. high Res. Chrom.* **1990**, *13*, 94-98.
- (20) Oortwijn H.; Walstra P. *Neth. Milk Dairy J.* **1979**, *33*, 134-154.
- (21) Weitz D.A.; Pine D. J., in *Dynamic Light Scattering*, Brown W., Ed. Clarendon Press, Cambridge **1993**; Chapter 16.
- (22) ten Grotenhuis E.; Paques M.; van Aken G. A. *J. Coll. Int. Sci.* **2000**, *227*, 495-504.
- (23) van Vliet T.; de Groot-Mostert A. E. A.; Prins A. *J. Phys. E* **1981**, *14*, 745-746.
- (24) Bird, R. B., Stewart, W. E., and Lightfoot, E. N. *Transport Phenomena* **1960**, John Wiley & Sons, Inc., New York.
- (25) von Smoluchowski M. *Z. Phys. Chem.* **1917**, *92*, 129-168.
- (26) Bremer L. G. B.; Walstra P.; van Vliet T. *Coll. Surf. A* **1995**, *99*, 121-127.
- (27) Walstra P.; Oortwijn H. *Neth. Milk Dairy J.* **1975**, *29*, 263-278.
- (28) Hunter, R. J. *Foundations of Colloid Science* **1987**, Oxford University Press, New York.
- (29) Vrij A. *Pure Appl. Chem.* **1976**, *48*, 471-483.
- (30) Barteri M.; Gaudiano M. C.; Rotella S.; Benagiano G.; Pala A. *Biochim. Biophys. Acta* **2000**, *1479*, 255-264.
- (31) Euston S. R.; Finnigan S. R.; Hirst R. L. *Food Hydrocolloids* **2000**, *14*, 155-161.
- (32) Hunt J. A.; Dalgleish D. A. *Food Hydrocolloids* **1994**, *8*, 175-187.
- (33) Smulders P. E. A. *Formation and stability of emulsions made with proteins and peptides*, **2001**, Thesis, Wageningen University.
- (34) Barnes H. A. and Walters K. *An Introduction to Rheology* **1989**, Elsevier, Amsterdam.
- (35) Tuinier R.; Vliegthart G. A.; Lekkerkerker H. N. W. *J. Chem. Phys.* **2000**, *113*, 10768-10775.
- (36) Syrbe A.; Fernandes P. B.; Dannenberg F.; Bauer W. J.; Klostermeyer N., in *Food Macromolecules and Colloids*, Dickinson E., Lorient D., Eds. Royal Society of Chemistry, Cambridge, UK **1995**.
- (37) Dickinson E.; Galazka V. B. *Food Hydrocolloids* **1991**, *5*, 281-296.

3

Control of strength and stability of emulsion gels by a combination of long- and short-range interactions*

Abstract

This paper discusses the change in phase behaviour and mechanical properties of oil-in-water emulsion gels brought about by variation of long- and short-range attractive interactions. The model system studied consisted of oil droplets stabilised by the protein β -lactoglobulin (β -lg). A long-range depletion attraction was obtained by addition of dextran. At short distances, the interaction is dominated by electrostatic repulsion between the adsorbed layers of β -lg. This interaction was varied by addition of Ca^{2+} ions and by changing the NaCl concentration. Combination of long- and short-range attraction resulted into a substantial decrease in the rate of serum separation and an increase in the emulsion-gel modulus at small deformations compared to depletion attraction alone. The flocculation process and the morphology of the flocs were investigated by diffusing wave spectroscopy and confocal scanning laser microscopy. Above a minimum concentration, dextran induced fast depletion-flocculation, leading to a network of emulsion droplets. This network quickly collapsed due to gravity. Addition of Ca^{2+} ions above a minimum concentration induced slow flocculation, and the flocs creamed before a network was formed. Addition of both dextran and Ca^{2+} ions resulted in a two-step mechanism of emulsion-gel formation. A network is quickly formed by depletion-flocculation and subsequently the bonds between the emulsion droplets are reinforced by Ca^{2+} ions. Due to this reinforcement, rearrangements of this network were suppressed resulting in a smaller rate of serum separation.

*Langmuir 19, **2003**, 6657-6663.

3.1 Introduction

The stability and mechanical properties of colloidal systems are of technological interest for numerous applications, e.g., drilling mud, paints, inks, cosmetics and foods. The properties of such materials are to a large extent determined by the interactions between the colloidal particles of which they consist. More specifically, for protein-stabilised emulsions these interactions are determined by the interaction between the oil droplets and by the adsorbed protein layer around the droplets.¹

In relatively dilute emulsions ($\phi < 0.4$ wt %) with repulsive droplet–droplet interactions, the droplets are distributed homogeneously over the emulsion and the emulsion behaves as a liquid. The droplets cream due to a density difference between the droplets and the continuous liquid, which results in the formation of a dense creamed layer on top of the emulsion. When the net interaction between the emulsion droplets becomes sufficiently attractive to overcome the Brownian motion of the emulsion droplets, they will flocculate. The relative rates of flocculation and creaming determine the structural evolution of an emulsion. If the rate of creaming exceeds the rate of flocculation, small flocs will be formed, which cream faster than individual droplets. This results in faster formation of a creamed layer. In the opposite case, the flocs grow large enough to overlap and form a network.^{2,3} Due to collapse of this network, which is similar to a large deformation compression, a serum layer will separate at the bottom of the emulsion.⁴

The morphology, stiffness, and strength of these colloidal networks can be tuned by varying the interaction between the particles in the network. Note that the term “strength” is used in relation to a non-linear (large) deformation or yielding, and “stiffness” in relation to linear (small) deformations. For example, a deeper well in the interaction potential curve usually yields a more open structure.^{2,5,6} However, also the shape of the interaction potential curve is important, which can be altered, e.g., by combining different types of interactions. As an example, the effect of a secondary energy minimum on the initial stages of flocculation was discussed in a recent paper by Behrens and Borkovec.⁷ These authors formulate a two-step flocculation mechanism, in which reversible flocculation into the secondary minimum precedes a slow coagulation into the primary energy minimum.

This paper treats the effect of a combination of interactions on the phase behaviour and gel strength of oil-in-water emulsions, stabilised by the milk protein β -lactoglobulin (β -lg). A long-range attraction was induced by addition of the polysaccharide dextran, which results

in a relatively weak depletion attraction.⁸⁻¹⁰ A change in short-range interaction was accomplished by addition of Ca^{2+} ions,¹¹⁻¹⁴ which bind to the proteins adsorbed at the oil-water interface,¹⁵ lowering the electrostatic repulsion between the droplet surfaces¹⁶ and increasing hydrophobicity of the adsorbed proteins.¹⁷ In addition, the effect of Ca^{2+} ions was compared to the effect of NaCl.

The effect of combined long- and short-range interactions was studied in detail by monitoring the flocculation process on a colloidal scale using diffusing wave spectroscopy (DWS) and confocal scanning laser microscopy (CSLM). An appropriate combination of dextran and Ca^{2+} ions is shown to lead to formation of a network of emulsion droplets with strong inflexible bonds, which improves gel stiffness and reduces the rate of serum separation.

3.2 Interactions between the emulsion droplets

In the present system, the total pair interaction potential, $U_T(h)$, at the surface-to-surface distance h is the sum of van der Waals, $U_{\text{vdw}}(h)$, electrostatic, $U_e(h)$, depletion, $U_{\text{dep}}(h)$, and hard-core steric interactions, $U_{\text{HC}}(h)$. To treat our system semi-quantitatively, we make some approximations to estimate the interaction potentials. We assume that the emulsion droplets can be modelled as spherical oil droplets covered by a negatively charged protein layer. The thickness, Δ , of the protein layer is assumed to be 3 nm, which is a reasonable estimate for β -lg molecules.¹⁸ The surface of the emulsion droplet is assumed to be positioned at the outer surface of the protein layer. The van der Waals interaction, $U_{\text{vdw}}(h)$, is expressed as $U_{\text{vdw}}(h) = -d_e A/[24(h + 2\Delta)]$, where d_e equals the diameter of an oil droplet which can be approximated by the diameter of the total emulsion droplet since $\Delta \ll d_e$. A is the Hamaker constant for the interaction between oil and water, which is taken as 4×10^{-21} J.¹⁹

The adsorbed layer of β -lg molecules carries a negative charge at neutral pH. This causes an electrostatic repulsion, which can be expressed by $U_e(h) = \pi \epsilon d_e \psi_0^2 \ln[1 + \exp(-\kappa h)]$.¹⁹ Here, ϵ is the dielectric constant of water ($= 6.9 \times 10^{-10}$ F·m), ψ_0 is the surface potential of the protein layer, κ is the reciprocal Debye length with a numerical value of $\kappa = 3.29(\Sigma((1/2)c_i z_i^2))^{1/2}$ nm in aqueous solutions at 25 °C, c_i is the electrolyte concentration in mol/l and z_i its valence. A more detailed description of the electric double layer is given in the Appendix.

Depletion of polymer from a layer around dispersed particles gives rise to an attractive interaction between these particles. Here we approximate the emulsion droplets by hard spheres with diameter d_e and volume fraction ϕ_e and the polysaccharide molecules by smaller spheres with diameter d_{ps} . It is assumed that the osmotic pressure of the polysaccharide in the aqueous phase increases linearly with concentration. The depletion interaction potential, $U_{dep}(h)$, is then given by²⁰

$$U_{dep}(h) = -\frac{c_{ps}RT}{6M} \cdot \pi(d_e + d_{ps})^3 \left[1 - \frac{3(d_e + h)}{2(d_e + d_{ps})} + \frac{(d_e + h)^3}{2(d_e + d_{ps})^3} \right] \text{ for } 0 \leq h \leq d_{ps}, \quad (3.1)$$

where c_{ps} is the polysaccharide concentration and M is the molecular mass of the polysaccharide. In our calculations, d_{ps} is taken twice the radius of gyration, r_g , of the polysaccharide molecule. Since the protein molecules are in this model positioned behind the surface of the emulsion droplet steric interactions are treated as $U_{HC}(h) = 0$ when $h > 0$ and $U_{HC}(h) \rightarrow \infty$ when $h < 0$.

The interaction potential between the droplets determines the occurrence and rate of flocculation. The expected onset of flocculation was calculated by a model of spinodal demixing. Spinodal demixing occurs when the osmotic compressibility, $\delta\Pi_e/\delta\phi_e$, due to interactions between the emulsion droplets becomes negative. The osmotic pressure due to the interacting emulsion droplets, Π_e , can be approached by a second-order virial expansion ($\Pi_e \sim \phi_e + B_2\phi_e^2$) up to a droplet volume fraction, ϕ_e , of 0.2. According to this model, spinodal demixing occurs if the volume fraction of emulsion droplets equals²¹

$$\phi_e = -\frac{1}{2B_2} = -\frac{V_e}{4\pi \int_0^\infty \left[1 - \exp\left(-\frac{U_T(h)}{k_B T}\right) \right] (d_e + h) d(d_e + h)}, \quad (3.2)$$

where V_e is the volume of an emulsion droplet, k_B is the Boltzmann constant, and T is the absolute temperature. It must be stressed that the absolute values of these interactions are at best good estimates due to the multitude of the assumptions made. We will use these values to discuss the experimental results.

3.3 Flocculation kinetics

During the initial stages of flocculation, the rate of flocculation of the emulsion droplets is characterised by the Smoluchowski time of flocculation, τ_s , which equals $(4\pi D d_e n_0)^{-1}$.²² Here D is the diffusion coefficient of the emulsion droplets and n_0 is the initial number of droplets per volume unit. The diffusion coefficient is equal to $k_B T / 3\pi\eta d_e$ for spheres, where η is the viscosity of the medium.

The initial rate of flocculation depends on the interaction potential between the droplets as expressed by

$$\tau_{s,F} = \tau_s \cdot \int_0^{\infty} \exp\left(\frac{U_T(h)}{k_B T}\right) \frac{d_e dh}{(h + d_e)^2}, \quad (3.3)$$

where the integral on the right side is known as the Fuchs factor.²³

By use of a fractal model, the effective volume fraction (defined as the volume fraction of flocculated oil droplets including the water enclosed by the flocs) of the flocculating emulsion, ϕ_{eff} , can be expressed as a function of the initial volume fraction of emulsion droplets, ϕ_e , $\tau_{s,F}$ and the fractal dimension D_f . This yields an expression to estimate τ_n , the time required to form a network of emulsion droplets²⁴

$$\tau_n = \tau_{s,F} \left(\phi_e^{\frac{-D_f}{3-D_f}} - 1 \right). \quad (3.4)$$

3.4 Experimental

3.4.1 Materials

β -Lactoglobulin (protein content 92.5 wt %) was purified from bovine milk.²⁵ Dextran (isolated from *Leuconostoc*; $M_w = 2 \times 10^6$ Da) was obtained from Sigma Chemicals (St. Louis, MO). Its radius of gyration was 32 nm, as determined from the intrinsic viscosity.⁴ NaCl (p. a.) and CaCl₂ (p. a.) and thiomersal (97 wt %) were obtained from Merck (Shuchardt, Germany). Sunflower oil (Reddy, Vandemoortele, The Netherlands) was purchased from a local retailer.

3.4.2 Sample preparation

Protein solutions were prepared by adding protein powder to the required amount of NaCl solution, followed by gentle stirring overnight, avoiding incorporation of air bubbles. The pH of all samples was between 6.6 and 6.8 and the NaCl concentration was 0.10 M. Thiomersal (0.02 wt %) was added to inhibit microbial growth.

Stock emulsions contained 40 wt % sunflower oil and 1 wt % β -lg. Emulsions were prepared by mixing oil into β -lg solution using an Ultra Turrax (Polytron, Switzerland) and subsequent homogenisation by 10 passes through a Delta lab-scale homogeniser operating at a pressure of 50 bar. The volume-over-surface-averaged droplet diameter, d_{32} , was determined using a laser diffraction apparatus (Coulter LS 230, Miami, FL). Stock emulsions used in this work had typical d_{32} values of 1.2 μ m.

A dextran solution was prepared by adding dextran to 0.10 M NaCl solution and stirring “au bain-marie” in boiling water for 4 hours.

Emulsion samples containing 10 wt % oil and various amounts of dextran and CaCl₂ were prepared by adding the stock emulsion to the required amounts of dextran solution and salt solution. In this way the droplet size distribution and the NaCl concentration of the emulsions were kept constant in all samples. All samples were mixed by gently shaking during 30 s just prior to an experiment. We note that fast flocculation already occurs during mixing and the gentle shaking may have broken up the larger flocs. All measurements were carried out at 25 °C.

3.4.3 Demixing experiments

Demixing of emulsions was followed by measuring the backscattering intensity of incident laser light along the height of an optical glass tube, using a Turbiscan MA 2000 apparatus (Ramonville St. Agne, France).²⁶ Emulsion samples were brought into these tubes using an automatic pipette and then stored. At selected times after bringing the sample into the tube, the backscattering profile was measured. This profile gives a qualitative indication of the distribution of the emulsion droplets along the height of the tube, since the backscattering intensity varies with the volume fraction of oil.

3.4.4 Confocal scanning laser microscopy (CSLM)

CSLM-imaging was performed using an inverted microscope (Leica DM Irbe, Heidelberg, Germany), combined with an argon laser setup (JDS Uniphase, San Jose, CA). A few drops of rhodamine B, a fluorescent label which is excited at 568 nm, were added to stain the protein and its fluorescence was detected at wavelengths between 600 and 700 nm.

3.4.5 Diffusing wave spectroscopy (DWS)

DWS measurements were carried out in a transmission geometry^{27,28} using a He/Ne laser ($\lambda = 547$ nm). The laser illuminated about 1 mm^2 of the sample, which was contained in a cuvette with an inner width, L , of 1.98 mm. The transport mean free path, l^* , of the samples was typically $100 \mu\text{m}$. The scattered light was focussed by a lens collector into a single mode fibre, attached to a photomultiplier (ALV, SO-SIPD, Langen/Hessen, Germany). The signal was analysed by a correlator board (ALV, flex-5000, Langen/Hessen, Germany) that calculated the intensity autocorrelation function, $g_2(t)$, from the transmitted light collected during 1 min of recording time. The decay time, $\tau_{1/2}$, was determined, which is defined as the time at which $g_2(t)-1$ had decayed to half of its initial value. Larger values of $\tau_{1/2}$ are indicative for a lower mobility of the emulsion droplets. All values of $\tau_{1/2}$ are much ($\gg 1000$ times) smaller than the recording time. Measurements were carried out during 30 min. During this time no significant topological changes (e.g., creaming) occurred within the samples.

3.4.6 Rheology

Dynamic measurements were carried out using a Bohlin VOR Rheometer (Huntingdon, U.K.). A concentric cylinder geometry (C 25) with a gap of 2.5 mm and a 1-g torsion bar were used. At the start of each measurement the samples were sheared at a rate of 10^2 s^{-1} to break up flocs that were formed between mixing the sample and performing the measurement (± 1 min). After this pre-shear treatment, the storage modulus, G' , was measured every minute during 30 minutes at a strain amplitude of 0.0046. Finally a strain sweep experiment was carried out.

3.4.7 ζ Potential measurements

The ζ potential of the emulsion droplets was determined using a zetasizer 2000 (type 1 256 Malvern Instruments, Southborough UK). Part of the 40 wt % stock emulsion was diluted by a factor of 10^5 with 0.1 M NaCl solution. The sample was injected into the apparatus and the average of four measurements was reported as ζ potential.

3.5 Results

Demixing experiments were carried out on 10 wt % oil-in-water emulsions at varying concentrations of dextran and Ca^{2+} ions. Four different types (A, B, C, and D) of demixing progressions were observed (Fig. 3.1). For each type a CSLM image was made 5 min after mixing the sample (Fig. 3.2) and the mobility of the emulsion droplets was recorded by DWS during 30 min after mixing the sample. Fig. 3.3 shows the normalised autocorrelation functions measured during the 30th minute of the measurement. All autocorrelation functions have single decay within the accuracy of our experiments. The development of $\tau_{1/2}$ is shown in Fig. 3.4. The interpretation of the behaviour of the emulsions will be discussed for each demixing type.

Demixing type A is typical for demixing due to creaming only. The CSLM picture shows single emulsion droplets, and the movement suggested free Brownian motion. This is in accordance with the DWS measurements, which showed a constant decay time during 30 min and no flocculation.

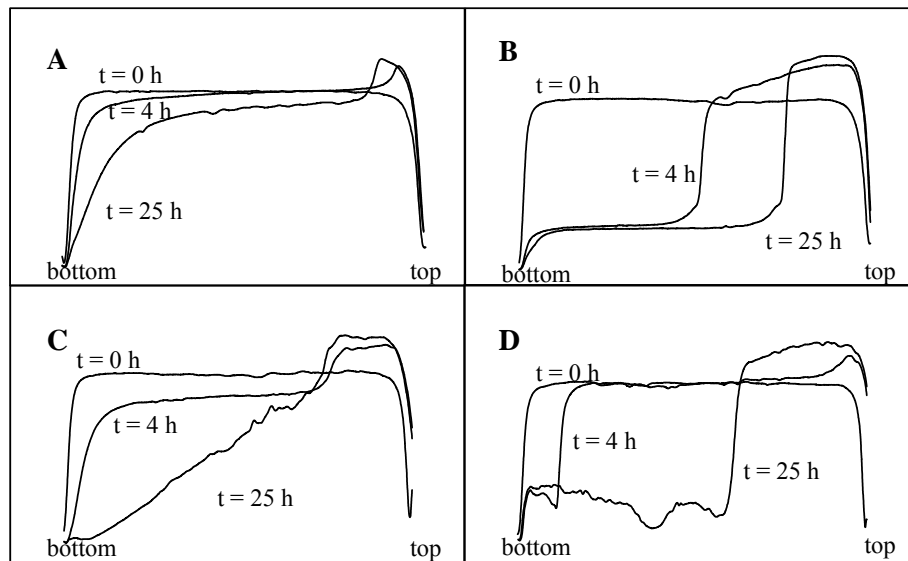


Fig. 3.1 Typical backscattering profiles of 10 wt % oil-in-water emulsions of four different types of demixing: type A, 0 wt % dextran, 0 mM Ca^{2+} ; type B, 1 wt % dextran, 0 mM Ca^{2+} ; type C, 0 wt % dextran, 100 mM Ca^{2+} ; type D, 1 wt % dextran, 100 mM Ca^{2+} . Horizontal axis is height along the tube, and vertical axis is backscattered intensity.

Type B was observed above a minimum polysaccharide concentration (c_{pf}) of 0.1 wt %. A sharp boundary between the serum layer and the emulsion was formed, which moved upward. CSLM pictures show the formation of large flocs, and we observed no significant motion of the flocs within the image acquisition time (1 s). These observations suggest the presence of a network of emulsion droplets. This suggestion was confirmed by the DWS experiments. The value of $\tau_{1/2}$ that was measured during the first minute after mixing the sample, $\tau_{1/2}(0)$, is larger than expected on the basis of the viscosity increase of the continuous phase caused by dextran. This is due to flocculation during mixing of the sample and during the first minute of the measurement. Subsequently, $\tau_{1/2}$ continued to increase and levelled off after 20 min. The behaviour of type B corresponds to fast flocculation of the emulsion droplets.

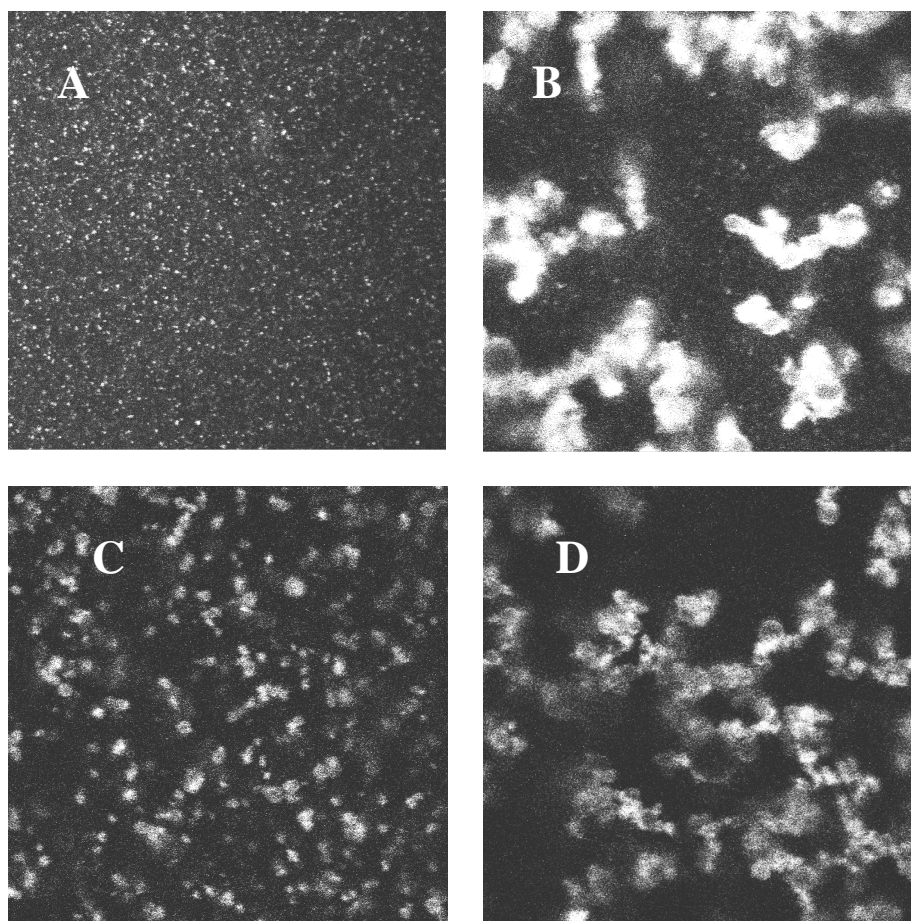


Fig. 3.2 CSLM pictures of the same systems as in Fig 3.1, 5 min after mixing the samples. Image size: $40\ \mu\text{m} \times 40\ \mu\text{m}$.

Type C was found above a minimum concentration of Ca^{2+} ions of 50 mM. Similar to type A, a creamed layer was formed, however, its formation proceeded quicker, and after 1 day the creamed layer began to shrink (see Fig. 3.5). The CSLM picture shows that small compact flocs were formed, which moved freely. DWS measurements showed that $\tau_{1/2}(0)$ was similar for types A and C, but for type C, $\tau_{1/2}$ slowly increased in time. This slow increase of $\tau_{1/2}$ can be attributed to slow flocculation resulting in the formation of the small flocs that were observed by CSLM.

Type D was found if dextran and Ca^{2+} ions were both present at a concentration higher than their respective minimum concentrations. CSLM pictures and DWS measurements indicate the formation of a network as a consequence of rapid flocculation, similar as for type B. However, the upward movement of the phase boundary was slower than for type B. For illustration, the heights of the emulsion networks at 1 wt % dextran and different concentrations of Ca^{2+} ions are plotted against time in Fig. 3.6.

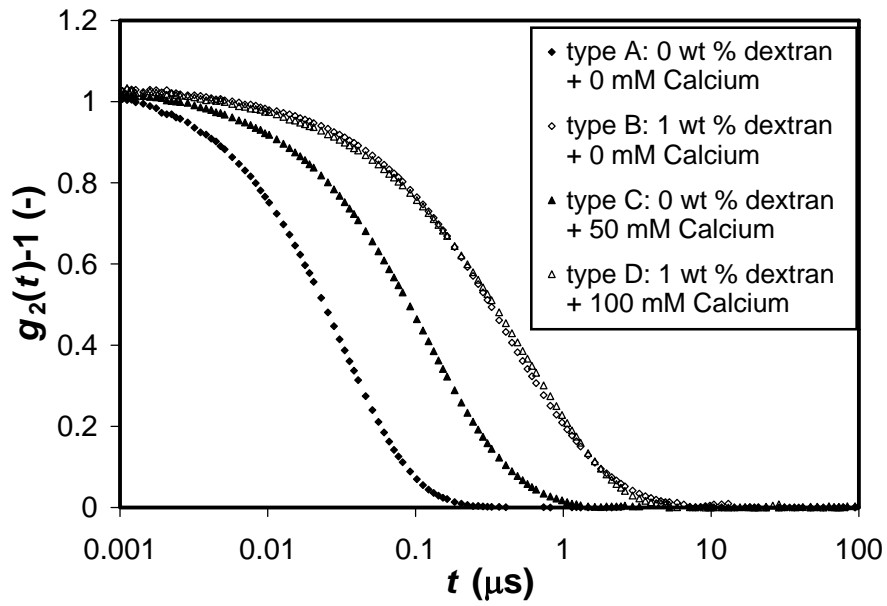


Fig. 3.3 Normalised autocorrelation functions, measured during the 30th minute after mixing, for the same systems as in Fig. 3.1.

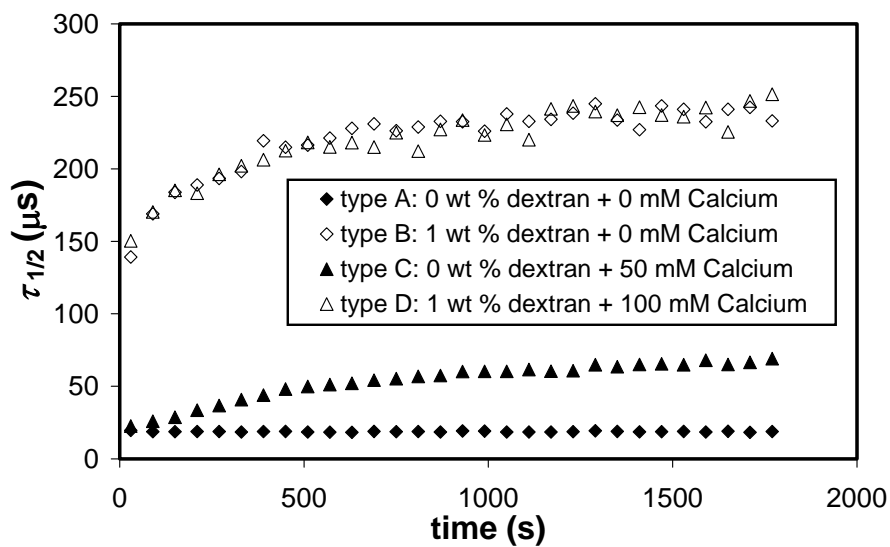


Fig. 3.4 Decay times of intensity autocorrelation functions plotted against time, for the same systems as in Fig. 3.1.

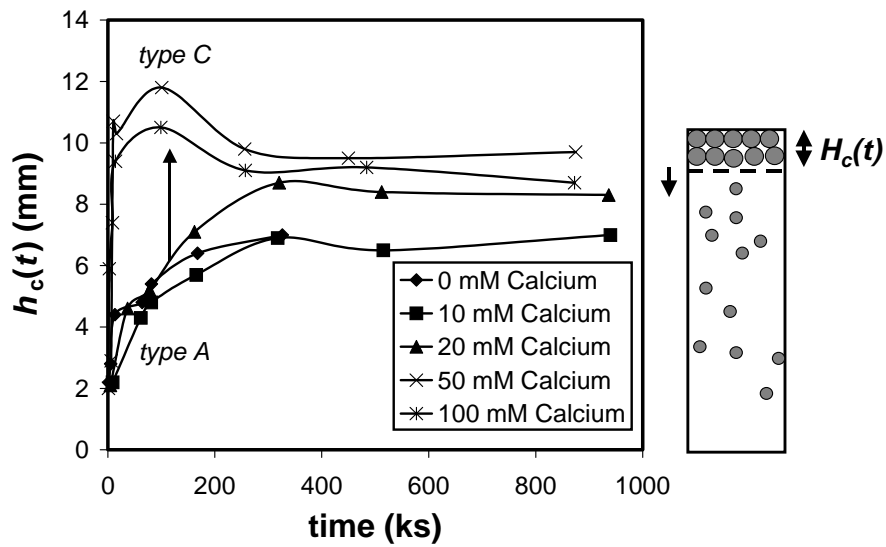


Fig. 3.5 Height of the creamed layer, $h_c(t)$, plotted against time for 10 wt % oil-in-water emulsions, containing various concentrations of Ca^{2+} ions. The figure reflects a transition from type A behaviour to type C behaviour between 20 and 50 mM.

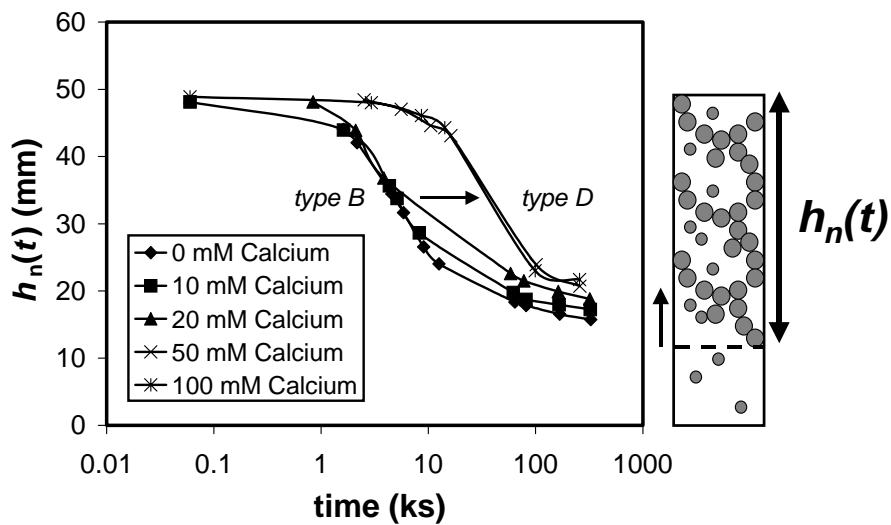


Fig. 3.6 Height of the flocculated emulsion network, $h_n(t)$, plotted against time for 10 wt % oil-in-water emulsions containing 1 wt % dextran and various amounts of Ca^{2+} ions. The figure reflects a transition from type B behaviour to type D behaviour between 20 and 50 mM.

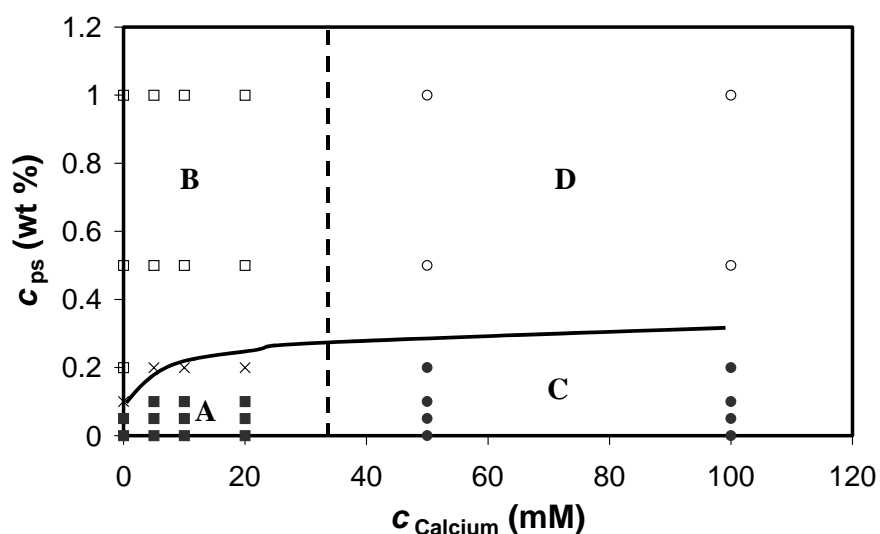


Fig. 3.7 Stability diagram of 10 wt % oil-in-water emulsions at varying concentrations of dextran and Ca^{2+} ions: \blacksquare , only creaming (type A); \times , transition between creaming and flocculation; \square , fast flocculation by dextran (type B); \bullet , slow flocculation induced by Ca^{2+} -ions (type C); \circ flocculation by a combination of mechanisms (type D). The drawn line indicates the estimated minimum polysaccharide concentration to induce flocculation. The dashed line indicates the estimated minimum concentration of Ca^{2+} ions for flocculation.

The four types of demixing behaviour at varying concentrations of dextran and Ca^{2+} ions are presented in the stability diagram of Fig. 3.7. The solid line indicates the transition from creaming to network formation due to depletion-flocculation. In the absence of Ca^{2+} ions, c_{pf} corresponds well with theory for spinodal demixing (eq. 3.2). This agreement between theory and experiment was observed earlier for different polysaccharides⁴ and for dextrans with different molecular weights (results not shown). However, c_{pf} was found to increase slightly with the Ca^{2+} concentration up to 20 mM Ca^{2+} ions. A lower value of c_{pf} was expected, because addition of Ca^{2+} ions decreases the range and strength of electrostatic repulsion. This effect was confirmed by measurement of c_{pf} as a function of NaCl concentration. These data are shown in Fig. 3.8, which shows that c_{pf} is lower at larger NaCl concentrations. The drawn and the dashed line in this figure denote the calculated spinodal demixing line for a varying potential and for a constant potential, respectively. For a constant ζ potential, we took -25 mV, which is the measured value at 0.1 M NaCl. For a varying ζ potential, we used the model described in the Appendix. Both

ways of incorporating the electrostatic interaction are in good agreement with our data between 0.01 and 0.1 M NaCl. This indicates that at these salt concentrations the range of the electrostatic repulsion (κ^{-1}) is more important for the position of the spinodal demixing boundary than the value of ψ_0 . Note that at NaCl concentrations below 0.01 M, depletion-flocculation is completely inhibited, even at very high dextran concentrations, because the electrostatic repulsion completely screens depletion attraction.

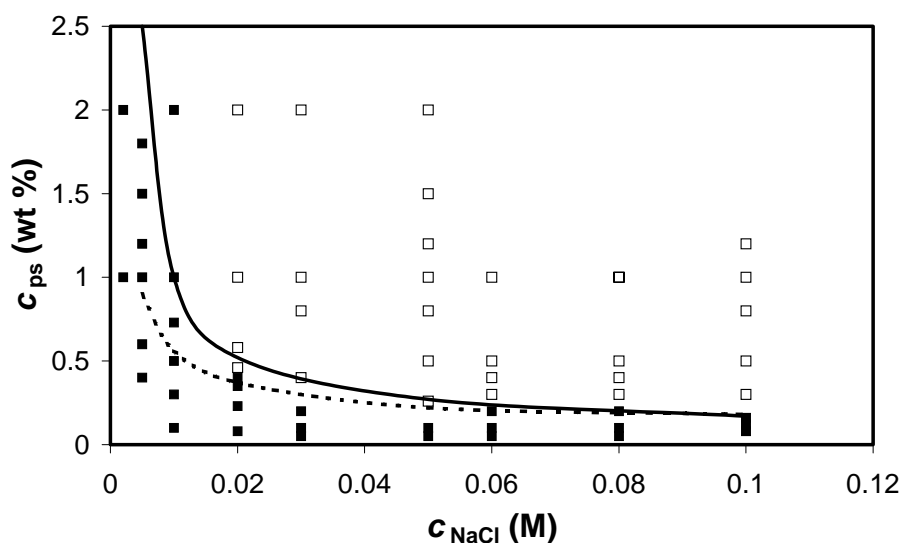


Fig. 3.8 Stability diagram of 10 wt % oil-in-water emulsions at varying concentrations of dextran and NaCl: ■, only creaming; □, fast flocculation by dextran. Calculated spinodal demixing lines: —, ζ depends on ionic strength (see Appendix); - - , ζ is constant (-25 mV).

An increase in c_{pf} , similar to that in Fig. 3.7 was observed earlier, if an excess amount of β -lg was present in the bulk. In that case the increase could be related to an increase in the low-shear viscosity in the bulk, affecting the interplay between flocculation and creaming kinetics.⁴ Perhaps Ca^{2+} ions have a similar effect on the viscosity which may be caused by a weak interaction between Ca^{2+} ions and the oppositely charged β -lg molecules in solution. A further study of this effect was however beyond the scope of the present work. Above 20 mM, the Ca^{2+} ions induce flocculation of emulsion droplets as indicated by the dashed line in Fig. 3.7. In region C this leads to accelerated creaming and in region D to retardation of the demixing process.

Another way to investigate the interaction between the emulsion droplets is by rheology. We performed dynamic rheological measurements on 30 wt % oil-in-water emulsions flocculated by 0.5 wt % dextran in the absence and presence of Ca^{2+} ions (Fig. 3.9). In the absence of Ca^{2+} ions, G' initially increased and levelled off after ~ 500 s. A sol–gel transition occurred within the first minute of the experiment, as indicated by the tangent of the loss angle ($\tan \delta = G''/G'$) becoming smaller than 1.²⁹ In the presence of 50 mM Ca^{2+} ions an initial increase of G' was observed as well, but here the increase continued during the whole experiment. After 30 min, G' was 1 order of magnitude higher than in the absence of Ca^{2+} ions. Also here we observed a sol–gel transition within 1 min, but $\tan \delta$ decreases to lower values than those in the absence of Ca^{2+} ions. This is indicative for a more elastic character of the system in the presence of Ca^{2+} ions at small deformations.

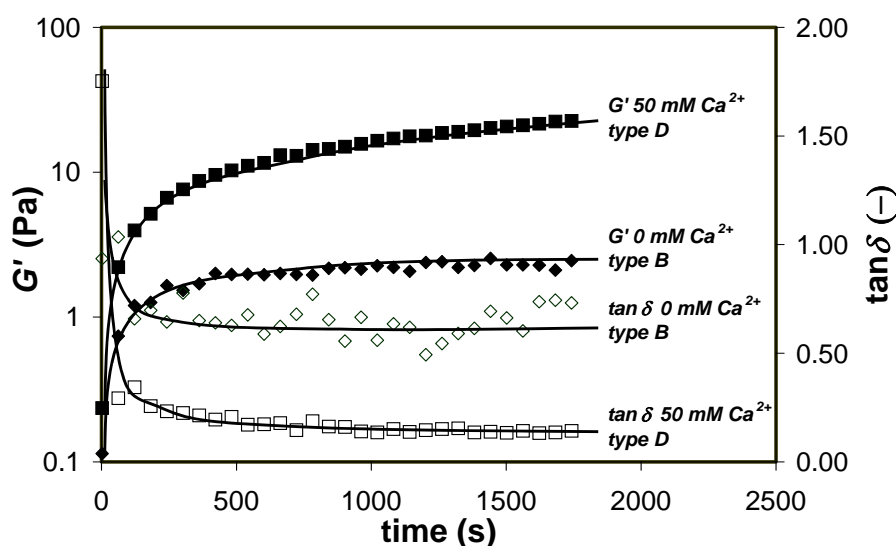


Fig. 3.9 G' and $\tan \delta$ as a function of time for 30 wt % oil-in-water emulsions flocculated by 0.5 wt % dextran in the absence and presence of 50 mM dextran. Lines are drawn to guide the eye.

The experimental results showed clear differences between emulsions containing dextran and Ca^{2+} ions in flocculation kinetics, floc morphology, and emulsion gel stiffness. On the basis of the results, we suggest a two-step process of emulsion gel formation. In the first step, fast depletion-flocculation accounts for network formation. In the second step, this network is slowly reinforced by a slow transition from weak depletion bonds to strong Ca^{2+} -intermediated protein-protein bonds. This reinforcement results into a stiffer and more elastic network.

3.6 Discussion

Here our hypothesis of a two-step process of emulsion gelation will be compared to model calculations. The pair potential curves between the emulsion droplets are given in Fig. 3.10 for various situations. At 0.1 M NaCl and in the absence of dextran and Ca^{2+} ions, electrostatic repulsion dominates close to $h = 0$ up to a few nanometers. According to eq. 3.2 this potential curve does not lead to flocculation, even though the interaction is slightly attractive at $h > 5$ nm. Addition of 1 wt % dextran leads to a decrease of the interaction energy minimum in the order of $10 k_B T$, and eq. 3.2 predicts spinodal demixing. Because the shallow minimum is not preceded by an energy maximum at larger h , the Fuchs factor will be close to 1 or actually somewhat smaller than 1 and fast flocculation will occur. At 1 wt % dextran, eq. 3.4 yields a value of τ_n of 20 s, assuming $D_f = 2.3$ which was experimentally found for other kinds of particle networks.² Due to the electrostatic energy barrier the equilibrium separation distance, h_{eq} , between two oil droplets will be close to the energy minimum of the interaction potential curve. According to the position of the energy minimum (Fig. 3.10A) a liquid layer of a few nanometers will remain between the emulsion droplets. Due to the presence of this layer, the bonds between the droplets in the flocs are flexible. Because of the relative shallow attractive energy well, the bonds can be disrupted by Brownian motion and gravity to be re-formed again between other droplets.³⁰ These rearrangements cause collapse of the emulsion network, which is observed as serum separation (Fig. 3.1B). A change in the molecular dimensions of the polysaccharide will lead to a change in the range of interaction, which is related to the radius of gyration of the polysaccharide. This effect is illustrated in Fig. 3.10A by the bold curves.

Addition of 50 mM Ca^{2+} ions to an emulsion stabilised by β -lg has two effects (Fig. 3.10B). The Debye length decreases from ~ 1 to ~ 0.5 nm leading to a substantial decrease in ζ and consequently a decrease in repulsion. In addition binding of one Ca^{2+} ion per molecule β -lg infers a small additional decrease in repulsion and an increased hydrophobicity of β -lg.^{16,17,31} Due to these factors, the energy barrier at short droplet separations is drastically lowered and formation of firm short-ranged bonds becomes possible, although its probability is low. This causes slow formation of small flocs, which cream separately.

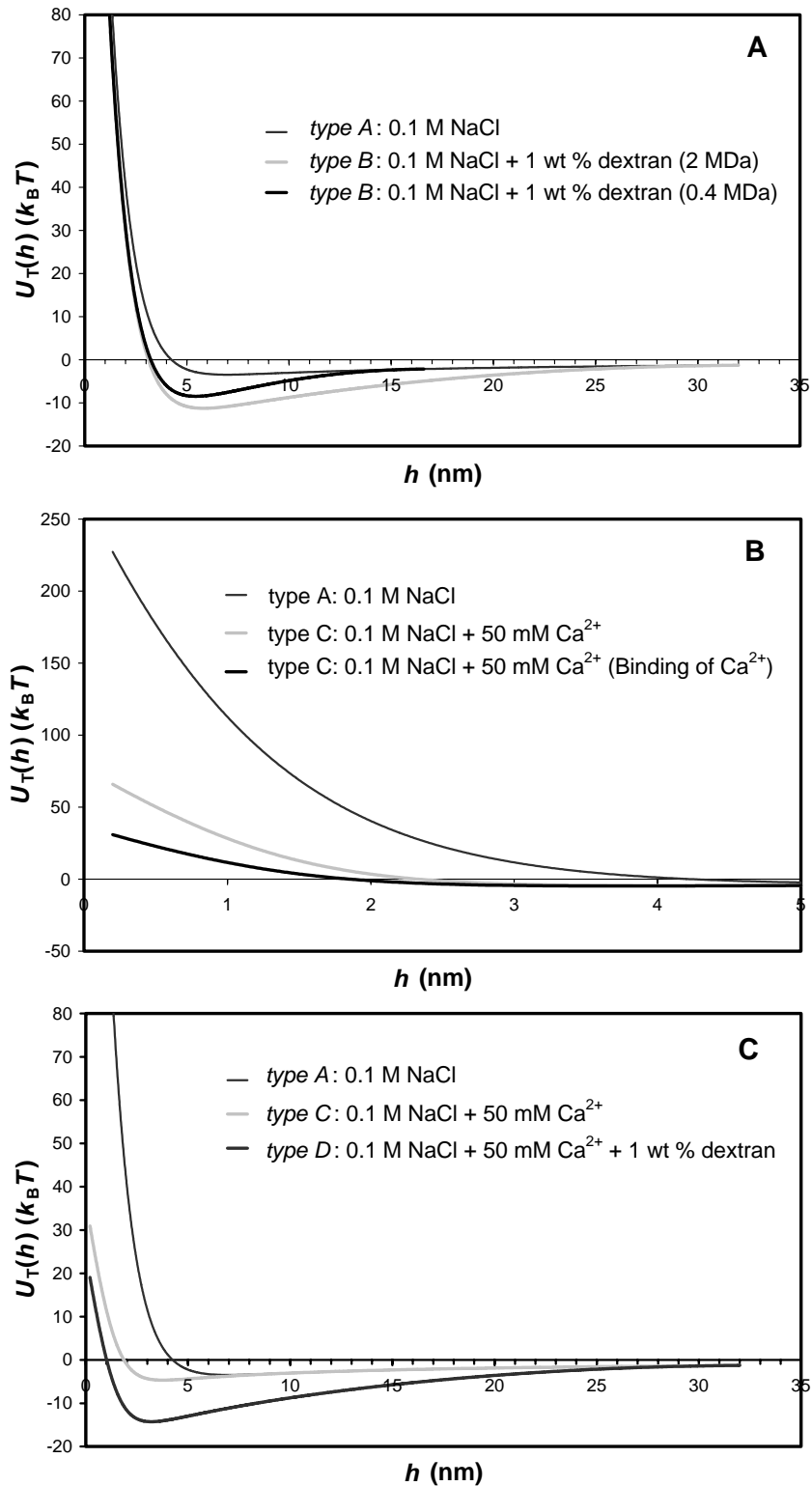


Fig. 3.10 Change of the interaction potential curves as a function of the distance h between two droplets surfaces on addition of **A**: 1 wt % dextran; **B**: 50 mM Ca^{2+} ; **C**: 1 wt % dextran + 50 mM Ca^{2+} . These plots are intended to show trends. Note that the scale of the horizontal axis varied between the panels.

When both dextran and Ca^{2+} ions are present in the system above their minimum concentrations, both changes in the potential curve occur (Fig. 3.10C). Again the depletion interaction will result in primary fast flocculation into the shallow energy minimum. A thinner aqueous layer between the emulsion droplets remains than in the absence of Ca^{2+} ions, which decreases the flexibility of the bonds. In addition, the decreased electrostatic repulsion allows a slow secondary process of reinforcement of droplet–droplet bonds, which decreases the probability of rupture of the bonds, and thus increases the network stiffness and strength. Accordingly, there is a lower probability for rearrangements, resulting in retardation of network collapse, which is in agreement with the experimental results (Fig. 3.6).

3.7 Conclusion

Flocculation and demixing of 10 wt % oil-in-water emulsions stabilised by β -lg were studied as a function of the concentrations of dextran, NaCl, and Ca^{2+} ions. Critical concentrations for flocculation were found for dextran and Ca^{2+} ions. The onset of depletion-flocculation was well predicted as function of the NaCl concentration via the total pair-potential between the oil droplets.

Depletion-flocculation leads to the formation of a network of emulsion droplets. The bonds between the droplets are formed by a weak long-range interaction, and as a consequence, the network quickly collapses due to gravity. Flocculation by Ca^{2+} ions proceeds much slower due to the presence of an electrostatic energy barrier, but the bonds are less flexible due to the higher strength and short range of the interactions. Because of the low flocculation rate, the flocs cream before they can form a network of emulsion droplets.

Combination of the two processes led to a two-step flocculation mechanism. First a weak network of emulsion droplets is formed by fast flocculation, and then the bonds between the droplets are slowly reinforced by Ca^{2+} -mediated protein–protein interactions. This two-step process was confirmed by the development of G' in time. As a consequence of this reinforcement of droplet-droplet bonds, rearrangements within the network are suppressed. This results into a retardation of network collapse and serum separation from the gelled emulsion.

These results show that mechanical properties and the stability against serum separation of flocculated colloidal systems against serum separation can be tuned by an appropriate combination of long-range and short-range interactions.

Acknowledgements

The authors thank Ab van der Linde and Fadel Aljawaheri for measuring the ζ -potential. Maarten Biesheuvel is acknowledged for useful discussions about electrostatic repulsive forces. Franklin Zoet is acknowledged for carrying out part of the experimental work.

Appendix

Electric double layer around protein stabilised emulsion droplets

In the calculation of the interaction potentials, we incorporate the measured ζ potential instead of the surface potential, ψ_0 . The ζ potential is located at a surface at a distance δ from the surface of charge, which is assumed to correspond to the outer surface of the adsorbed protein molecules. An estimate for the ζ potential can also be calculated from the charge density, σ , of the protein layer, which is related to the surface coverage and the number of elementary charges, z , per protein molecule. The charge of a β -lg molecule at pH 6.7 is mainly determined by seven free carboxyl groups of which the pK -value is between 4 and 4.5.³² The charge density is related to the surface potential, ψ_0 , by¹⁹

$$\sigma = \frac{z\Gamma_s F}{M \left(1 + 10^{(pK-pH)} \exp\left(-\frac{\psi_0 F}{RT}\right) \right)} \quad (\text{A1})$$

and

$$\sigma = \epsilon\kappa\psi_0. \quad (\text{A2})$$

Here Γ_s is the number of protein molecules per m^2 , F is Faraday's constant, R the gas constant, and T the absolute temperature. Finally, ζ is related to ψ_0 by $\zeta = \psi_0 \exp(-\delta\kappa)$.¹⁹ The measured value of ζ (-25 mV) is in good agreement with values reported by other

authors³³ and corresponds to ψ_0 when $\delta = 1.2$ nm. Eq. A1 and A2 were used to calculate the dependence of ζ on the ionic strength. The calculated values of ζ are used in eq. 2 to calculate the dependence of c_{pf} on the ionic strength and to calculate the interaction potential curves in parts B and C of Fig. 3.10.

References

- (1) Dickinson E. *Coll. Surf. B.* **2001**, *20*, 197-210.
- (2) Bremer L. G. B.; Bijsterbosch B. H.; Walstra P.; van Vliet T. *Adv. Coll. Int. Sci.* **1993**, *46*, 117-128.
- (3) Poon W. C. K.; Haw M. D. *Adv. Coll. Int. Sci.* **1997**, *73*, 71-126.
- (4) This thesis, chapter 2; Blijdenstein T. B. J.; van Vliet T.; van der Linden E.; van Aken G. A. *Food Hydrocolloids* **2003**, *17*, 661-669.
- (5) Berli C. L. A.; Quemada D.; Parker A. *Coll. Surf. A* **2003**, *215*, 201-204.
- (6) Tuinier R.; de Kruif C. G. *J. Coll. Int. Sci.* **1999**, *218*, 201-210.
- (7) Behrens S. H.; Borkovec M. *J. Coll. Int. Sci.* **2002**, *225*, 460-465.
- (8) Cao Y. H.; Dickinson E.; Wedlock D. J. *Food Hydrocolloids* **1990**, *4*, 185-195.
- (9) Demetriades K.; McClements D. J. *J. Agric. Food Chem.* **1998**, *46*, 3929-3935.
- (10) Manoj P.; Fillery-Travis A.; Watson A. D.; Hibberd D.; Robins M. M. *J. Coll. Int. Sci.* **1998**, *207*, 283-293.
- (11) Kulmyrzaev A.; Chanamai R.; McClements D. J. *Food Res. Int.* **2000**, *33*, 15-20.
- (12) Agboola S. A.; Dalgleish D. G. *J. Food Sci.* **1995**, *60*, 399-402.
- (13) Chen J.; Dickinson E.; Iveson G. *Food Structure* **1993**, *12*, 135-146.
- (14) Ye A.; Singh H. *Food Hydrocolloids* **2000**, *14*, 337-346.
- (15) Silvestre M. P. C.; Decker E. A.; McClements D. J. *Food Hydrocolloids* **1999**, *13*, 419-424.
- (16) Pappas C. P.; Rothwell J. *Food Chemistry* **1991**, *42*, 183-201.
- (17) Jeyarajah S.; Allen J. C. *J. Agric. Food Chem.* **1994**, *42*, 80-85.
- (18) Barteri M.; Gaudiano M. C.; Rotella S.; Benagiano G.; Pala A. *Biochim. Biophys. Acta* **2000**, *1479*, 255-264.
- (19) Hunter R. J. *Foundations of Colloid Science* **1987**, Oxford University Press, New York.
- (20) Vrij A. *Pure Appl. Chem.* **1976**, *48*, 471-483.
- (21) de Hek H.; Vrij A. *J. Coll. Int. Sci.* **1981**, *84*, 409-422.
- (22) von Smoluchowski M. *Z. Phys. Chem.* **1917**, *92*, 129-168.
- (23) Overbeek J.Th.G., in *Colloid Science I*, Kruyt H.R., Ed. Elsevier Publishing Company, Amsterdam **1952**; Chapter 7.
- (24) Bremer L. G. B.; Walstra P.; van Vliet T. *Coll. Surf. A* **1995**, *99*, 121-127.
- (25) de Jongh H. H. J.; Gröneveld T.; de Groot J. *J. Dairy Sci.* **2001**, *84*, 562-571.
- (26) Mengual O.; Meunier G.; Cayré I.; Puech K.; Snabre P. *Coll. Surf. A* **1999**, *152*, 111-123.

- (27) Weitz D.A.; Pine D. J., in *Dynamic Light Scattering*, Brown W., Ed. Clarendon Press, Cambridge **1993**; Chapter 16.
- (28) ten Grotenhuis E.; Paques M.; van Aken G. A. *J. Coll. Int. Sci.* **2000**, 227, 495-504.
- (29) Barnes H. A. and Walters K. *An Introduction to Rheology* **1989**, Elsevier, Amsterdam.
- (30) Bos M. T. A.; van Opheusden J. H. J. *Phys. Rev. E* **1996**, 53, 5044-5050.
- (31) Baomy J. J.; Brule G. *Le Lait* **1988**, 68, 33-48.
- (32) Walstra, P. *Physical Chemistry of Foods* **2003**, Marcel Dekker, Inc., New York.
- (33) Kulmyrzaev A.; Shubert H. *Food Hydrocolloids* **2004**, 18, 13-19.

4

Dextran-induced depletion-flocculation in oil-in-water emulsions in the presence of sucrose*

Abstract

The phase behaviour and mechanical properties of 10 wt % oil-in-water emulsions, stabilised by β -lactoglobulin (β -lg) and flocculated by the polysaccharide dextran were studied as a function of sucrose concentration. The sucrose concentration affected neither the polysaccharide concentration above which depletion-flocculation occurred, nor the elastic modulus and maximum linear strain of the emulsion gels formed. Furthermore, only a minor change in size of dextran molecules was measured over the range of sucrose concentrations studied. From this we deduce that the depletion potential between the oil droplets was not significantly affected by addition of sucrose. However, the sucrose concentration did affect the rate of macroscopic phase separation, which could be attributed to a larger viscosity and density of the aqueous phase. Thus, in unheated systems sucrose has a kinetic effect on serum separation in depletion-flocculated emulsions but no significant effect on droplet-droplet interactions.

4.1 Introduction

The stability against creaming and the texture of relatively dilute ($\phi < \phi_{\max}$) oil-in-water emulsions can be tuned in two general ways.¹ Firstly, the rheological properties of the aqueous phase can be changed, which affect the kinetics of flocculation and creaming of the oil droplets.² Secondly, the interaction forces between the emulsion droplets can be tuned, which determine whether the emulsion droplets flocculate or not.³ Oil-in-water emulsions for food applications often contain a combination of ingredients that may affect both rheological properties and droplet-droplet interactions at the same time.

Addition of polysaccharides that do not adsorb at the emulsion droplets, can induce a depletion interaction between the emulsion droplets and an increase in viscosity of the aqueous phase.⁴⁻⁶ Above a minimum polysaccharide concentration, the droplet-droplet interaction becomes sufficiently attractive to overcome the thermal entropy of the oil droplets, which leads to flocculation. If the flocculation rate is much greater than the creaming rate, the oil droplets can form a space-filling network,^{7,8} here denoted as an emulsion gel. However, emulsion gels formed by a depletion attraction often collapse under gravity, separating a substantial amount of serum due to rearrangements within the emulsion droplet network.^{9,10}

The presence of sugars, e.g. sucrose, can affect physico-chemical properties of proteins, emulsions and polysaccharides in various ways. Addition of sugars primarily leads to a viscosity increase, especially at high concentrations (> 30 wt %). Moreover, they affect the conformational stability of globular proteins¹¹ and the hydrophobic interactions between unfolded proteins. As a consequence, sugars affect heat-induced and cold gelation of milk proteins^{12,13} and pH-induced gelation of casein stabilised emulsion gels.¹⁴ Recently, Kim et al.¹⁵ observed a decrease in the extent of salt-induced flocculation of whey protein stabilised emulsions on addition of sucrose at temperatures below the protein denaturation temperature. This effect was attributed to the increased protein conformational stability. Above the denaturation temperature, droplet flocculation was promoted by sucrose due to increased hydrophobic interactions.

Sugars also affect the solvent quality of water for polysaccharides by enhancing hydrophobic interactions, which for example enables pectin to gel at low pH.¹⁶

Furthermore, the change in solvent quality may also lead to a change in the effective size of the molecular chains, which would in turn affect the range of the depletion potential.

In this paper, we discuss the effect of sucrose on the phase behaviour of depletion flocculated emulsion gels. A model emulsion, stabilised by bovine β -lactoglobulin (β -lg), was used and depletion-flocculation was induced by the polysaccharide dextran. To be able to separate the effects of sucrose on droplet interactions from its effects on the aqueous phase rheology, the effect of sucrose on the rheological properties of dextran solutions was determined separately.

4.2 Materials and methods

4.2.1 Materials

β -Lactoglobulin (92.5 wt %) was purified from bovine milk.¹⁷ Dextran (isolated from *Leuconostoc*; molecular weight, $M_w = 2 \times 10^6$ Da; radius of gyration, $r_g = 32$ nm, overlap concentration, $c^* = 1.4$ wt %) was obtained from Sigma Chemicals (St. Louis, USA). NaCl (p. a.) and thiomersal (97 %) were obtained from Merck (Shuchardt, Germany). Sucrose was obtained from BDH Chemicals (Poole, U.K.). Sunflower oil (Reddy, Vandemoortele, the Netherlands) was purchased from a local retailer.

4.2.2 Methods

A detailed description of the sample preparation, creaming measurements and diffusing wave spectroscopy has been given elsewhere.⁹ Briefly, all aqueous solutions were made at pH 6.7 and a NaCl concentration of 0.1 M. A 40 wt % oil-in-water emulsion was prepared by mixing the oil into a protein solution and homogenising the mixture by 10 passes through a lab-scale homogeniser (Delta instruments, Drachten, the Netherlands) at a pressure of 50 bar. This procedure yielded typical values of the Sauter droplet diameter, d_{32} , of 1 μ m at an overall protein content of 1 wt %.

Emulsion samples containing 10 wt % oil and various concentrations of protein and dextran were prepared by mixing various amounts of dextran solution, sucrose solution and salt solution with the stock emulsion. In this way the droplet size distribution and the NaCl concentration of the emulsions were the same in all samples. Mixing was performed by gentle shaking during 30 s. We note that flocs already started to form during shaking.

4.2.3 Demixing measurements

We measured the backscattering intensity of incident laser light along the height of an optical glass tube,¹⁸ using a Turbiscan MA 2000 apparatus (Ramonville St. Agne, France). Emulsion samples were put in the glass tubes using an automatic pipette and then stored at 25 °C. Subsequently, the backscattering profile was measured at selected times after putting the sample into the tube.

4.2.4 Diffusing wave spectroscopy (DWS)

DWS measurements were carried out in transmission^{19,20} using a He/Ne laser ($\lambda = 633$ nm) and a cuvette with an inner width, L , of 2.5 mm. The transport mean free path in the samples ranged from 100 μm in the absence of sucrose up to 500 μm at a sucrose concentration of 30 wt %. Intensity autocorrelation functions, $g_2(t)$, were measured at time intervals of 1 minute during 30 minutes. The characteristic decay time, $\tau_{1/2}$, defined as the time at which $g_2(t) - 1$ had decayed to half of its initial value, was determined from the autocorrelation functions.

4.2.5 Rheology

The apparent viscosity of dextran solutions was determined using an Ubbelohde viscometer. The densities of the solutions at varying dextran and sucrose concentrations, required to calculate the apparent viscosity, were determined by weighing 10 ml of each solution.

Steady and oscillatory shear measurements were carried out at controlled strain (-rate) at 25 °C using a Bohlin VOR Rheometer (Huntingdon, UK) equipped with a concentric cylinder geometry (C 25). A pre-shear treatment at 100 s^{-1} during 60 s was applied and 30 minutes after this treatment the storage modulus, G' , was determined in a dynamic experiment at a frequency of 1 Hz at increasing strain (strain-sweep experiment).

4.2.6 Emulsion washing

Some emulsions were washed to remove non-adsorbed protein from the aqueous phase. In this treatment, the emulsions were centrifuged at 10,000 g for 30 minutes. The aqueous phase was drained from the vessel while the dense creamed layer was gently lifted up. During this procedure the droplet size distribution of the emulsion remained constant. Subsequently the emulsion was redispersed in the required amount of 0.1 M NaCl solution. This procedure was repeated 3 times.

4.3 Results and discussion

4.3.1 Effect on flocculation threshold

The effect of sucrose on the total droplet-droplet interaction was studied firstly by determining the minimum polysaccharide concentration, c_{pf} , above which depletion-flocculation occurs. This minimum concentration was determined experimentally by preparing 10 wt % emulsion samples at different concentrations of sucrose and dextran and subsequently measuring their phase behaviour by turbidimetry. Below c_{pf} , the oil droplets creamed separately and formed a creamed layer on top of the sample. Above c_{pf} , fast flocculation caused network formation within approximately 20 s after sample preparation.²¹ Gravity-induced network contraction led to the appearance of a sharp phase boundary between an emulsion-rich and an emulsion-poor phase, which moved upward. In the stability diagram (Fig. 4.1) this process is denoted as serum separation.

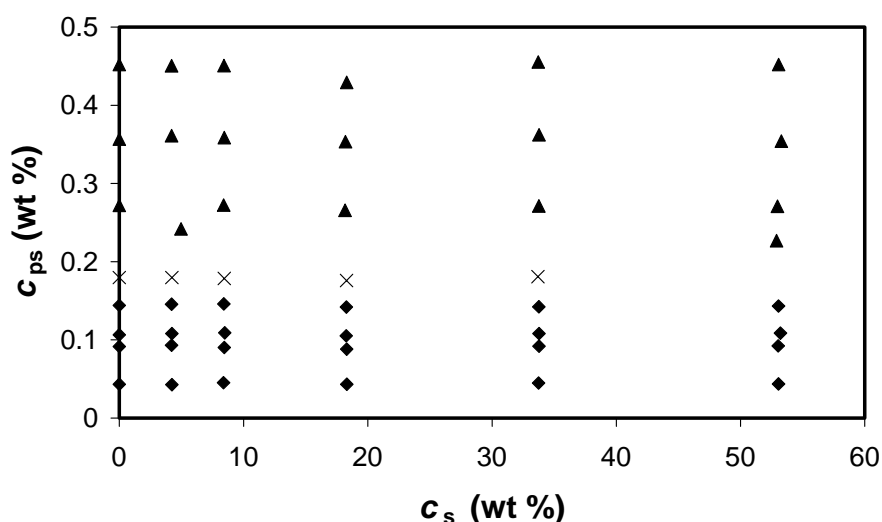


Fig. 4.1 Stability diagram of 10 wt % oil-in-water emulsions as a function of sucrose, c_s , and dextran, c_{ps} , concentration: ◆, non-flocculating emulsion (creaming only); ×, slightly flocculating emulsion (enhanced creaming); ▲, flocculated emulsion (serum separation).

At higher sucrose concentration, the turbidity of the emulsions was lower due to a decrease in the refractive index difference between the oil droplets and the aqueous phase. However, the turbidity remained sufficiently high to interpret the backscattering profiles.

From the stability diagram (Fig. 4.1), c_{pf} can be estimated to be ~ 0.2 wt % in the absence of sucrose. This value is in reasonable agreement with the theoretically predicted value of 0.17 wt %, calculated using a model of spinodal demixing, which is described in detail elsewhere.^{9,22} On increasing the sucrose concentration, no significant change in c_{pf} was found.

4.3.2 Effect on dextran rheology

Sucrose may affect the diameter of the dextran molecules by changing the solvent quality. To investigate this dependency, the relative viscosity, η_r , was determined for 0.56 and 1.1 wt % dextran dissolved in 0.1 M NaCl solutions at different sucrose concentrations. Results are plotted in Fig. 4.2.

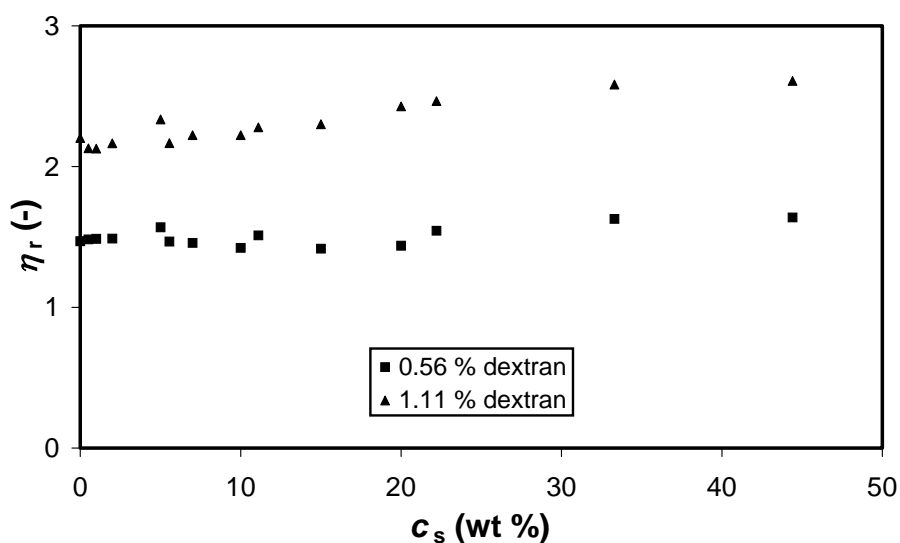


Fig. 4.2 Relative viscosity of 0.56 and 1.11 wt % dextran, dissolved in a solution of 0.1 M NaCl at different sucrose concentrations.

For both dextran concentrations, the variation between the data points showed no significant trend in the relative viscosity with the sucrose concentration. An estimate of the variation in the radius of the dextran molecules can be made using the Einstein relation ($\eta_r - 1) \sim r_g^3$. This yields a variation in radius of gyration of 32 ± 1 nm for the range of sucrose concentrations studied. Based on depletion theory, this variation in the radius of gyration

would correspond to a variation in theoretically predicted value for c_{pf} of 0.02 wt %. This is within the experimental error of the experimental observations in Fig. 4.1. Therefore we may conclude that addition of sucrose does not lead to a variation in the radius of the dextran molecules that is large enough to cause a significant change in c_{pf} .

4.3.3 Effect on flocculation kinetics

The effect of sucrose on the kinetics of dextran-induced flocculation was determined by monitoring the mobility of the oil droplets using DWS. We measured autocorrelation functions of 10 wt % oil-in-water emulsions at different sucrose concentrations, in the presence and absence of 1 wt % dextran. The extracted values of $\tau_{1/2}$ are a measure of the droplet mobility. At dextran concentrations below c^* , the viscosity increase due to dextran is negligible and therefore an increase in $\tau_{1/2}$ in time can be ascribed to dextran-induced flocculation.²⁰ However, the presence of sucrose complicates the situation because sucrose also leads to an increase in $\tau_{1/2}$ by itself. This increase is caused by a higher viscosity of the aqueous phase, reducing the mobility of the oil droplets. Moreover, the higher refractive index of the solution causes lower optical contrast of the droplets leading to a larger mean free path length, l^* , of the scattered light and an increase in $\tau_{1/2}$. We separated the increase in $\tau_{1/2}$ due to sucrose from the increase in $\tau_{1/2}$ due to dextran-induced flocculation by dividing $\tau_{1/2}$ -values measured in the presence of dextran, $\tau_{1/2}(t)$, by the corresponding values in the absence of dextran, $\tau_{1/2}(0)$, at the same sucrose concentration. Consequently, the resulting normalised decay times reflect a decrease in droplet mobility due to flocculation.

The results are plotted in Fig. 4.3. In all cases the normalised decay times that were recorded during the first minute after mixing were much greater than 1, indicating that flocculation largely occurs during mixing.²¹ The normalised decay times increased in time and levelled off after 20 min. The evolution of the normalised decay times did not significantly vary with the sucrose concentration up to 30 wt %.

These results indicate that sucrose caused no substantial changes in the flocculation kinetics after mixing of the samples, despite of a viscosity increase due to sucrose. A possible explanation for this is that the flocs are mainly formed during and shortly after mixing, where the flocculation process is mainly controlled by convection and therefore not strongly dependent on the viscosity. Altogether, DWS measurements showed that sucrose has no significant effect on the kinetics of flocculation and gel formation.

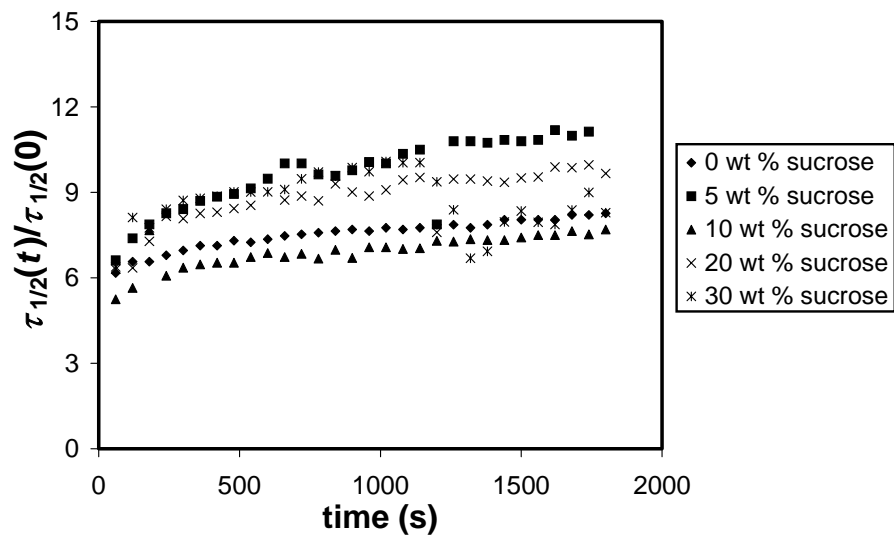


Fig. 4.3 Normalised decay times of autocorrelation functions as a function of time, measured in 10 wt % oil-in-water emulsions at 1 wt % dextran and different sucrose concentrations. The decay times $\tau_{1/2}(t)$ are normalised to the decay times of emulsions with corresponding sucrose concentrations in the absence of dextran $\tau_{1/2}(0)$.

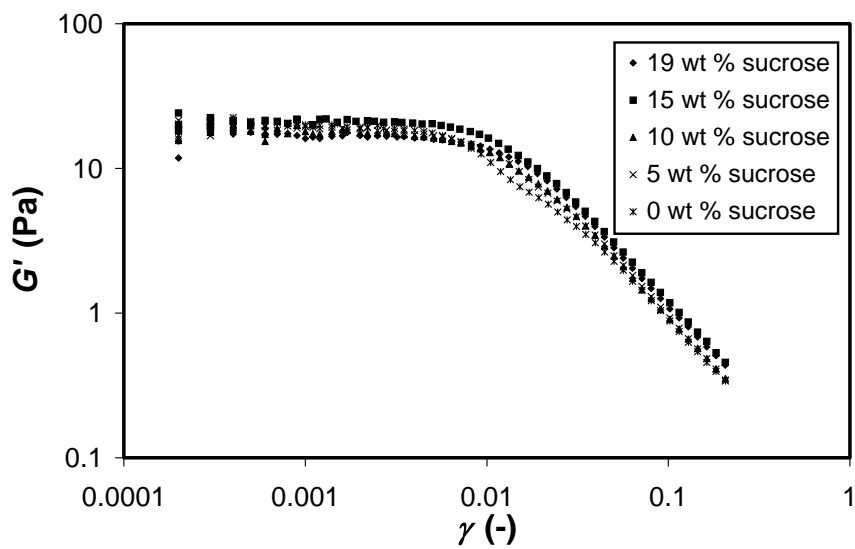


Fig. 4.4 Apparent elastic moduli as a function of shear strain amplitude, γ , for 30 wt % oil-in-water emulsions, containing 2 wt % dextran and different concentrations of sucrose.

4.3.4 Effect on emulsion gel rheology

The effect of sucrose on the visco-elastic properties of the emulsion gels was investigated by performing strain-sweep experiments on 30 wt % oil-in-water emulsions, containing 2 wt % dextran and different concentrations of sucrose. Fig. 4.4 shows that all systems had elastic moduli of about 20 Pa up to 19 wt % sucrose. The maximum linear strain did not depend on sucrose content. These two observations suggest that the strength of the interdroplet bonds was not significantly affected.

4.3.5 Effect of sucrose on droplet flocculation

The experimental results show that sucrose does not affect c_{pf} and the size of the dextran molecules. This demonstrates that the net interaction between the droplets, which in our systems is dominated by the long-range depletion interaction caused by the presence of dextran, is not significantly changed by sucrose.

Comparison between the experimental results by Kim et al.¹⁵ and ours shows that the effect of sucrose on flocculation of emulsions stabilised by β -lactoglobulin depends on the sensitivity to sucrose of the origin of the interaction that causes flocculation. Salt-induced flocculation in the absence of dextran is dominated by the relatively short-range van der Waals interaction between the droplets and molecular interactions between the adsorbed protein layers, which vary with the sucrose concentration. Dextran-induced flocculation is dominated by the long-range depletion potential, which is independent of the sucrose concentration. In the latter, the short-range interactions will only be important for the relatively slow enhancement of the firmness of the bonds between the droplets.²¹

4.3.6 Effect of sucrose on network contraction

At dextran concentrations above c_{pf} , contraction of the droplet network leads to the separation of serum from the emulsion phase. We determined the rate of serum separation by monitoring the position of the phase boundary in time. We defined $H_n(t)$ as the height, $H(t)$, of the contracting emulsion gel at time t , divided by the height of the network at time zero, H_0 . Fig. 4.5 shows the development of $H_n(t)$ for 10 wt % emulsions containing 1 wt % dextran in the aqueous phase. In the presence of 5-30 wt % sucrose, the rate of serum separation was slightly increased, leading to a somewhat lower value of H_n after 25 ks (see inset Fig. 4.5). Above 30 wt % sucrose, the rate of serum separation clearly decreased. The same trend was observed for 10 wt % emulsions containing 0.5 wt % of dextran and also

for 10 wt % emulsions that had been washed. By washing, unadsorbed protein was removed in order to eliminate the effect of protein present in the aqueous phase on the flocculation process.⁹

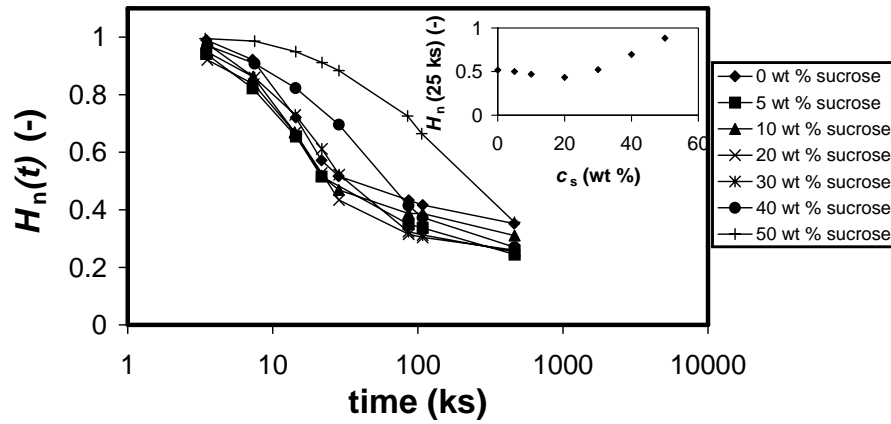


Fig. 4.5 $H_n(t)$ plotted against time on a logarithmic scale for a 10 wt % oil-in-water emulsion at 1 wt % dextran at different sucrose concentrations. $H_n(t)$ represents the height of the emulsion gel network at time t divided by the initial height of the emulsion H_0 . The inset shows H_n after 25 ks for different sucrose concentrations.

The trend observed in the initial rate of network contraction may in principle have two causes, namely a change in the properties of the aqueous phase and a change in structure of the emulsion gels. We separate these possibilities from each other by using the following simple model. Due to gravity, the network of flocculated emulsion droplets exerts a pressure P onto itself, which increases along the height of the sample. At the top of the sample this pressure is given by

$$P = \Delta\rho g \phi H_0. \quad (4.1)$$

Here $\Delta\rho$ is the density difference between the emulsion droplets and the aqueous phase, g is the acceleration due to gravity and ϕ is the volume fraction of the oil droplets. We assume that the network mainly contracts at the top of the sample, because there the pressure is highest. This was confirmed by measured creaming profiles.⁹ The initial rate of serum separation can now be modelled as the superficial velocity of water permeating through the gel column with height H_0 .^{10,23} The initial superficial velocity is given by Darcy's law

$$v_i = \frac{BP}{\eta H_0} = \left(\frac{dH(t)}{dt} \right)_{t=0}, \quad (4.2)$$

where B is the permeability constant, which describes the porosity of the network of the oil droplets, and η the viscosity of the aqueous phase. Combination of eqs. 4.1 and 4.2 yields

$$\frac{v_i}{\Delta\rho g \phi} = B \cdot \frac{1}{\eta}. \quad (4.3)$$

The initial velocity was determined from the slope of $H(t)$ versus t , during the first 2 ks of the experiment. Fig. 4.6 shows a plot of $v_i/(\Delta\rho g \phi)$ against $1/\eta$, for systems in which v_i , $\Delta\rho$ and η were varied by changing the sucrose concentration. This was done for two series of washed emulsions containing 0.5 wt % or 1 wt % dextran. The figure shows that $v_i/(\Delta\rho g \phi)$ is proportional to $1/\eta$ over the whole range of sucrose concentrations, which indicates that B is independent on the sucrose concentration. This suggests that the structure of the emulsion gel is not significantly affected by the sucrose concentration. Consequently, the change in initial rate of serum separation must be due to changes in viscosity and density of the aqueous phase.

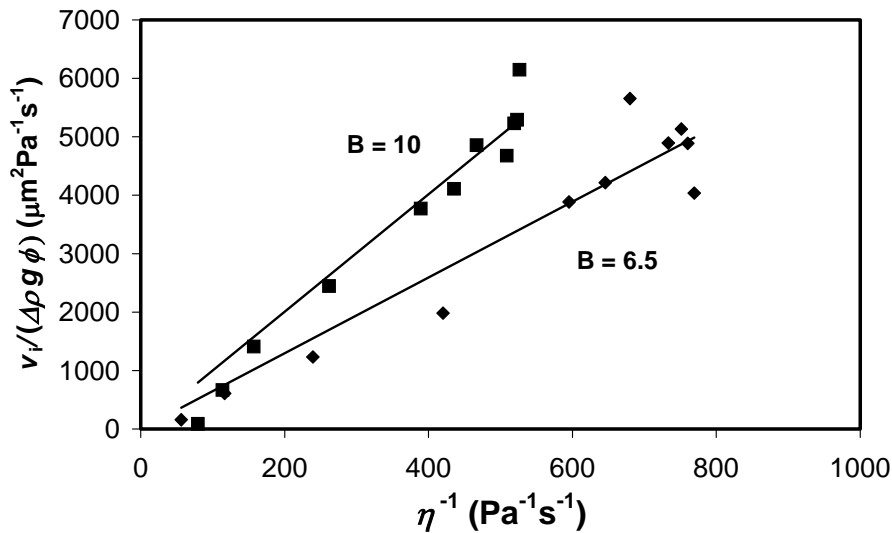


Fig. 4.6 Initial rate of network contraction divided by $\Delta\rho$, g and ϕ , plotted against $1/\eta$ for emulsions containing 0.5 (◆) and 1 (■) wt % dextran and different concentrations of sucrose. The drawn lines were obtained by linear regression.

4.3.7 Serum separation at high dextran concentrations

In general, the results indicate that at dextran concentrations up to 1.1 wt %, the effect of the sucrose concentration on phase behaviour and network contraction can be explained on the basis of the increase in the viscosity and density of the continuous phase. At dextran concentrations above 1.4 wt % the polymer chains start to overlap, which complicates the system considerably.

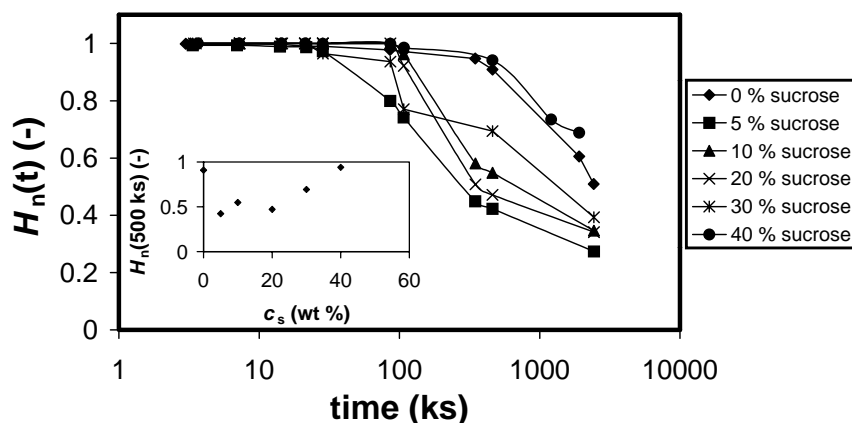


Fig. 4.7 $H_n(t)$ plotted against time on a logarithmic scale for a 10 wt % oil-in-water emulsion at 5 wt % dextran at different sucrose concentrations. $H_n(t)$ represents the height of the emulsion gel network at time t divided by the initial height of the emulsion H_0 . The inset shows H_n after 500 ks for different sucrose concentrations.

At 5 wt % dextran (Fig. 4.7), a delay time was observed during which no serum separation occurred. After this delay time, $H_n(t)$ varies with the sucrose concentration in a similar way as at low dextran concentrations (Fig. 4.5). However, an important difference with Fig. 4.5 is that $H_n(t)$ decreases very strongly between 0 and 5 wt % sucrose. The reason for this strong decrease is not yet clear and requires an additional study. However, we would like to make a few suggestions for this decrease. Firstly, at these dextran concentrations, the emulsion gel network is embedded in a network of entangled dextran molecules. The low-shear viscosity of this dextran network is partly responsible for the presence of a delay time²⁴ in addition to the mechanical properties of the emulsion gel network.^{10,25} Already at low concentration, sucrose may reduce the interactions between the chain elements, leading to a reduction in the low-shear viscosity of the dextran network and consequently a

large reduction in $H_n(t)$. Secondly, changes in viscosity of the continuous phase due to the presence of an entangled dextran network may influence the droplet aggregation process, leading to a more compact structure of the flocs of which the emulsion gel consists.²⁶ This would lead to a higher porosity of the emulsion gel, facilitating serum separation. Thirdly, gradual reinforcement of the droplet-droplet bonds during the delay time may play a role. This gradual reinforcement is caused by unfolding of adsorbed protein molecules, leading to a larger exposure of hydrophobic and free sulfhydryl groups,²⁷ which may lead to interdroplet disulphide bonds.²⁸ Although depletion-flocculated emulsion droplets remain separated by a few nanometer due to electrostatic repulsion, some disulphide bonds between the droplet surfaces may be formed at a slow rate. The presence of sucrose may inhibit unfolding of the adsorbed proteins.¹⁵ As a result slow formation of hydrophobic- and disulfide-bonds between the flocculated droplets during the delay time is inhibited, facilitating rearrangements within the droplet network and serum separation.

4.4 Conclusion

This paper shows the effects of sucrose on depletion-flocculation in oil-in-water emulsions, the resulting rheological properties of the emulsion gels and their phase behaviour. Below the overlap concentration of the dextran molecules, the minimum polysaccharide concentration for depletion-flocculation and the size of the polysaccharide molecules were unaffected by sucrose addition. Also the elastic modulus and the maximum linear strain of the emulsion gels were unaffected. Based on these results, we conclude that sucrose does not have a significant effect on the droplet-droplet interaction when this interaction is dominated by a depletion interaction caused by dextran. We also showed that changes in the kinetics of network contraction in the emulsion gels can be ascribed to changes in viscosity and density of the aqueous phase caused by sucrose.

Above the overlap concentration of the dextran molecules, a delay time is observed before serum separation starts to occur and the rate of serum separation depends in a more complicated way on the sucrose concentration.

These results show that at practically relevant concentrations of dextran, addition of sucrose above ~20 % stabilises an emulsion by reducing the rate of serum separation. This decrease is mainly due to an increase of the viscosity of the aqueous phase.

References

- (1) Robins M. M.; Watson A. D.; Wilde P. J. *Curr. Op. Coll. Int. Sci.* **2003**, *7*, 419-425.
- (2) Dickinson E. *Food Hydrocolloids* **2003**, *17*, 25-39.
- (3) Dickinson E. *Coll. Surf. B* **2001**, *20*, 197-210.
- (4) Cao Y. H.; Dickinson E.; Wedlock D. J. *Food Hydrocolloids* **1990**, *4*, 185-195.
- (5) Lekkerkerker H. N. W.; Poon W. C. K.; Pusey P. N.; Stroobants A.; Warren P. B. *Europhys. Lett.* **1992**, *20*, 559-564.
- (6) Vrij A. *Pure Appl. Chem.* **1976**, *48*, 471-483.
- (7) Bremer L. G. B.; Bijsterbosch B. H.; Walstra P.; van Vliet T. *Adv. Coll. Int. Sci.* **1993**, *46*, 117-128.
- (8) Poon W. C. K.; Haw M. D. *Adv. Coll. Int. Sci.* **1997**, *73*, 71-126.
- (9) This thesis, chapter 2: Blijdenstein T. B. J.; van Vliet T.; van der Linden E.; van Aken G. A. *Food Hydrocolloids* **2003**, *17*, 661-669.
- (10) Manoj P.; Fillery-Travis A.; Watson A. D.; Hibberd D.; Robins M. M. *J. Coll. Int. Sci.* **1998**, *207*, 283-293.
- (11) Semenova M. G.; Antipova A. S.; Belyakova L. E. *Curr. Op. Coll. Int. Sci.* **2002**, *7*, 438-444.
- (12) Kulmyrzaev A.; Bryant C.; McClements D. J. *J. Agric. Food Chem.* **2000**, *48*, 1593-1597.
- (13) Kulmyrzaev A.; Cancelliere C.; McClements D. J. *J. Sci. Food Agr.* **2000**, *80*, 1314-1318.
- (14) Dickinson E.; Merino L. M. *Food Hydrocolloids* **2002**, *16*, 321-331.
- (15) Kim H.-J.; Decker E. A.; McClements D. J. *J. Agric. Food Chem.* **2003**, *51*, 766-772.
- (16) Oakenfull D.; Scott A. *J. Food Sci.* **1984**, *49*, 1093-1098.
- (17) de Jongh H. H. J.; Gröneveld T.; de Groot J. *J. Dairy Sci.* **2001**, *84*, 562-571.
- (18) Mengual O.; Meunier G.; Cayré I.; Puech K.; Snabre P. *Coll. Surf. A* **1999**, *152*, 111-123.
- (19) Weitz D.A.; Pine D. J., in *Dynamic Light Scattering*, Brown W., Ed. Clarendon Press, Cambridge **1993**; Chapter 16.
- (20) ten Grotenhuis E.; Paques M.; van Aken G. A. *J. Coll. Int. Sci.* **2000**, *227*, 495-504.
- (21) This thesis, chapter 3: Blijdenstein T. B. J.; Hendriks W. P. G.; van der Linden E.; van Vliet T.; van Aken G. A. *Langmuir* **2003**, *19*, 6657-6663.
- (22) de Hek H.; Vrij A. *J. Coll. Int. Sci.* **1981**, *84*, 409-422.
- (23) van Vliet T and Walstra P. *Food Colloids* Bee R. D., Richmond P., and Mingins J. Eds, The Royal Society of Chemistry, Cambridge **1989**, 206-217.
- (24) Vélez G.; Fernández M. A.; Muñoz J.; Williams P. A.; English R. J. *J. Agric. Food Chem.* **2003**, *51*, 265-269.
- (25) Parker A.; Gunning P. A.; Kim Ng.; Robins M. M. *Food Hydrocolloids* **1995**, *9*, 333-342.
- (26) Yan Y. D.; Burns J. L.; Jameson G. J.; Biggs S. *J. Coll. Int. Sci.* **2002**, *255*, 91-97.
- (27) Kim H.-J.; Decker E. A.; McClements D. J. *Langmuir* **2002**, *18*, 7577-7583.
- (28) Monahan F. J.; McClements D. J.; Kinsella J. E. *J. Agric. Food Chem.* **1993**, *41*, 1826-1829.

5

Serum separation and rheology of depletion- and bridging-flocculated emulsions: A comparison*

Abstract

Stability against demixing, rheology and microstructure of emulsions that were flocculated by depletion or bridging were compared. Flocculation by depletion and bridging was induced by addition of the polysaccharide carboxy-methylcellulose (CMC) to emulsions that were stabilised by β -lactoglobulin (β -lg) at pH 6.7 and 3.0 respectively. Depletion-flocculated emulsions generally have a lower initial demixing rate than bridging-flocculated emulsions, but after long times they are compressed to a higher oil content by gravity. Differences in the initial demixing rate are shown to be caused by differences in porosity between the gels. In bridging-flocculated emulsions, large irreversible flocs are formed by flow during mixing, resulting in larger permeability than in depletion-flocculated emulsions. Rheological measurements showed that bridging-flocculated emulsions can withstand larger stresses than depletion-flocculated emulsions. Greater network strength and a lower probability of rearrangements explain why bridging flocculation systems can retain more water at longer times.

5.1 Introduction

Polymer molecules such as polysaccharides can be used to control the mechanical properties and stability of oil-in-water emulsions against demixing. In addition to increasing the viscosity or gelling of the aqueous phase, polysaccharides can induce flocculation of emulsion droplets.¹ When flocculation of the droplets proceeds faster than creaming due to gravity, it leads to the formation of a network of oil droplets and the system is denoted as an emulsion gel.²⁻⁴ These emulsion gels are sensitive to gravity-induced network breakdown, which leads to serum separation.^{5,6} Serum separation limits the shelf-life of emulsions and hence control of this process is desirable.

The stability of the emulsion droplet network against gravitational stress is related to its microstructure, which is in turn dependent on the type of droplet-droplet interaction.^{7,8} Generally, two types of polysaccharide-induced droplet-droplet interactions are distinguished, i.e. depletion- and bridging-flocculation.¹ Which of these two mechanisms prevails, depends on the interaction between the polysaccharide and the emulsion droplet surface.

The focus of the present paper is to show that the two flocculation mechanisms lead to different mechanical properties and different rates and amounts of serum separation. To this end, a model system was used in which the type of flocculation mechanism could be tuned by changing the pH. This system consisted of an oil-in-water emulsion, stabilised by an adsorbed layer of β -lactoglobulin, which has an iso-electric point (IEP) of 5.2.⁹ Flocculation was induced by addition of the polysaccharide carboxy-methylcellulose (CMC). Above the IEP (pH = 6.0 or 6.7), both β -lg and CMC are negatively charged causing an electrostatic protein-polysaccharide repulsion, which leads to depletion-flocculation above a minimum CMC concentration. Below the IEP (pH 3.0), β -lg and CMC are oppositely charged, causing an electrostatic protein-polysaccharide attraction that leads to bridging-flocculation within a concentration range of CMC.

Differences in phase behaviour and serum separation will be discussed in terms of differences in droplet-droplet bond strength, microstructure and network rheology. In addition, attention will be paid to the importance of sample preparation.

5.2 Background

5.2.1 Flocculation mechanisms

If a polysaccharide does not bind to the droplet surface, depletion of polysaccharide from a region around the emulsion droplets induces droplet-droplet attraction (Fig. 5.1A).¹⁰⁻¹² The attractive energy is determined by the polysaccharide concentration and can amount to a few $k_B T$ in the energy minimum. The range of the interaction is determined by the radius of gyration of the polysaccharide molecule. Because of this, bonds formed by depletion are weak, reversible and flexible.

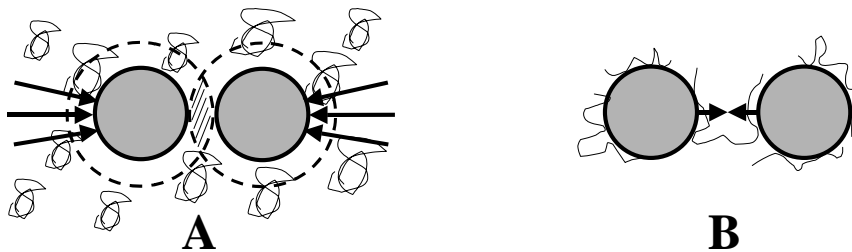


Fig. 5.1 Sketches of the mechanisms of **A**: depletion- and **B**: bridging-flocculation.

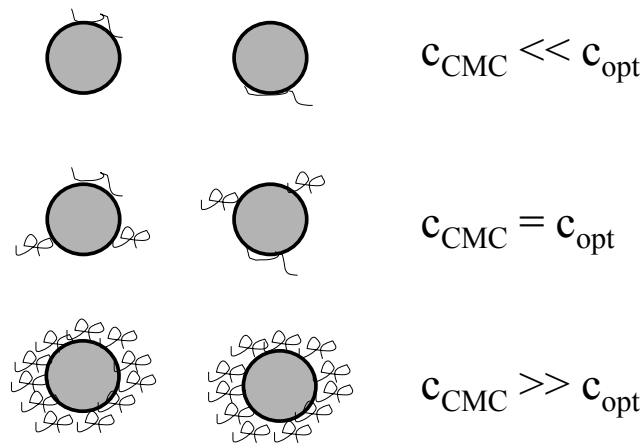


Fig. 5.2 Sketch of the bridging mechanism as a function of c_{CMC} .

When a single polysaccharide molecule adsorbs on two or more emulsion droplets, the droplets are interconnected by a polysaccharide bridge (Fig. 5.1B). According to Healy and La Mer,¹³ the optimum polysaccharide concentration for bridging-flocculation is the concentration at which half of the droplet interface is covered with polysaccharide (Fig. 5.2). The attraction is determined by the interaction between the polysaccharide and the

droplet surface, which is often of electrostatic origin and on the order of hundreds of $k_B T$. Hence, bonds formed by bridging are relatively strong and irreversible. Moreover, bonds are inflexible compared to depletion bonds, because of the polysaccharide link between two interfaces.

Bridging-flocculation has been shown to occur for e.g. protein-stabilised emulsions containing the polysaccharide carrageenan.^{14,15} Corresponding with the bridging concept,¹³ the degree of flocculation, and the gel modulus both went through a maximum as a function of the polysaccharide concentration.

5.2.2 Emulsion gel formation and stability

In this section, a theoretical framework is described that will be used to qualitatively interpret the experimental data on emulsion demixing. Three types of demixing can be distinguished by their demixing profile, which was determined by measuring the turbidity as a function of the height of the emulsion (Fig. 5.3).^{2,10} Demixing type A denotes creaming of single droplets, type B refers to gravity-induced collapse of an emulsion gel and type C denotes accelerated creaming of small discrete flocs.

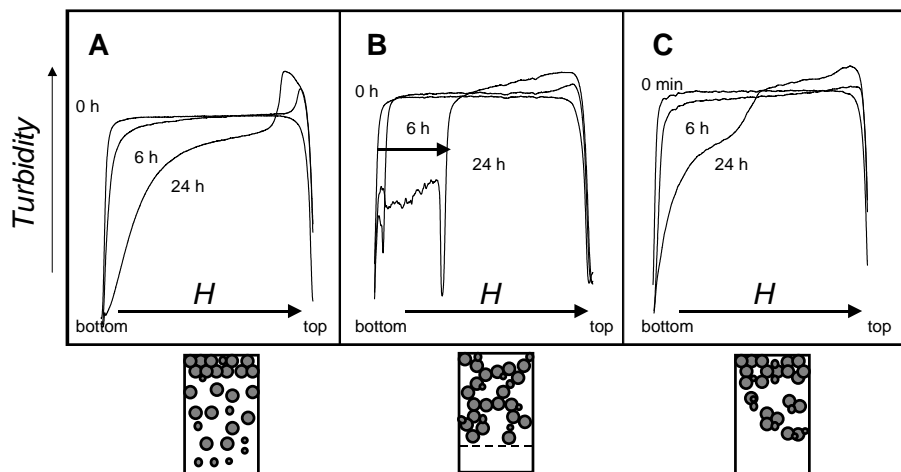


Fig. 5.3 Creaming profiles of three main types of demixing as determined by scanning the backscattering intensity as a function of height: **A**: creaming of single droplets; **B**: phase separation: contraction of emulsion gel; **C**: creaming of small aggregates and consolidation of creamed layer.

In the case of type B, flocculation proceeds fast and already occurs during mixing of the polysaccharide solution and the emulsion. After mixing, an emulsion gel consisting of a network of emulsion droplets is formed rapidly. The pressure, P , exerted on the emulsion

droplet network due to the density difference between the oil droplets and the aqueous phase is given by $P = \Delta\rho g H_0 \phi$,⁶ where $\Delta\rho$ is the density difference between oil and the aqueous phase, g the acceleration due to gravity, H_0 the initial height of the emulsion gel and ϕ the volume fraction of oil. As a consequence of this pressure difference, the phase boundary starts moving as denoted by the arrow in Fig. 5.3 with an initial rate, $(dH/dt)_{t=0}$, which is abbreviated by v_i . We use $h_n(t)$ for the height, $H(t)$, of the collapsing emulsion gel network at time t divided by the total height of the emulsion, H_0 .

The rate at which the network collapses is determined by its elasticity upon compression and its permeability. Shortly after mixing, the droplet network has not significantly been deformed and does not provide an elastic counter pressure yet and the rate of collapse under gravity is mainly determined by the permeability of the network. Under these conditions, the velocity can then be described by d'Arcy's law which reads $v_i = BP(\eta H_0)^{-1}$, where B is the permeability coefficient, and η the viscosity of the aqueous phase.

At longer times, when gel deformation becomes significant, the mechanical properties of the emulsion gel also start to play a role⁶. Generally, when P is larger than σ_{\max} , the maximum stress the emulsion gel network can withstand, the emulsion gel will start to rearrange and collapses (Fig. 5.4)⁵. When P is smaller than σ_{\max} , the network will respond by increasing elastic resistance with increasing compression. The boundary between the two regions where either elastic compression or network collapse occurs is situated around the height in the gel column, H_B , where $\sigma_{\max} = P$.

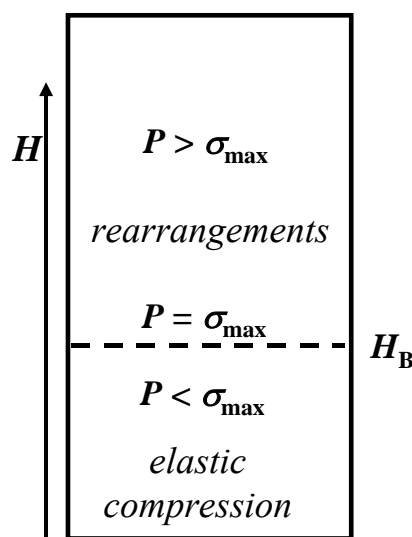


Fig. 5.4 Sketch of the force acting on an emulsion gel column and the resulting mechanisms of network contraction.

An indication of σ_{\max} can be obtained from dynamic rheological measurements under shear deformation. For uniaxial compression, where the volume decrease of the emulsion gel is proportional to the degree of collapse, the compression modulus, E , is related to the elastic shear modulus, G' , by $E = 2G'$.¹⁶ Similarly, σ_{\max} can be approximated using $\sigma_{\text{lin}} = 2G' \gamma_{\text{lin}}$, where γ_{lin} and σ_{lin} are the maximum linear strain and stress respectively, assuming that the system behaves linearly up to fracture.

Finally, we calculate the final average oil content in the contracted emulsion gels by using $\phi(t) = \phi_0 H_0 / H(t)$.

5.3 Experimental

5.3.1 Materials and sample preparation

Materials

β -Lactoglobulin (protein content 92.5 wt %) was purified from bovine milk.¹⁷ Carboxymethylcellulose, Blanose 7HOF, was obtained from Hercules (Zwijndrecht, The Netherlands). NaCl (p. a.) and thiomersal (97 wt %) were obtained from Merck (Schuchardt, Germany). Sunflower oil (Reddy, Vandemoortele, the Netherlands) was purchased from a local retailer. 1-bromohexadecane and 1-bromo-octane were obtained from Fluka Chemika (Buchs, Switzerland).

Sample preparation

Solutions of β -lg or CMC were prepared by adding the dry matter to the required amount of salt solution (0.1 M NaCl), followed by gently stirring overnight, avoiding incorporation of air bubbles. Thiomersal (0.02 wt %) was added to inhibit microbial growth. The pH was set at 6.7 using 1 M HCl or NaOH.

Stock emulsions contained 1 wt % β -lg and 40 wt % sunflower oil or a mixture of 1-bromohexadecane and 1-bromo-octane. Emulsions were prepared by mixing oil into a β -lg solution using an Ultra Turrax (Polytron, Switzerland). Subsequently, this pre-emulsion was homogenised by 10 passes through a lab-scale homogeniser (Delta Instruments, Drachten, the Netherlands) operating at a pressure of 50 bar. Stock emulsions had typical d_{32} -values of 1.2 μm as determined from laser diffraction (see section 5.3.2).

Emulsion samples containing various amounts of oil and CMC at pH 6.7 were prepared by adding the stock emulsion to the required amounts of CMC solution and salt solution. In this way the droplet size distribution and the NaCl concentration of the emulsions were kept constant in all samples. Emulsion samples at pH 6.0 and 3.0 were prepared in a similar way after separately lowering the pH of the stock emulsion, CMC solution and salt solution with 1 M HCl. The droplet size distribution of the emulsion was unaffected by the pH decrease.

All samples were mixed by gently shaking until the sample appeared homogeneous to the unaided eye (~30 s). All experiments were carried out at 25 °C.

Characterisation of CMC

The molecular conformation of CMC was determined at pH 6.7 and 3.0 by using size-exclusion chromatography combined with multiple-angle laser-light-scattering (SEC-MALLS). CMC was dissolved in 0.08 M NaNO₃ to which phosphate buffer was added. the pH was adjusted to 6.7 or 3.0 and the total ionic strength was 0.1 M. Measurements yielded distributions of molecular mass, M_w , and radius of gyration, r_g . In addition, r_g is plotted against M_w on a double logarithmic scale. The slope, ν , of this line is a measure of the conformation of the molecule. Weight averages of M_w and r_g , the overlap concentration, c^* , and ν are given in Table 5.1 for pH 6.7 and pH 3.0. At pH 3.0, which is near the pK of CMC, larger values of M_w and r_g were obtained indicating slight aggregation of the polysaccharide, probably due to the lower charge density. The overlap concentration is only slightly affected by this aggregation and ν is approximately 0.3, indicating a compact spherical conformation and a slight degree of branching.¹⁸

Table 5.1 Molecular dimensions of CMC at pH 6.7 and 3.0 as obtained from SEC-MALLS characterisation. M_w is the weight averaged molecular weight, r_g the radius of gyration, c^* the overlap concentration and ν describes the dependence $r_g \sim M_w^\nu$.

pH	M_w (MDa)	r_g (nm)	c^* (mg/l)	ν
6.7	2.00 +/- 0.02	128.5 +/- 0.3	243 +/- 0.2	0.28
3.0	5.43 +/- 0.16	185.6 +/- 1.1	219 +/- 3	0.28

5.3.2 Flocculation experiments

Demixing and flocculation

Demixing of emulsions was followed by turbidimetry as described previously,^{2,10} using a Turbiscan MA 2000 apparatus (Ramonville St. Agne, France). The initial height of the emulsions samples was 43 +/- 1 mm. The state of flocculation of emulsion samples was investigated by light microscopy using an Axioscope (Carl Zeiss instruments, Oberkochen, Germany). Samples containing 10 wt % oil were diluted ten times without changing the pH and ionic strength. The apparent size distribution of the emulsion samples was determined using a laser diffraction apparatus (Coulter LS 230, Miami, USA). The circuit of the apparatus was filled with tap water or, when specified, with a 0.1 M salt solution at a set pH. A few droplets of the emulsion samples, which had aged for 24 hours, were diluted into this circuit and consequently two measurements of 90 seconds were carried out.

Diffusing wave spectroscopy (DWS)

DWS measurements were carried out in a transmission geometry^{19,20} using a He/Ne laser ($\lambda = 633$ nm) and a beam expander. The laser illuminated about 1 cm² of the sample that was contained in a sample cell with an inner width, L , of 1.2 mm. The transport mean free path, l^* , of the samples was typically 100 μ m. The decay time, $\tau_{1/2}$, was extracted as described before.² Measurements were carried out during 30 minutes at intervals of one minute.

5.3.3 Rheology

Dynamic measurements were carried out using a Bohlin VOR rheometer (Huntingdon, U.K.). A concentric cylinder geometry (C 25) with a gap of 2.5 mm and a 1-g torsion bar were used. At the start of each measurement the samples were sheared at a rate of 10² s⁻¹. After this pre-shear treatment, the emulsion was left to gel for 30 minutes at subsequently G' was determined as a function of strain amplitude (strain sweep experiment).

5.4 Results and discussion

5.4.1 Flocculation experiments

Emulsion demixing

Demixing of emulsion samples with various CMC-concentrations, c_{CMC} , at pH 6.7 or pH 3.0 was investigated by turbidimetry and the state of flocculation was observed microscopically. The results are presented in the stability diagram of Fig. 5.5. In the absence of CMC, demixing proceeded according to type A (see section 5.2.2) at all pH values. This indicates that oil droplets creamed separately and no flocculation occurred, which was confirmed by the microscopic observations (Image in Fig. 5.5).

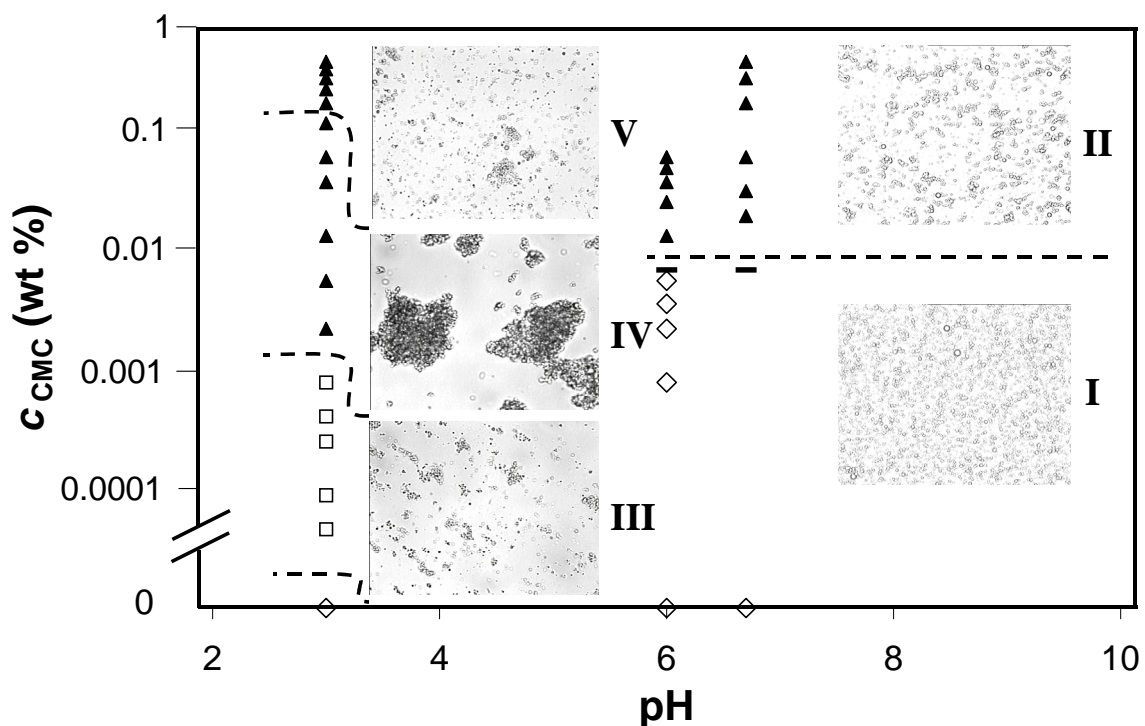


Fig. 5.5 Stability diagram of 10 wt % oil-in-water emulsions at pH 6.7 and pH 3.0. \diamond : type A; —: transition between type A and B; \blacktriangle : type B; \square : type C. Images of emulsions in different stability regions (image size: 100 x 80 μm) are included in the diagram. Image I represents emulsions in the absence of CMC, irrespective of pH; Image II represents depletion-flocculated emulsion droplets at pH 6.0 and 6.7; Images III - V represent the regions within the dashed lines at pH 3.0.

At pH 6.0 and 6.7, emulsions flocculate by depletion above 0.008 wt % CMC. This is shown in Fig. 5.5 by a transition from demixing type A to type B. Microscopic images I and II show a transition from discrete emulsion droplets to small rearranging flocs. Additionally, particle size measurements were performed (Fig. 5.6). At pH 6.7, the apparent d_{32} was similar to that of the stock emulsion for all CMC-concentrations. Apparently, the flocs formed above 0.008 wt % CMC had disintegrated into discrete emulsion droplets, showing that flocculation was reversible upon dilution. The minimum polysaccharide concentration, c_{pf} , for the occurrence of flocculation was calculated using a model for spinodal demixing.¹⁰ This yielded a value of c_{pf} of 5×10^{-3} wt %, which is in satisfactory agreement with the experimental value of 8×10^{-3} wt %. We conclude that at pH 6.0 and 6.7, droplets flocculated by means of the depletion mechanism.

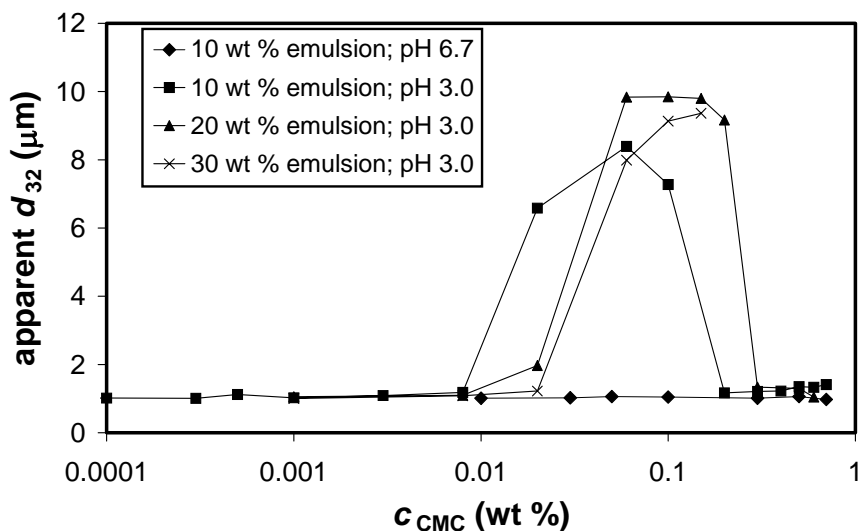


Fig. 5.6 Apparent d_{32} for pH 3 and 6.7, measured directly after dilution. At pH 3.0, d_{32} is given for 10, 20 and 30 wt % oil-in-water emulsion.

At pH 3.0, demixing type C is observed upon addition of 10^{-5} - 10^{-3} wt % CMC. Here, small flocs were observed microscopically (image III), which creamed rapidly. Between 10^{-3} and 10^{-1} wt % CMC, the flocs that are observed microscopically (image IV) at pH 3.0 are much larger than those at pH 6.0 and 6.7. This observation in diluted emulsions shows that bonds are irreversible upon dilution. The emulsions separate a clear serum and this behaviour can be classified as demixing type B. Above 10^{-1} wt % CMC, the microscopic image V shows smaller flocs but demixing still proceeds according to type B, although some emulsion droplets remained in the serum layer. This suggests that the flocculation process has

become less effective at higher CMC-concentrations. Fig. 5.6 shows a maximum in apparent d_{32} as a function of c_{CMC} at the three oil concentrations studied at pH 3.0. Moreover, the CMC-concentration at which this optimum was found was proportional to the oil concentration. For all oil concentrations, the optimum value of c_{CMC} corresponded to an interfacial coverage of approximately 1 mg/m^2 . This observation is in agreement with values found by others for bridging-flocculated suspensions²¹ or emulsions.^{14,15} Based on the concentration dependence of flocculation and the irreversible character of the flocs we conclude that at pH 3.0 flocculation mainly proceeds by the bridging mechanism.

At even larger c_{CMC} at pH 3.0, the apparent d_{32} decreased to the original droplet diameter, but demixing still occurs according to type B indicating the presence of a droplet network. At these concentrations, bridging is suppressed (Fig. 5.2) but the excess of non-adsorbed CMC-molecules induces depletion-flocculation.²¹

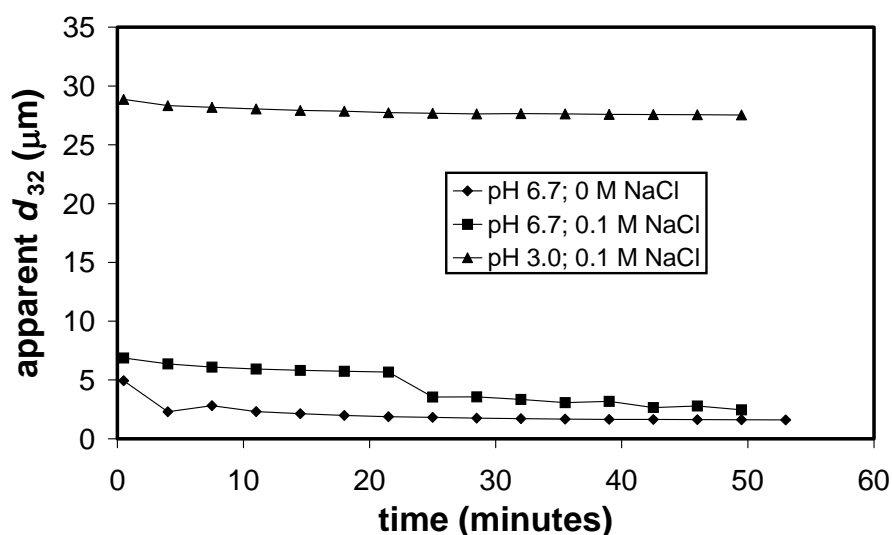


Fig. 5.7 Apparent d_{32} as a function of time after dilution of an emulsion made at pH 3.0 at different pH and salt concentration in the vessel of the Coulter Laser.

Cause of bridging interaction

We investigated the cause of bridging interaction by diluting a few drops of bridging-flocculated samples in solutions with different pH and ionic strength in the circuit of the Coulter Laser. The apparent d_{32} was monitored during 30 minutes after dilution (Fig. 5.7). When the sample was diluted at pH 3.0 with 0.1 M NaCl, the apparent d_{32} remains $30 \mu\text{m}$, which is comparable to the floc size observed microscopically. When diluted at pH 6.7,

the apparent d_{32} decreased instantly and continued to decrease slightly in time, indicating that flocs slowly disintegrate when diluted at pH 6.7. This decrease was stronger when no salt was added. In addition, it was observed that complex coacervates were formed in mixed solutions of β -lg and CMC at pH 3.0 (data not shown), but not at pH 6.7. These observations suggest that the occurrence of bridging is mainly caused by electrostatic protein-polysaccharide interactions.

Flocculation kinetics

Information on the flocculation kinetics of 20 wt % emulsions at pH 3.0 was obtained from the evolution of decay times, measured by DWS. All measured autocorrelation functions showed a single decay and the extracted values of $\tau_{1/2}$ are plotted in Fig. 5.8. On addition of CMC, the decay times measured during the first minute were already much larger than in the absence of CMC. Apparently, flocculation has already occurred during mixing and during the first minute of recording. This feature is similar to that observed for depletion flocculated emulsions² and indicates that the flocculation process is fast, i.e. controlled by the rate of droplet encounter.

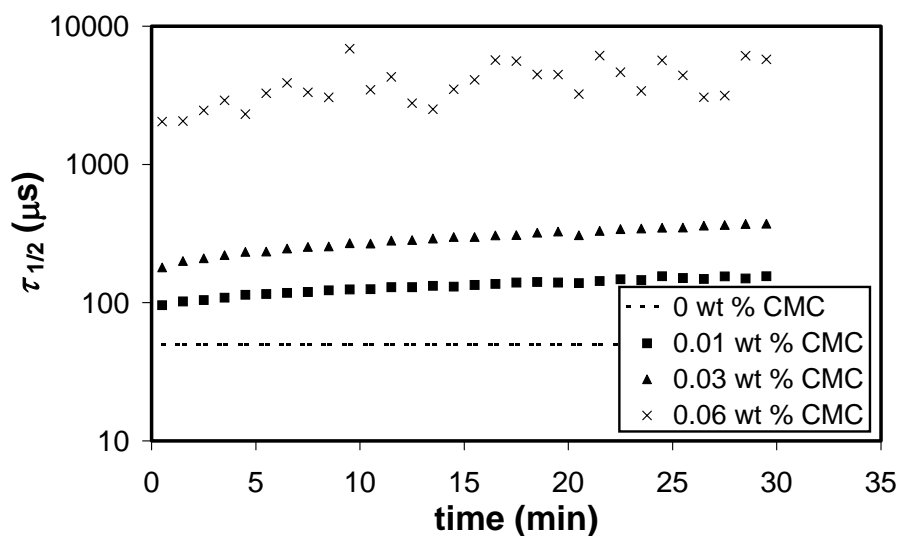


Fig. 5.8 Decay times of autocorrelation functions of 20 % oil-in-water emulsions at pH 3.0 containing different amounts of CMC. Measurements were carried out during 30 minutes after mixing.

5.4.2 Network contraction

Collapse of the emulsion gel networks was monitored for emulsions gelled by depletion or by bridging (resp. at pH 6.7 or 3.0). The initial rate of network contraction, v_i , and the relative network height after 150 hours, $h_n(150)$, were extracted from the data. Figs. 5.9 and 5.10 show v_i and $h_n(150)$ for both mechanisms as a function of c_{CMC} . For emulsions gelled by depletion, a decrease in v_i with c_{CMC} is observed. The latter has been previously observed by other researchers for polymer-induced depletion-flocculation^{11,22-24} and can be explained by two factors. Firstly, the viscosity of the aqueous phase increases and, secondly, the attraction caused by depletion increases with increasing c_{CMC} . Respectively, these factors retard the flow of liquid through the network and reinforce the droplet-droplet bonds, which decreases the rate and probability for rearrangements. As a consequence, no substantial difference in $h_n(150)$ was found up to 0.1 wt % CMC. Above this concentration, $h_n(150)$ strongly increases and approaches unity, which indicates that no contraction occurs during the experiment. This result corresponds to the presence of a delay time²³ larger than 150 hours.

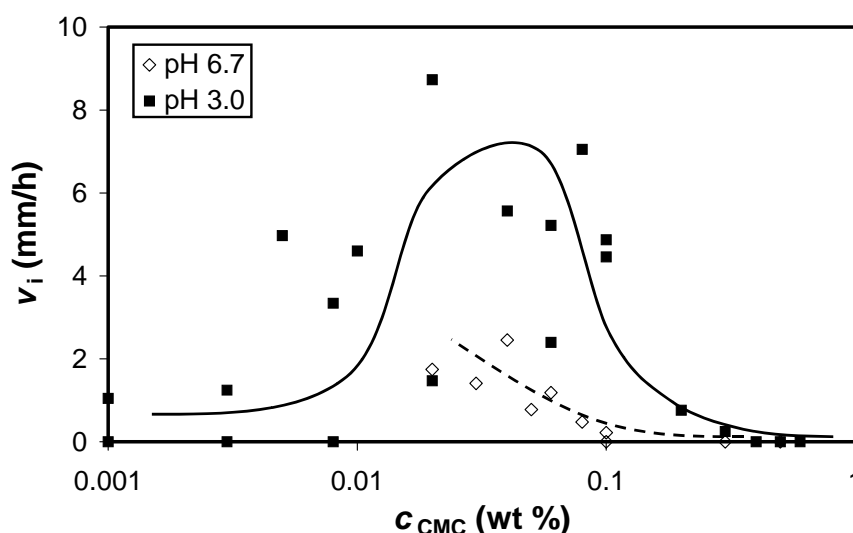


Fig. 5.9 Initial network contraction velocity, v_i , for 10 wt % oil-in-water emulsions at pH 3.0 and pH 6.7 as a function of c_{CMC} . The drawn and the dashed line provide a guide to the eye.

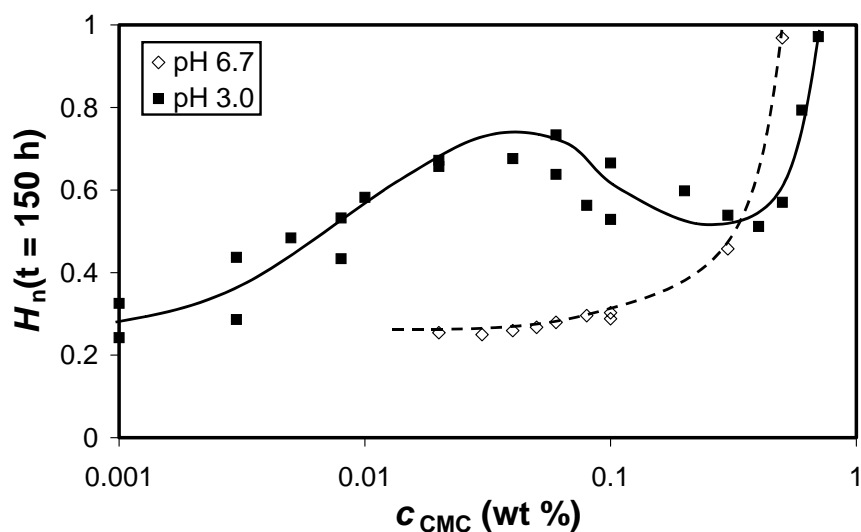


Fig. 5.10 Relative network height after 150 hours, $H_n(150)$, for 10 wt % oil-in-water emulsions at pH 3.0 and pH 6.7 as a function of c_{CMC} . The drawn and the dashed line provide a guide to the eye.

For emulsions gelled by bridging, a maximum in v_i can be observed as a function of c_{CMC} and the values of v_i are generally larger than for depletion flocculated emulsion gels. We note that substantial scatter of the data points can be observed, indicating that the formation of microstructure of the emulsion gels is not very reproducible. The values of $h_n(150)$ increase with c_{CMC} , reaching a maximum around the optimum flocculation condition of 0.06 wt % CMC. Above this concentration $h_n(150)$ decreases due to a decreased effectivity of bridging. Above 0.3 wt % CMC, a steep increase in $h_n(150)$ is found, similar to that observed at pH 6.7. Similar results were found at 5, 20 and 30 wt % oil (results not shown). The larger values of v_i and $h_n(150)$ for bridging flocculated emulsions are probably related to the higher strength and lower flexibility of bridging-flocculated emulsion droplets compared to depletion-flocculated droplets.

5.4.3 Rheology

Rheological measurements were performed to obtain more information on the network strength. The elastic modulus, G' , was determined as a function of the strain amplitude, γ , for 20 wt % density matched oil-in-water emulsions that contained 0.12 wt % CMC. Results are plotted in Fig. 5.11. The depletion-flocculated emulsion shows a gradual decrease in G' with strain applied, which is consistent with literature data on depletion

flocculated emulsions.^{25,26} For the bridging-flocculated system, a higher storage modulus was measured. The modulus is constant up to $\gamma = 0.02$ and shows a sudden decrease at larger γ . This sudden decrease is indicative for microscopic fracture of the emulsion gel. Apart from a larger storage modulus, bridging flocculated systems have a smaller value of $\tan\delta$ ($= G''/G'$), indicating a more elastic behaviour at small deformations. The maximum linear strain, γ_{\max} , was defined at the strain amplitude where the measured elastic modulus had decreased to 95 % of the low strain value. A summary of the data extracted from the rheological measurements is shown in Table 5.2.

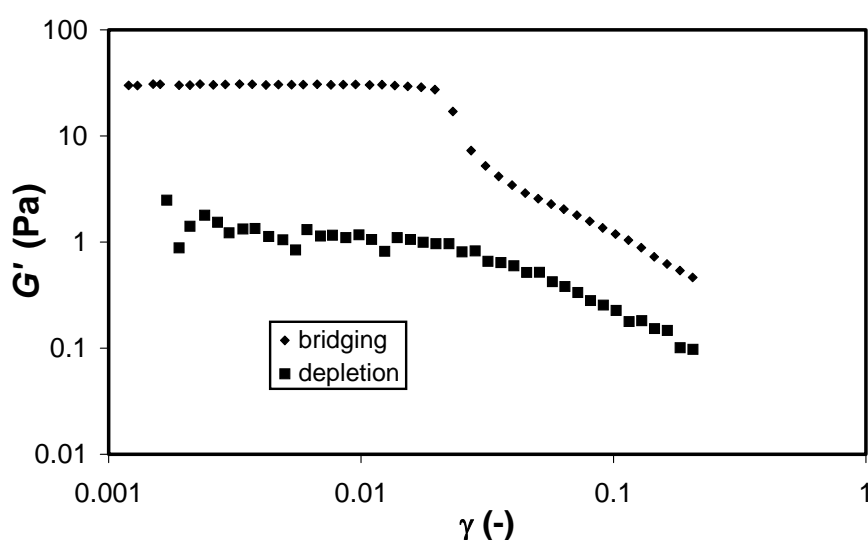


Fig. 5.11 G' as a function of strain amplitude for 20 wt % oil-in-water emulsions, containing 0.12 wt % CMC at pH 6.7 and pH 3.0.

Table 5.2 Rheological data of a bridging- and a depletion-flocculated emulsion: 20 wt % oil, 0.12 wt % CMC. H_B is the height of the region in which linear deformation occurs. For the calculation of H_B we used $\Delta\rho = 80 \text{ kg}\cdot\text{m}^{-3}$ and $g = 9.81 \text{ m}\cdot\text{s}^{-2}$.

pH	G' (Pa)	$\tan\delta$ (-)	γ_{lin} (-)	σ_{lin} (Pa)	H_B (mm)
6.7	1.2	0.29	0.0077	0.019	0.12
3.0	30	0.09	0.017	1.1	6.7

5.4.4 Discussion

Results showed that the initial rate of network collapse is smaller for depletion-flocculated emulsion gels than for bridging-flocculated ones (Fig. 5.9). This result can be understood on the basis of the microstructure of the systems. Microscopic images of bridging-flocculated emulsions have shown that flocs were large and had a heterogeneous and compact structure upon dilution (Fig. 5.5). Because flocculation already occurs during mixing, the structure of the flocs and the resulting droplet network are influenced by the flow during mixing. The droplet-droplet bonds formed are firm and irreversible and as a consequence, the flocs formed by bridging grow up to a range of relatively large sizes during mixing, whereas flocs formed by weak depletion forces can be broken down to smaller sizes or even single droplets.²⁷ The range of cluster sizes in bridging-flocculated emulsions implies larger but less reproducible permeability and initial demixing velocity compared to depletion flocculated emulsions.

The final height, $h_n(150)$, of the contracted emulsion gels was about 0.25 for depletion-flocculated emulsion gels (Fig. 5.10). This corresponds to a volume fraction of droplets of about 0.4. This value is the same when the emulsions demix by creaming only, but it is smaller than the maximum packing fraction of spherical particles ($\phi_m = 0.6-0.7$). This shows that the droplets pack at a somewhat lower volume fraction than expected, which is probably due to gradual formation of stronger surface bonds between the droplets. Moreover, it shows that the emulsion gels that were formed at moderate c_{CMC} contract up to equilibrium within 150 hours. Apparently, collapse of the droplet network mainly proceeds by rearrangements within the droplet network. According to the model presented in section 5.2.2 and the values given in Table 5.2, H_B (see Fig. 5.4) is negligible compared to H_0 . This confirms that the network is too weak to withstand the gravitational stress and collapses by rearrangements.

For bridging-flocculated emulsion gels, values of $h_n(150)$ are in general substantially higher up to 0.7, which corresponds with $\phi(150) = 0.14$ (Fig. 5.10). This indicates that the network rearranges to a limited extent only. For bridging-flocculated emulsions, H_B is smaller but significant compared to H_0 (Table 5.2), indicating that a significant part of the network offers elastic resistance against the compressive force (Fig. 5.4). Nevertheless, in the major part of the gel P would be larger than σ_{in} , implying that gravity-induced rearrangements are possible. Based on the strain dependence of G' , the system would

break in the region above H_B , leading to an inhomogeneous structure of large fragments. Consequently, rearrangements will mainly occur between and not within the fragments, implying a low probability for rearrangements. Moreover, the pores between the fragments become smaller upon rearrangements, which ultimately stops serum separation.

Based on the model and our experimental results, we propose that more water can be retained in bridging-flocculated emulsions, because of the elastic resistance against compression and a lower probability of rearrangements within the flocs. More detailed information on the microstructure of flocculated emulsions will be provided in a forthcoming publication.²⁸

5.5 Conclusion

The process of serum separation and rheology clearly differ between emulsions gelled by depletion- and bridging-flocculation. In depletion flocculated emulsions, the initial velocity of serum separation due to network contraction is generally low, but the system can rearrange up to a random closed packing ($\phi \approx 0.45$) of the oil droplets. In bridging-flocculated emulsions, the initial rate of serum separation is larger, but more serum is retained at longer times.

It was argued that a difference in initial serum separation was caused by a difference in microstructure, which was determined by flow during mixing of the emulsion samples. In bridging-flocculated emulsions, flow leads to an inhomogeneous structure of large flocs and large channels, leading to a high initial permeability.

Differences in the final amount of serum separated could be partly attributed to the rheological parameters of the emulsion gels. Emulsions gelled by bridging are stronger than those gelled by depletion and offer more resistance against gravity-induced collapse.

This work has shown that different types of droplet-droplet interaction affect the microstructure formed during mixing, leading to differences in demixing behaviour. Apparently, flow is an important parameter to control the stability and mechanical properties of emulsion gels and more research on this is recommended.

Acknowledgements

The authors thank Kees Olieman and Roelie Holleman for SEC-MALLS characterisation of CMC.

References

- (1) Dickinson E. *Food Hydrocolloids* **2003**, *17*, 25-39.
- (2) This thesis, chapter 3: Blijdenstein T. B. J.; Hendriks W. P. G.; van der Linden E.; van Vliet T.; van Aken G. A. *Langmuir* **2003**, *19*, 6657-6663.
- (3) Bremer L. G. B.; Bijsterbosch B. H.; Walstra P.; van Vliet T. *Adv. Coll. Int. Sci.* **1993**, *46*, 117-128.
- (4) Poon W. C. K.; Haw M. D. *Adv. Coll. Int. Sci.* **1997**, *73*, 71-126.
- (5) Buscall R.; White L. R. *Journal of the Chemical Society Faraday Transactions. I. Physical Chemistry* **1987**, *83*, 873-891.
- (6) van Vliet T and Walstra P. *Food Colloids* Bee R. D.; Richmond P.; and Mingins J. Eds, The Royal Society of Chemistry, Cambridge **1989**, 206-217.
- (7) Biggs S.; Habgood M.; Jameson G. J.; Yan Y. *Chem. Eng. J.* **2000**, *80*, 13-22.
- (8) Yan Y. D.; Burns J. L.; Jameson G. J.; Biggs S. *Chem. Eng. J.* **2000**, *80*, 23-30.
- (9) McKenzie H. A. *Milk proteins: chemistry and molecular biology* **1971**, Academic Press, London.
- (10) This thesis, chapter 2: Blijdenstein T. B. J.; van Vliet T.; van der Linden E.; van Aken G. A. *Food Hydrocolloids* **2003**, *17*, 661-669.
- (11) Cao Y. H.; Dickinson E.; Wedlock D. J. *Food Hydrocolloids* **1990**, *4*, 185-195.
- (12) Vrij A. *Pure Appl. Chem.* **1976**, *48*, 471-483.
- (13) Healy T.; La Mer V. K. *J. Coll. Sci.* **1964**, *19*, 323-332.
- (14) Dickinson E.; Pawlowsky K. *J. Agric. Food Chem.* **1997**, *45*, 3799-3806.
- (15) Dickinson E.; Pawlowsky K. *Food Hydrocolloids* **1998**, *12*, 417-423.
- (16) Whorlow R. W. *Rheological Techniques* **1980**, Ellis Horwood, Chichester.
- (17) de Jongh H. H. J.; Gröneveld T.; de Groot J. *J. Dairy Sci.* **2001**, *84*, 562-571.
- (18) Lloyd L.L.; Kennedy J. F.; Knill C. J., in *Light Scattering: Principles and Development*, Brown W., Ed. Clarendon Press, Oxford **1996**; Chapter 15.
- (19) Weitz D.A.; Pine D. J., in *Dynamic Light Scattering*, Brown W., Ed. Clarendon Press, Cambridge **1993**; Chapter 16.
- (20) ten Grotenhuis E.; Paques M.; van Aken G. A. *J. Coll. Int. Sci.* **2000**, *227*, 495-504.
- (21) Furusawa K.; Ueda M.; Nashima T. *Coll. Surf. A* **1999**, *153*, 575-581.
- (22) Demetriades K.; McClements D. J. *J. Agric. Food Chem.* **1998**, *46*, 3929-3935.
- (23) Manoj P.; Fillery-Travis A.; Watson A. D.; Hibberd D.; Robins M. M. *J. Coll. Int. Sci.* **1998**, *207*, 283-293.
- (24) Tuinier R.; de Kruif C. G. *J. Coll. Int. Sci.* **1999**, *218*, 201-210.
- (25) Moates G. K.; Watson A. D.; Robins M. M. *Coll. Surf. A* **2001**, *190*, 167-178.
- (26) Blijdenstein T. B. J.; Nicolas Y.; van der Linden E.; van Vliet T.; Paques M.; van Aken G. A., Knaebel A.; and Munch J. P. *Proceedings of the 3rd international symposium on food rheology and structure* Fischer, P., Marti, I., and Windhab, E. Eds, ETH, Zürich **2003**, 343-346.
- (27) Gregory J. *Coll. Surf.* **1988**, *31*, 231-253.
- (28) This thesis, chapter 6: Blijdenstein T. B. J.; van der Linden E.; van Vliet T.; van Aken G. A. **2003** in *preparation*.

6

Scaling behaviour of delayed demixing, rheology and microstructure of emulsions flocculated by depletion and bridging*

Abstract

This paper describes an experimental comparison of microstructure, rheology and demixing of bridging- and depletion-flocculated oil-in-water emulsions.

The elasticity of flocculated emulsions versus the emulsion volume fraction showed scaling behaviour with exponents of 2 and 5 for depletion- and bridging-flocculated emulsions, respectively. These exponents reflect a difference in bond type between the depletion- and the bridging mechanism. Depletion-flocculated emulsions exhibited a critical volume fraction for percolation in contrast to bridging-flocculated emulsions.

CSLM-imaging showed that bridging-flocculated emulsions were heterogeneous over larger length scales than depletion-flocculated emulsions. As a consequence, G' as determined from DWS corresponded well with G' as measured macroscopically for the depletion-flocculated emulsions, but this correspondence was not found for the bridging-flocculated emulsions. The heterogeneity of bridging-flocculated emulsions was confirmed by DWS-echo-measurements, indicating that their structure breaks up into large fragments upon oscillatory shear deformation larger than 1 %.

Gravity-induced demixing occurred in both emulsions, but the demixing processes differed. After preparation of bridging-flocculated emulsions, serum immediately started separating, whereas depletion-flocculated systems at polysaccharide concentrations in the overlap regime usually showed a delay time before demixing. The delay time was found to scale with the network permeability, B , the viscosity, η , of the aqueous phase and the density-difference between oil and water, $\Delta\rho$, as $t_{\text{delay}} \sim B^{-1} \cdot \eta \cdot \Delta\rho^{-1}$. The results are in line with the mechanism proposed by Starrs et al.,¹ where erosion of the droplet network leads to widening of the channels within the droplet networks, enhancing drainage of liquid.

*Article in preparation.

6.1 Introduction

Mechanical properties and stability against gravity-induced demixing are important parameters for practical applications of oil-in-water emulsions. Polysaccharides are often used to control these parameters, e.g. by inducing flocculation, which leads to the formation of a network of oil droplets.²⁻¹¹ A challenging scientific problem is to obtain control over demixing kinetics and mechanical properties. To this end, we studied the microscopic dynamics of the droplet networks.

The rheological properties of an emulsion gel are primarily determined by their volume fraction and the main type of interaction between the emulsion droplets. The two main types of polysaccharide-induced interaction types are depletion¹² and bridging.¹³ In case of non-adsorbing polysaccharides, depletion of polysaccharide from a region around the oil droplets induces a weak attraction, leading to reversible and flexible droplet-droplet bonds. In case of strong adsorption of the polysaccharide onto the oil droplet surface, individual polysaccharide molecules can adsorb on different droplets. This leads to strong and inflexible polymer bridges between the droplets. Additionally, the rheological properties depend on the microstructure of a flocculated emulsion, which is determined by the interplay between the droplet interactions and the preparation conditions of emulsions.^{11,14,15}

In case of emulsion gels, gravity-induced demixing proceeds by compression of the droplet network, which leads to separation of serum liquid. Therefore, the mechanism of network compression is related to rheological properties of the network, such as the yield stress.^{16,17} If the gravitational stress is smaller than the yield stress, the elasticity of the network can prevent substantial compression, whereas in the opposite case, the network collapses via rearrangements. In addition, the rate of serum separation is related to the pore size of the network.^{11,18} In depletion-flocculated emulsions, demixing is often preceded by a delay time, during which the emulsion appears stable. This delay time is apparent especially at polysaccharide concentrations at which chain overlap occurs.¹⁸⁻²⁰ At present, no complete theoretical framework has been established to describe this delay time and the subsequent process of network compression, but this phenomenon appears to be universal for gelled emulsions as well as for other gelled colloidal systems.^{18,21}

Over the last decade, a number of experimental techniques have become widely available to study the microstructure of colloidal systems. Examples are confocal scanning laser microscopy (CSLM) and diffusing wave spectroscopy (DWS).²²⁻²⁵ Progress has been made in relating particle mobility to the elastic properties of fractal colloidal gels.^{26,27} Moreover, the DWS-echo technique can be used to investigate structural changes caused by controlled oscillatory shear, as has been shown for e.g. densely packed emulsions²⁸ and colloidal glasses.²⁹ The combination of DWS-echo with CSLM-imaging^{30,31} was shown to be applicable to flocculated emulsions.³²

The focus of the present paper is twofold. Firstly, we investigated the scaling behaviour of the shear elasticity of emulsions versus the volume fraction of droplets, flocculated by the two mechanisms. The scaling behaviour is interpreted in terms of percolation and fractal approaches and the results will be supported by microscopic and micro-rheological data. Secondly, we present data on the effects of flocculation mechanism, oil content, polysaccharide concentration and density difference on the delay time and the subsequent process of serum separation in depletion-flocculated emulsions. The results will be interpreted on the basis of microstructure, rheological behaviour and literature data on delayed creaming.

6.2 Theoretical background

6.2.1 Elasticity modulus

Gelled systems usually show a power-law scaling behaviour between the storage modulus, G' , and the volume fraction, ϕ , of dispersed particles, e.g., oil droplets. The scaling exponent contains information on the prevailing type of deformation in the strands of emulsion droplets, originating from the type of droplet-droplet interaction. The scaling behaviour can be interpreted in two ways.

For particle gels, use can be made of models that consider the elasticity to originate from the elastic properties of the fractal clusters of which the gel consists. In these models, the network elasticity scales as $G' \sim \phi^n$. For example, Mellema et al.³³ developed a categorisation of the scaling exponent based on fractal geometry of flocs and formalism developed by Kantor and Webman.³⁴ In this approach, the scaling exponent is given by $n = \alpha/(3 - D_f)$, where D_f is the fractal dimension of the clusters forming the gel. The parameter α is a number between 1 and 4, related among other things to the amount of curvature

within the strands, determining whether deformation energy arises from energy bending or stretching.

Percolation theory^{35,36} predicts scaling behaviour according to $G' \sim (\phi - \phi_p)^\theta$. Here, the exponent θ depends on the type of interaction force between the droplets. Purely isotropic force percolation yields $\theta = 2 \pm 0.2$ ³⁷ and purely central force percolation with a vector character of the force yields $\theta = 4.4 \pm 0.6$.³⁸ In a system where both types of forces are present, Kantor and Webman found $2.9 < \theta < 3.6$. In the percolation approach, a critical percolation threshold, ϕ_p is recognised. This threshold is related to the magnitude of the attractive interaction, U , between the emulsion droplets via the tentative relation $\phi_p(U) \approx (0.55 - 0.60)\exp(-U/2.1k_B T)$,³⁹ where k_B is the Boltzmann constant and T the absolute temperature. In case of strong attraction, clusters grow and finally form an infinite cluster. In case of weak attraction, rearrangements in the clusters and cluster break up compete with cluster growth and counteract network formation.^{7,15}

6.2.2 Diffusing wave spectroscopy

Diffusing wave spectroscopy, DWS, is a dynamic light scattering technique, in which intensity fluctuations measured in scattered light are used to probe the mobility of light scattering particles,²³ e.g. emulsion droplets.⁴⁰ The relative displacement of the emulsion droplets due to Brownian motion, $x(t)$, is related to the intensity autocorrelation function, $g_2(t)$, by^{23,28}

$$g_2(t) - 1 = \beta \left(\int_0^\infty P(s) e^{-x(t)s/l^*} ds \right)^2, \quad (6.1)$$

where β is an instrumental factor, $P(s)$ is the distribution function of optical path length s and l^* is the transport mean free path of the scattered light. The factor $x(t)$ equals $k_0 \langle \Delta r^2(t) \rangle / 3$, where k_0 is the length of the wave vector which equals $2\pi/\lambda$, with λ the wavelength of the laser light, and $\langle \Delta r^2(t) \rangle$ the mean squared displacement of the oil droplets. Integration of eq. 6.1 has been performed for transmission and backscattering geometries in a rectangular cell,²³ yielding two expressions in which $P(s)$ is described by the sample width, L , and l^* . By using these equations, we obtain $\langle \Delta r^2(t) \rangle$ from $g_2(t)$,

measured in transmission and backscattering geometry. By matching the resulting $\langle \Delta r^2(t) \rangle$, calculated from transmission and backscattering measurements, l^* can be found. For gelled systems, the Brownian motion is arrested because the particles are held in the strands of the network. The arrested diffusion of particles in a fractal network that does not significantly rearrange, $\langle \Delta r^2(t) \rangle$, can at short time scales be approximated by a stretched exponential (eq. 6.2),^{26,41}

$$\langle \Delta r^2(t) \rangle = \delta^2 \left\{ 1 - \exp \left[- \frac{t}{\tau_c} \right]^p \right\}. \quad (6.2)$$

Here, δ^2 denotes a characteristic maximum mean squared displacement of the vibrating emulsion droplets and τ_c the characteristic vibration time. The exponent p equals 1 for free diffusion of the particle and about 0.7 for particles bound in a fractal network.²⁶ The elastic shear modulus G' can be calculated using the relation $G' = 6\pi\eta/\tau_c$.^{26,27} Here, η represents the viscosity of the medium in which the particles are suspended.

When oscillatory shear is applied to the system, this gives an extra contribution to the particle mobility and the full expression of the relative displacement of the oil droplets reads^{28,32}

$$x(t, t_0) = \frac{1}{3} k_0 \langle \Delta r^2(t) \rangle + \frac{1}{15} [k_0 l^* \gamma_0 |\sin(\omega(t + t_0)) - \sin(\omega t_0)|]^2 + \Phi(t), \quad (6.3)$$

where the first term represents Brownian motion. The second term represents the oscillatory deformation, where γ_0 equals the strain amplitude, ω is the angular frequency of the oscillation and t_0 is an arbitrary chosen starting time within the oscillation. The intensity autocorrelation function under oscillatory shear is obtained by substitution of eq. 6.3 into eq. 6.1 and integration over all values of t_0 within one oscillation period. An echo peak in $g_2(t)$ is predicted after each period of oscillation.

If oscillation induces rearrangements in the particle network, these rearrangements contribute to $x(t)$ by the third term in eq. 6.3, $\Phi(t)$. As a consequence the maximum in $g_2(t)$ at each oscillation period will be lower than $g_2(t)$ in quiescent condition.²⁸

6.3 Experimental

6.3.1 Materials

β -Lactoglobulin (protein content 92.5 wt %) was purified from bovine milk.⁴² Dextran (isolated from *Leuconostoc*; $M_w = 2 \times 10^6$ Da) was obtained from Sigma Chemicals (St. Louis, USA). Carboxy-methylcellulose, Blanose 7HOF, was obtained from Hercules (Zwijndrecht, The Netherlands). NaCl (p. a.) and thiomersal (97 wt %) were obtained from Merck (Schuchardt, Germany). Sunflower oil (Reddy, Vandemoortele, the Netherlands) was purchased from a local retailer. 1-Bromo-hexadecane and 1-bromo-octane were obtained from Fluka chemicals (Buchs, Switzerland).

6.3.2 Sample preparation

Solutions of β -lg or CMC were prepared by adding the material to the required amount of salt solution, followed by gently stirring overnight, avoiding incorporation of air bubbles. Dextran solutions were prepared by adding the material to a 0.1 M NaCl solution, containing 0.02 wt % thiomersal to inhibit microbial growth, and stirring 4 hours in a bath of boiling water. Solutions contained 0.1 M NaCl. The pH was set at 6.7 using 1 M HCl or NaOH.

Stock emulsions contained 40 wt % of dispersed phase and 1 wt % β -lg. Emulsions were prepared by stirring oil or a mixture of oil and bromo-alkanes into a β -lg solution using an Ultra Turrax (Polytron, Switzerland). Subsequently, this pre-emulsion was homogenised by 10 passes through a lab-scale homogeniser (Delta Instruments, Drachten, the Netherlands) at a pressure of 50 bar. Stock emulsions had typical d_{32} -values of 1.0 μm as determined from laser diffraction (Coulter LS 230, Miami, USA). All samples were mixed by gently shaking until the sample appeared homogeneous to the unaided eye (~ 30 s). All experiments were carried out at 25 °C.

6.3.3 Rheology

Dynamic measurements, also denoted as macro-rheological measurements, were carried out using a Bohlin VOR rheometer (Huntingdon, U.K.). A concentric cylinder geometry (C 25) with a gap of 2.5 mm and a 1-g torsion bar were used. At the start of each measurement, the samples were sheared at a rate of 10^2 s^{-1} during 60 s and after this pre-

shear treatment the emulsion was left to gel for 30 minutes. Hereafter, G' was determined as a function of frequency (0.1 – 6 Hz) and strain amplitude (0.00028 – 0.28).

6.3.4 DWS and CSLM

The microstructure of oil-in-water emulsions was investigated at rest and under oscillatory shear using the oscillatory shear cell described by Nicolas et al.³¹ This cell was mounted on a Confocal Scanning Laser Microscope (Perkin Elmer UltraView RS, Wellesley, USA) providing the possibility to carry out DWS measurements simultaneously with imaging. DWS was carried out in transmission and backscattering geometry,²³ using a HeNe laser, (Melles Griot, $\lambda = 633$ nm).

In order to make the emulsion droplets visible for CSLM-imaging the adsorbed protein layer was stained by addition of Rhodamine. This fluorescent label was excited at 568 nm and its fluorescence was detected at wavelengths between 600 and 700 nm.

Emulsion samples were brought into the shear cell, directly after mixing. Intensity fluctuations were recorded during half an hour in transmission and subsequently one hour in backscattering geometry. Within these recording times, adequate time averages of the intensity autocorrelation function were obtained ($g_2(0) - 1 > 0.4$). Simultaneously, the microstructure was determined by CSLM.

Subsequently, DWS-echo measurements were carried out while a sinusoidal oscillating strain was applied. Hereby, the strain amplitude, γ_a , was increased in small steps from 0.00038 to 0.038.

6.3.5 Demixing experiments

Demixing of emulsions was monitored by turbidimetry as described previously,^{10,43} using a Turbiscan MA 2000 apparatus (Ramonville St. Agne, France). The initial height, H_0 , of the emulsions samples was 43 ± 1 mm. The height of the collapsing gel at time t was defined as $H(t)$. We normalised this height to the final emulsion height, H_f , yielding $h'(t) = (H(t) - H_f) / (H_0 - H_f)$.⁴⁴

6.4 Results and discussion

6.4.1 Elasticity modulus

Dynamic rheological measurements were carried out on density-matched emulsions that were flocculated by A) depletion and B) bridging. Measurements were performed over a frequency range from 0.01 to 6 Hz. We plotted G' according to the two theoretical approaches described above (Fig. 6.1 and 6.2).

By plotting G' against ϕ on double logarithmic scale, (Fig. 6.1), we find that the bridging-flocculated emulsions give a substantially steeper slope, n , than depletion-flocculated emulsions. In Table 6.1, the values of n and α are shown, recognising that strictly, these values only have a meaning when $\phi_p = 0$ and D_f is known. Here we assume an arbitrary, but realistic value for D_f between 2.0 and 2.5.⁴⁵ By following the method of van der Linden and Sagis,³⁶ $G'^{(1/\theta)}$ was plotted against the volume fraction of emulsion droplets, ϕ , for different values of θ . Optimal linear regression was obtained for $\theta = 1.8$ and $\theta = 5.1$ for depletion-flocculated and bridging-flocculated emulsions, respectively. From these curves we also obtained ϕ_p , which was zero for bridging-flocculated systems but not for depletion-flocculated emulsions. Subsequently, double-logarithmic plots of G' versus $(\phi - \phi_p)$ were made and these are shown in Fig. 6.2.

On the basis of these two considerations of our data we make the following relation to the droplet-droplet interactions.

In depletion-flocculated emulsions, droplets are gently pushed together by a long-range depletion force but a repulsive layer of adsorbed protein prevents direct droplet-droplet contact.¹⁰ This implies that deformation energy is due to stretching of the droplet-droplet bonds, and not to rotation of the droplets around each other. Therefore, this type of droplet-droplet interaction has characteristic features, resembling an isotropic force, in line with $\theta = 1.8$.³⁷ Deformation via stretching also corresponds to the low value of α in the model of Mellema et al.³³

In bridging-flocculated emulsions, a strong attraction acts between the CMC-molecules and the droplet interface. As a consequence, the droplets will become strongly surface-to-surface bound by a number of CMC-molecules.⁴⁶ Because of this, bending of droplet-droplet bonds will also contribute to the deformation energy, in addition to stretching. Therefore, the bridging-type of interaction has characteristic features of the percolation models that take bending deformation into account.^{34,38} These models predict $3.6 < \theta < 5.0$, which reasonably corresponds to our experimental result. The contribution of bending was also reflected by the higher value of α .³³

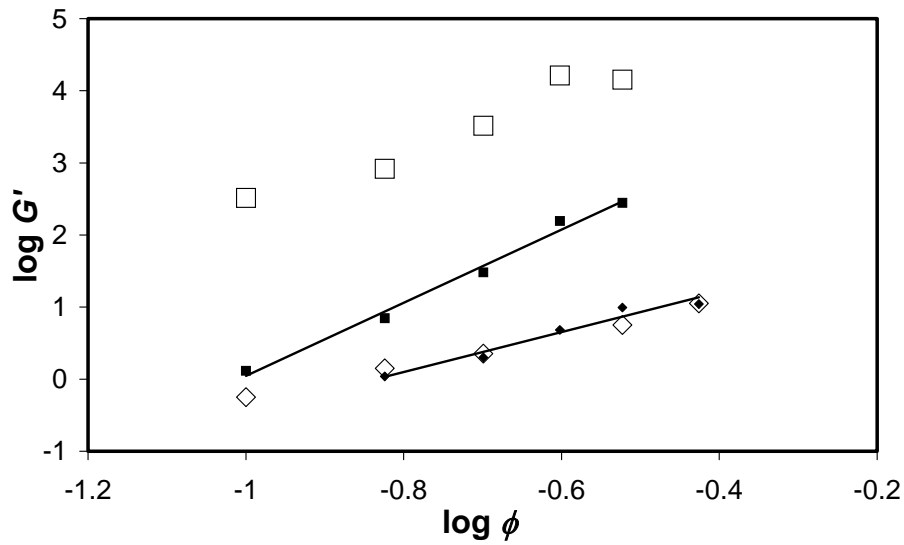


Fig. 6.1 Double logarithmic plot of G' , (Pa), versus ϕ for \blacklozenge , depletion flocculated emulsions at $c_{\text{dextrans}} = 2$ wt % and \blacksquare , bridging flocculated emulsions where c_{CMC} corresponds to a maximum surface coverage of $1 \text{ mg}\cdot\text{m}^{-2}$. G' was determined by rheology at 1 Hz (filled symbols) and by DWS in transmission and backscattering (open symbols).

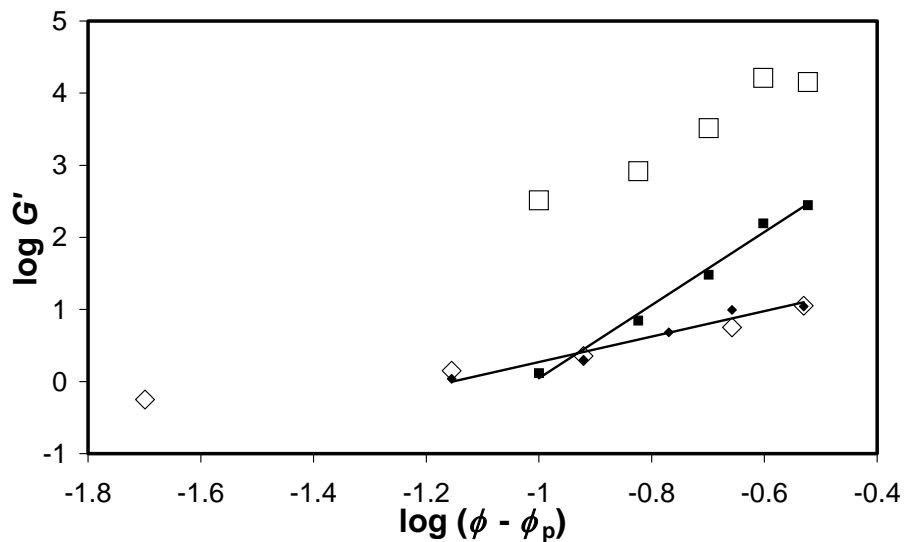


Fig. 6.2 Double logarithmic plot of G' , (Pa), versus $(\phi - \phi_p)$ for the same data as in Figure 6.1.

Table 6.1 Scaling exponents n , α and θ , and the percolation threshold concentration ϕ_p for depletion- and bridging-flocculated emulsions.

	n	α	θ	ϕ_p
depletion	2.9 +/- 0.1	2.3 +/- 0.7	1.8 +/- 0.2	0.08 +/- 0.03
bridging	5.1 +/- 0.3	3.3 +/- 0.7	5.1 +/- 0.3	0.00 +/- 0.01

6.4.2 The percolation threshold

Critical volume fractions for percolation of emulsion droplets were extracted from the linear plots of $G^{(1/\theta)}$ versus ϕ and these are also shown in Table 6.1. The existence of a percolation threshold in depletion-flocculated emulsions can be understood on the basis of the relatively weak interaction between the droplets. An estimate of ϕ_p was also made using the relation found by Segrè,³⁹ yielding $\phi_p = 0.1$, which agrees well with the experimental value. In the bridging-flocculated emulsions, the percolation concentration was zero, which is in accordance with the much stronger bridging attraction between the oil droplets.

6.4.3 Imaging

Fig. 6.3 shows CSLM-images of the microstructure of depletion- and a bridging-flocculated emulsion at different oil contents. In most systems, a fixed structure of flocculated emulsion droplets was observed microscopically. In the system of image A in Fig. 6.3, thermal vibrations of the fine droplet strands could be discriminated, but no rearrangements of the network structure. These observations indicate the existence of an emulsion gel.

The microstructure of the emulsion gels differs in the degree of heterogeneity. The depletion-flocculated networks appear homogeneous at length scales above 10 μm , whereas the bridging-flocculated network is heterogeneous up to the floc size of about 100 μm . This difference in heterogeneity agrees with observations made by light microscopy that were reported before.¹¹ It can be attributed to flow during mixing of the stock emulsion and the polysaccharide solution. In the following sections, the consequences of this heterogeneity will be discussed.

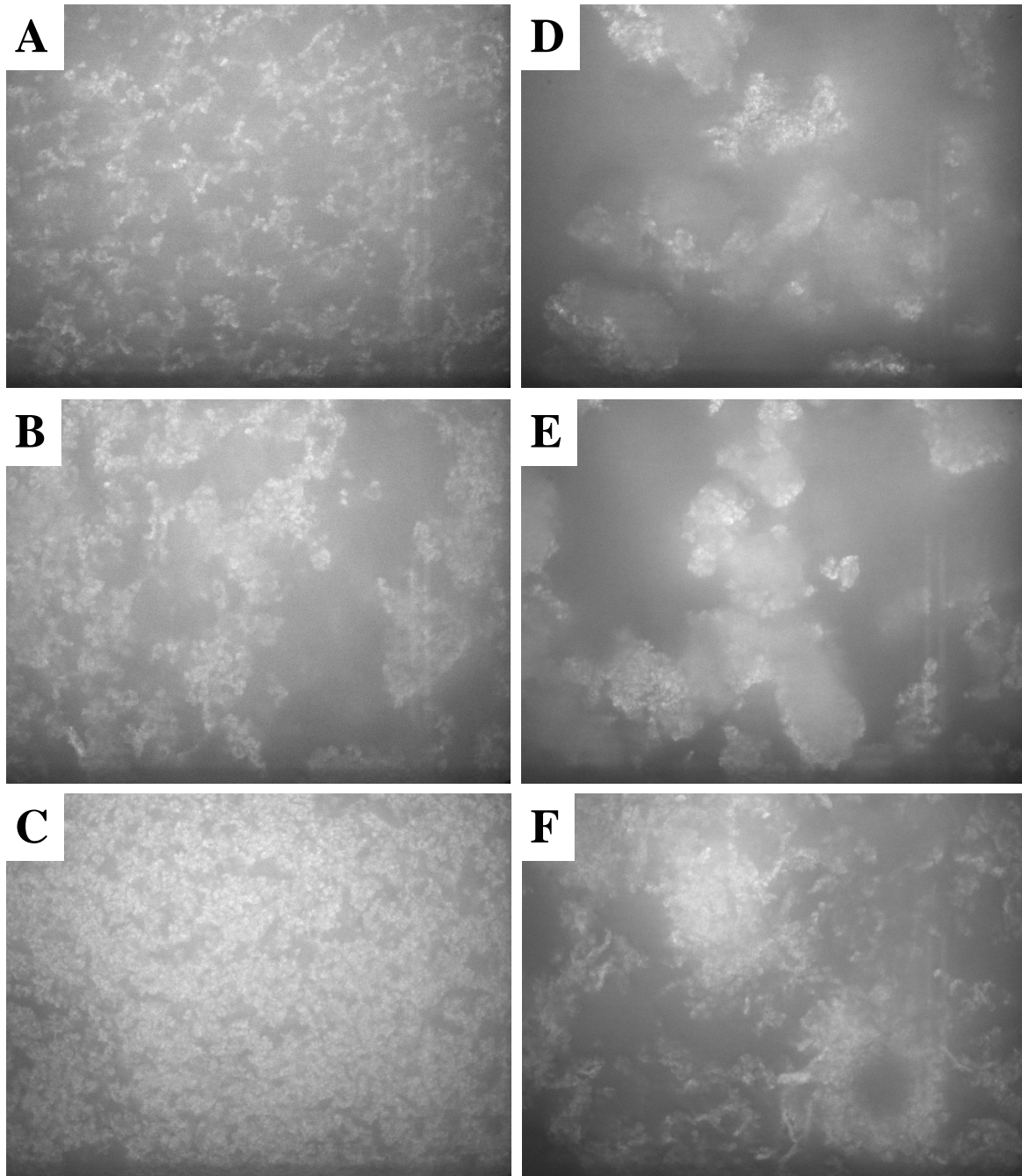


Fig. 6.3 CSLM-images of oil-in-water emulsion at 10 (A & B), 20 (C & D) and 30 (E & F) wt % oil. Image size: $130 \times 100 \mu\text{m}$. In A, B and C emulsions contained 2 wt % dextran inducing depletion-flocculation. In D, E and F, emulsions contained $1 \text{ mg}\cdot\text{m}^{-2}$ CMC, which induced bridging flocculation.

6.4.4 DWS at rest

Intensity autocorrelation functions were measured for density-matched emulsions in backscattering and transmission geometry. Curves of the mean squared displacement of the emulsion-droplets were obtained and fitted with eq. 6.2. The results are shown in Fig. 6.4 for a series of depletion-flocculated emulsions. We note that the measured mean squared displacement does not completely level off to a maximum value. At larger timescales, some motion occurs at larger length scales.⁴⁷ This is not included in the model used here, which only takes into account the vibrational movement.

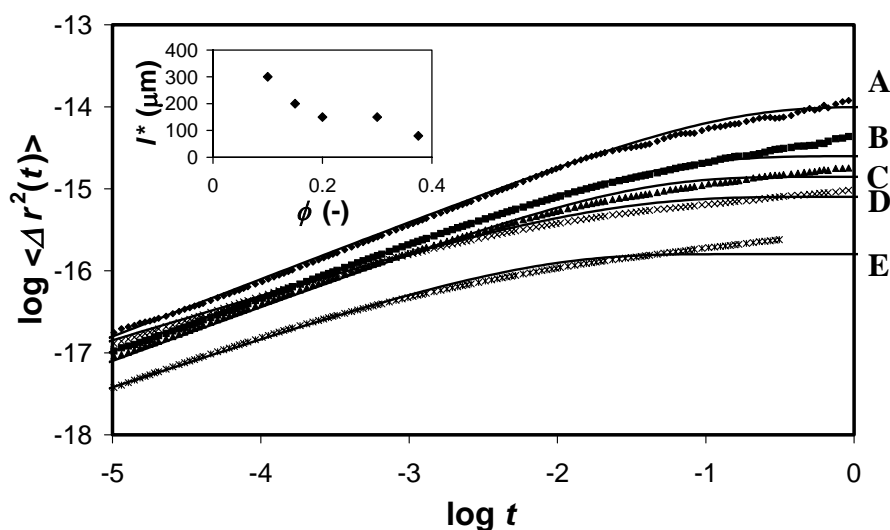


Fig. 6.4 Mean squared displacement, $\langle \Delta r^2(t) \rangle$, of depletion-flocculated emulsions at volume fractions of oil. Drawn lines are fits of eq. 6.2 to the experimental data. **A:** $\phi = 0.10$; **B:** $\phi = 0.15$; **C:** $\phi = 0.20$ **D:** $\phi = 0.30$ **E:** $\phi = 0.38$. The inset shows l^* as a function of ϕ .

The extracted parameters (p , δ^2 and τ_c) are presented in Table 6.2. Values of τ_c were transformed into G' and these values were included in the plots of the macroscopic moduli obtained by rheology in Fig 6.1 and 6.2.

For depletion-flocculated emulsions, the values of p are generally slightly lower than 0.7, especially at larger ϕ . A tentative explanation for the lower values of p is the presence of thick strands in which the mobility is arrested more strongly than in thin strands. Thick strands indicate that the structure is somewhat more heterogeneous than an ideal fractal network. Nevertheless, good agreement was found well above ϕ_p between G' obtained

from rheology and DWS by making use of the model of Krall and Weitz,²⁶ which is an encouraging result for the application of light-scattering-based microrheology. Only near ϕ_p , DWS seems to overestimate G' , probably due to dead ends in the network. Dead ends show features of elasticity on the micro-level, but do not contribute to the elasticity measured macroscopically.

The bridging-flocculated systems showed a large difference between G' as measured by micro- and macro-rheology throughout the whole range of oil contents. This result is consistent with the fact that the length scale of heterogeneity in bridging-flocculated emulsions, as observed by CSLM is on the order of the probing length of DWS. The parameters p and δ^2 are consistently smaller in bridging-flocculated systems. This indicates that in the bridging-flocculated emulsions, the droplet mobility is even more strongly arrested than in depletion-flocculated systems. This is probably due to the stronger interaction and the higher compactness of the flocs. The parameters do not strongly depend on ϕ , which is consistent with the CSLM-observation that the floc size and structure, is independent on ϕ . Apparently, the floc size and structure is determined by the intensity of mixing of the samples, which was constant in our experiments.

Table 6.2 Fit parameters p , δ^2 and τ_c extracted from the evolution of $\langle \Delta r^2(t) \rangle$ in different emulsion samples. For depletion-flocculated samples, $c_{\text{dextran}} = 2$ wt % and for bridging-flocculated samples, the surface coverage is $1 \text{ mg}\cdot\text{m}^{-2}$.

Interaction type	ϕ (-)	p (-)	δ^2 (nm^2)	τ_c (ms)
depletion	0.1	0.70	10000	100
	0.15	0.66	2500	40
	0.2	0.66	1400	25
	0.3	0.58	700	10
	0.375	0.60	160	5
bridging	0.1	0.40	200	9
	0.15	0.47	170	6
	0.2	0.35	33	3
	0.25	0.35	300	3
	0.3	0.40	27	6

6.4.5 DWS-echo

Intensity autocorrelation functions were recorded in transmission geometry under oscillatory shear at a frequency of 100 Hz. By using this frequency, peaks are located at correlation times at which the signal had not decayed entirely due to Brownian motion.^{28,32} However, at this frequency we are limited to measurement of samples with a modulus larger than about 20 Pa. In samples with lower moduli, excessive resonance in the samples between the plates would increase the internal strain amplitude dramatically.⁴⁸

Values of γ_0 were extracted from the initial decay and the echo peaks of autocorrelation functions^{28,32} were measured at the various applied strain amplitudes, γ_a . Results for γ_0 are shown in Fig. 6.5.

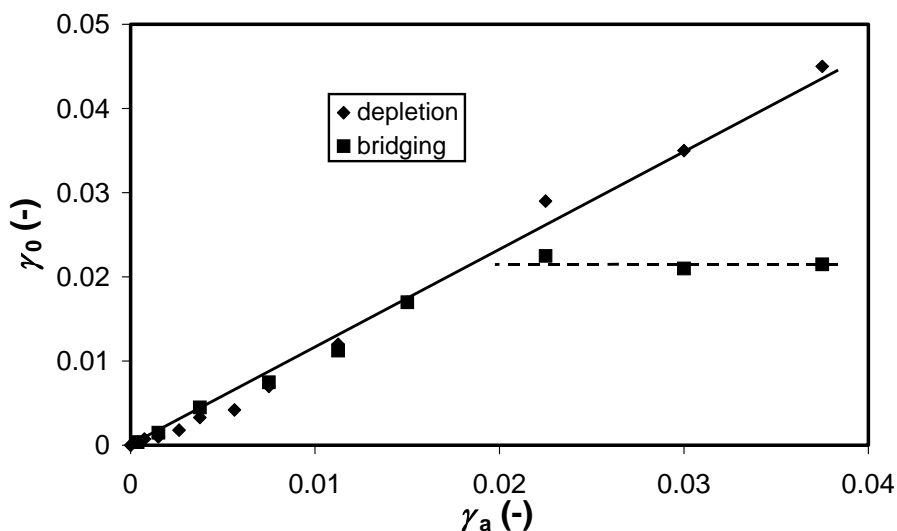


Fig. 6.5 Microscopic deformation, γ_0 , obtained from DWS-echo measurements plotted against the applied deformation, γ_a , for a depletion- and a bridging-flocculated emulsion. Lines are drawn to guide the eye. The drawn line represents the depletion-flocculated emulsions. The dashed line represents the bridging-flocculated emulsions.

In depletion-flocculated emulsion gels, a linear relation is found between γ_0 and γ_a , which indicates that the deformation is rather homogeneously distributed over the system. In bridging-flocculated emulsion gels, the microscopic strain initially increases with the externally applied strain, but above 1-2 % strain, no further increase is observed anymore. We infer that fracture occurs within the samples and that the strain inside the fragments has

reached a maximum value. The fragments (which are larger than l^*) slip along each other when large strain amplitudes are applied. This observation reflects an important difference between the bridging- and depletion flocculated systems. Fracture was also observed in macro-rheological experiments on bridging-flocculated emulsions, whereas depletion-flocculated systems showed yielding behaviour.¹¹

6.4.6 Demixing kinetics

Typical curves of the process of network contraction are shown in Fig. 6.6. At short ageing times, both curves of depletion-flocculated emulsions containing dextran show a smaller degree of network compression than bridging-flocculated emulsions and show a delay time, especially at high polysaccharide concentration. The same result as for the emulsions that contained dextran was reported for depletion-flocculated emulsions containing CMC at pH 6.7.¹¹ Finally, depletion-flocculated emulsions are compressed to a high oil content of 40-45 wt %. In bridging-flocculated emulsions, network compression stops at a low level of compression compared to depletion-flocculated structures. These differences will be discussed in more detail in the following section.

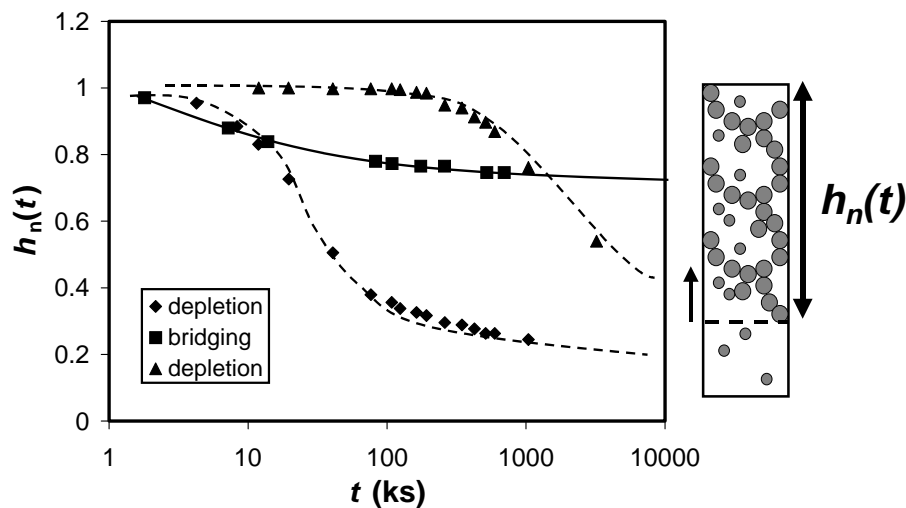


Fig. 6.6 Examples of the process of network contraction for two depletion-flocculated emulsions and one bridging-flocculated emulsion, all at 10 wt % oil. \blacklozenge , 1 wt % dextran; \blacktriangle , 5 wt % dextran (both pH 6.7; depletion) \blacksquare , 0.06 wt % CMC (pH 3.0; bridging).

6.4.7 Delay times

Another feature of demixing in depletion-flocculated emulsions is the presence of a delay time before network compression starts.^{18,21} During the delay time, channels of expelled liquid are formed within the gel network.²¹ The channels cause erosion of the droplet network, which amplifies the growth of the channels. When the channels have become sufficiently large, the gel collapses.¹ Other recent work has shown that the evolution of collapse of colloidal silica gels at different conditions can be scaled along the time axis onto a master curve.⁴⁴ Scaling our data on the time axis to the delay time, t_{delay} , the time at which $h'(t)$ decayed to 0.1, yielded a similar master curve (Fig. 6.7). The same master curve was obtained independent of oil content, polysaccharide concentration or density difference. Delay times as a function of ϕ are shown in Fig. 6.8, as a function of the polysaccharide concentration in Fig. 6.9, and as a function of the density difference between the emulsion droplets and the aqueous phase in Fig. 6.10.

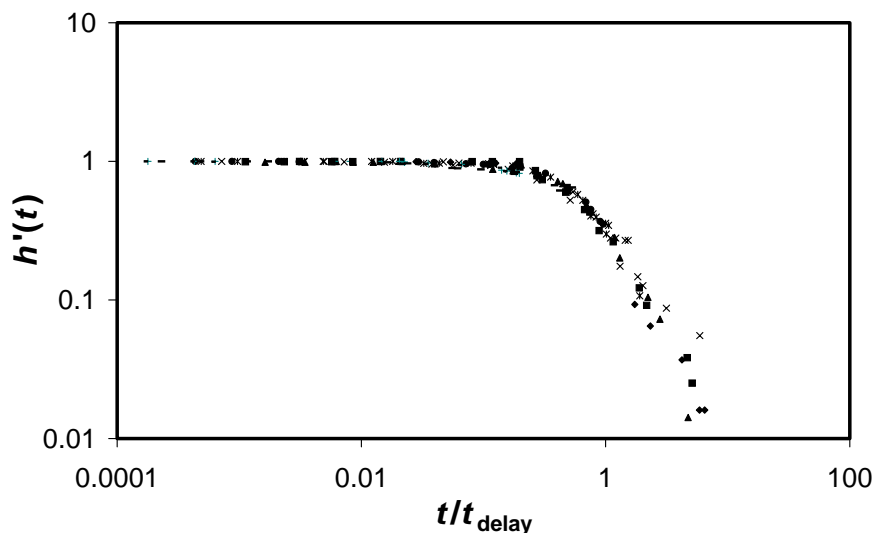


Fig. 6.7 Master curve of the normalised network height, h' of 10 wt % oil-in-water emulsions at 5 wt % dextran as a function of scaled time.

Because the occurrence of a delay time is related to the erosion of the droplet network caused by the flow through the channels, in porous structures the strands will be more vulnerable to the erosion process than in dense structures. On the basis of this a dependency of t_{delay} of the permeability B would be expected as $t_{\text{delay}} \sim B^{-1}$. For fractal gels, B is related to ϕ by¹⁴ $B \sim \phi^{[2/(D_f - 3)]}$ and for a realistic value of $D_f \approx 2$, this relation yields $t_{\text{delay}} \sim \phi^2$. This result is in line with our data and those of Manoj et al.,¹⁸ showing a scaling of $t_{\text{delay}} \sim \phi^{2.1}$.

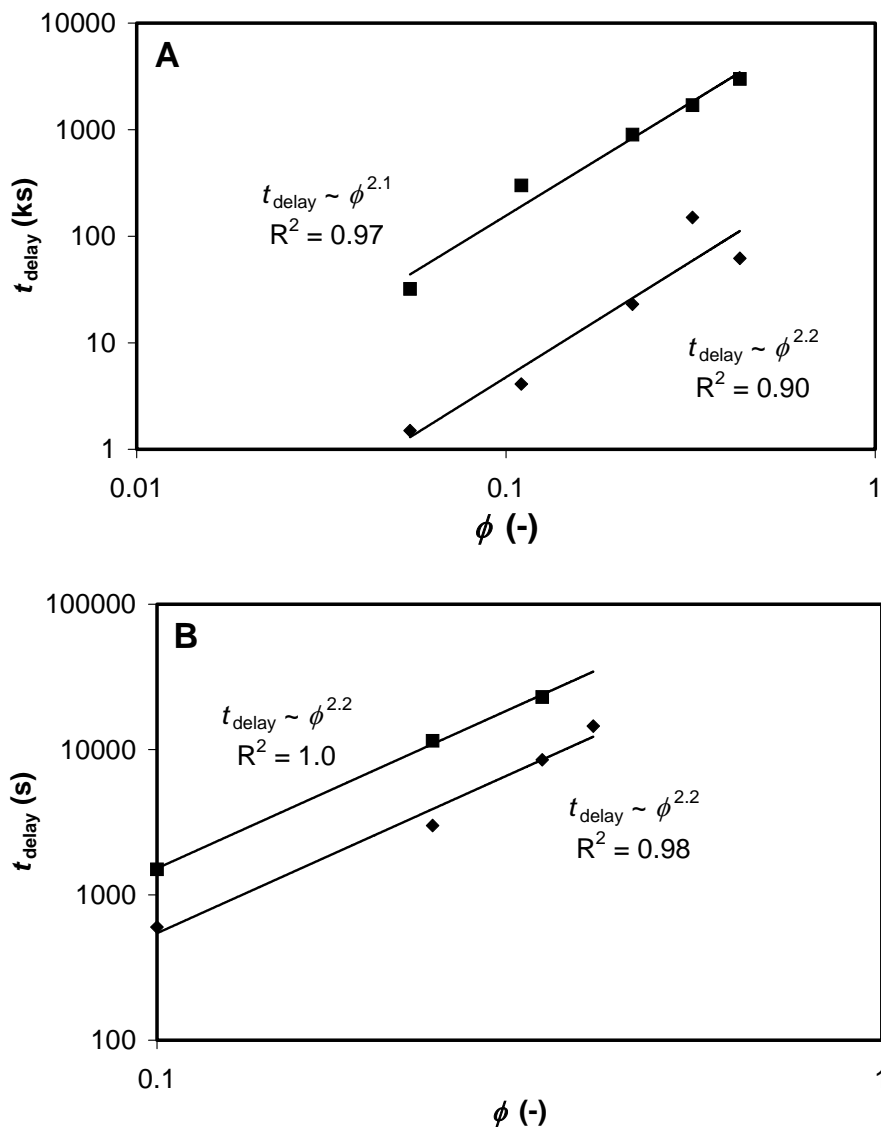


Fig. 6.8 Delay times of depletion-flocculated emulsions plotted against oil fraction on log-log scale. Chart A: ◆, 1 wt % dextran; ■, 5 wt % dextran. The delay times in chart B were taken from Manoj et al. 1998. ◆, 0.2 wt % HEC; ■, 0.35 wt % HEC. In both data sets, a scaling exponent of 2.1-2.2 is found.

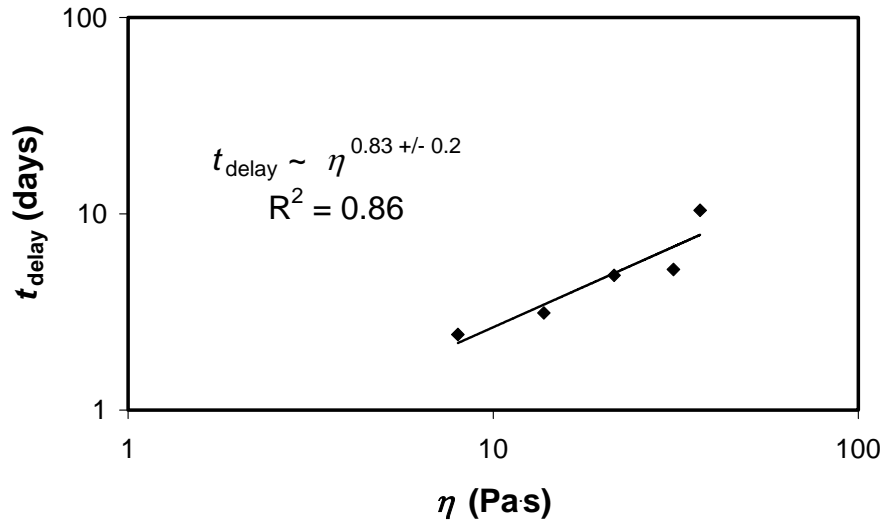


Fig. 6.9 Delay times of depletion-flocculated emulsions as a function of low-shear viscosity of the continuous phase.

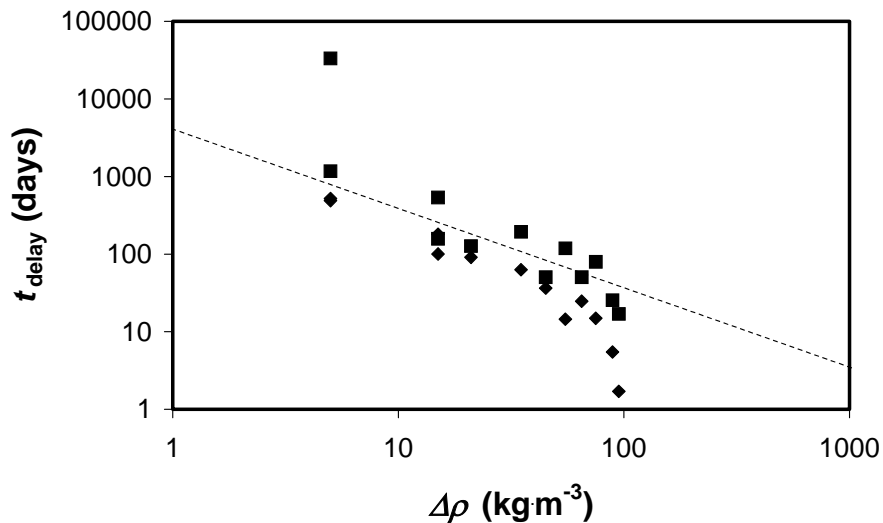


Fig. 6.10 Delay times of depletion-flocculated emulsions as a function of the density difference between the dispersed and the continuous liquid. The dashed line represents the relation $t_{\text{delay}} \sim \Delta\rho$.

When delay times measured in emulsions flocculated by dextran are plotted against the viscosity of the dextran solution, we find $t_{\text{delay}} \sim \eta^{(0.83 \pm 0.2)}$. Scaling of the delay time with the polysaccharide concentration was found by Parker et al.¹⁹ for oil-in-water emulsions at different polysaccharide concentrations in the overlap regime. A power law exponent of 3.9 ± 0.4 was found for a variety of non-adsorbing polysaccharides. This exponent is equal to the theoretical exponent for the increase of the apparent viscosity with polymer concentration in the overlap regime.^{49,50} Indeed, such exponents (3.5-4.4) were found for

the viscosity increase of polysaccharide solutions in the overlap regime. The results of Parker et al.¹⁹ therefore confirm the relation $t_{\text{delay}} \sim \eta$. This observation is in line with recent work reported by Vélez et al.,⁵¹ who also related the delay time to the strong viscosity increase in the entangled polysaccharide solutions. The effect of the polysaccharide concentration on the depletion attraction, which would reinforce the droplet network, is apparently dominated by the strong effect of the viscosity.

Data on the effect of density difference show a decrease of t_{delay} with $\Delta\rho$. These data show the importance of gravity as a driving force for the rearrangements that lead to serum separation. The pressure, P , exerted on the network is given by $P = \Delta\rho g H \phi$, where g is the acceleration due to gravity and H the height of the sample. According to this relation, a dependence of $t_{\text{delay}} \sim \Delta\rho^{-1}$ would be expected, which is shown in chart 6.10 by the dashed line. Most of the data points reasonably resemble this behaviour, although a few data points at high and low $\Delta\rho$ deviate from the expected line. This might be due to a number of reasons, e.g. formation of protein-protein bonds at long ageing times.

Summarising, the scaling behaviour of the delay-times shows a relation $t_{\text{delay}} \sim B^{-1} \cdot \eta \cdot \Delta\rho^{-1}$, where η is the low-shear viscosity of the continuous phase and where $B \sim \phi^{-2}$. Building on the ideas of Starrs et al.²¹, we propose that channels are present within the droplet network, but initially, these are too small to allow measurable serum separation. The width of these channels limits serum separation. The channels must become wider before substantial serum separation will take place. Widening of the channels occurs by means of structural rearrangements, which are driven by gravity, but limited by the viscous drag of the medium in which the network is embedded and by the initial channel size.

The idea of network erosion is also in line with the differences between depletion- and bridging-flocculated emulsions. In depletion-flocculated emulsions, erosion of droplets from the network is most likely, because the interdroplet bonds are relatively weak. As a consequence, the erosion process can amplify itself and the structure can collapse to a rather close packing. On the contrary, in bridging-flocculated emulsions, much larger channels are present initially, allowing immediate serum separation. However, upon drainage of liquid, these channels are compressed and eventually disappear, because erosion of the network is highly unlikely due to the strong polysaccharide bridges. At this stage, the process of drainage and serum separation has ended.

6.5 Conclusion

Scaling the emulsion gel elasticity with $(\phi - \phi_p)$ yielded scaling exponents $\theta = 1.8$ and $\theta = 5.1$ for depletion- and bridging-flocculated emulsions respectively. Interpretation of the scaling exponent via different theoretical approaches consistently reflected the two types of interaction between the droplets. The existence of a percolation threshold in depletion-flocculated emulsions was explained by the magnitude of the droplet-droplet interaction.

Rather good agreement was found between G' from DWS and G' from macro-rheology in depletion-flocculated systems well above ϕ_p . In bridging-flocculated systems, a large deviation was found between micro- and macro-rheological measurements. This was explained by the structural heterogeneity at length scales above the probing length of DWS. The heterogeneity of the bridging-flocculated emulsions was also shown by CSLM-imaging, fracture/yielding behaviour, and comparison between micro- and macroscopic deformation during oscillatory shear.

Serum separation from emulsion gels was confirmed to be driven by gravity. At short times, an important difference between the two systems is the possible presence of a delay-time before demixing in depletion-flocculated emulsions, when the polysaccharide concentration is in the overlap regime. Because of the much smaller channel-size of depletion-flocculated emulsions, demixing is strongly impeded, whereas liquid can immediately drain from the heterogeneous bridging-flocculated systems. The delay time in depletion-flocculated systems was found to scale with the network permeability, the aqueous phase viscosity and the density difference between oil and the aqueous phase as $t_{\text{delay}} \sim B^{-1} \cdot \eta \cdot \Delta\rho^{-1}$.

At long times, self-amplifying erosion of the network structure of depletion-flocculated systems allows collapse until a random close packing of the emulsion droplets is reached. In bridging-flocculated emulsions the demixing process arrests itself because the droplet-droplet bonds are stronger and the network does not erode.

Our results provide possibilities to control rheology and the type of demixing process of emulsion gels by selecting a polysaccharide, based on its interaction with the oil droplet/water interface. In addition a step is made to control of the delay time before demixing of depletion-flocculated emulsions.

References

- (1) Starrs L.; Poon W. C. K.; Hibberd D.; Robins M. *J. Phys. Cond. Matt.* **2002**, *14*, 2485-2505.
- (2) Bibette J.; Mason T. G.; Gang H.; Weitz D. A.; Poulin P. *Langmuir* **1993**, *9*, 3352-3356.
- (3) Poulin P.; Bibette J.; Weitz D. A. *Eur. Phys. J. B* **1999**, *7*, 277-281.
- (4) Meller A.; Gisler T.; Weitz D. A.; Stavans J. *Langmuir* **1999**, *15*, 1918-1922.
- (5) Tuinier R.; de Kruif C. G. *J. Coll. Int. Sci.* **1999**, *218*, 201-210.
- (6) Manoj P.; Watson A. D.; Hibberd D.; Fillery-Travis A.; Robins M. M. *J. Coll. Int. Sci.* **2000**, *228*, 200-206.
- (7) Berli C. L. A.; Quemada D.; Parker A. *Coll. Surf. A* **2003**, *215*, 201-204.
- (8) Dickinson E. *Food Hydrocolloids* **2003**, *17*, 25-39.
- (9) Robins M. M.; Watson A. D.; Wilde P. J. *Curr. Op. Coll. Int. Sci.* **2003**, *7*, 419-425.
- (10) This thesis, chapter 3: Blijdenstein T. B. J.; Hendriks W. P. G.; van der Linden E.; van Vliet T.; van Aken G. A. *Langmuir* **2003**, *19*, 6657-6663.
- (11) This thesis, chapter 5: Blijdenstein T. B. J.; van Winden A. J. M.; van Vliet T.; van der Linden E.; van Aken G. A. *submitted* **2003**
- (12) Vrij A. *Pure Appl. Chem.* **1976**, *48*, 471-483.
- (13) Healy T.; La Mer V. K. *J. Coll. Sci.* **1964**, *19*, 323-332.
- (14) Bremer L. G. B.; Bijsterbosch B. H.; Walstra P.; van Vliet T. *Adv. Coll. Int. Sci.* **1993**, *46*, 117-128.
- (15) Bos M. T. A.; van Opheusden J. H. J. *Phys. Rev. E* **1996**, *53*, 5044-5050.
- (16) Buscall R.; White L. R. *Journal of the Chemical Society Faraday Transactions. 1. Physical Chemistry* **1987**, *83*, 873-891.
- (17) van Vliet, T and Walstra, P. *Food Colloids* Bee, R. D., Richmond, P., and Mingins, J. Eds, The Royal Society of Chemistry, Cambridge **1989**, 206-217.
- (18) Manoj P.; Fillery-Travis A.; Watson A. D.; Hibberd D.; Robins M. M. *J. Coll. Int. Sci.* **1998**, *207*, 283-293.
- (19) Parker A.; Gunning P. A.; Kim Ng.; Robins M. M. *Food Hydrocolloids* **1995**, *9*, 333-342.
- (20) Robins M. M. *Curr. Op. Coll. Int. Sci.* **2000**, *5*, 265-272.
- (21) Poon W. C. K.; Starrs L.; Meeker S. P.; Moussaïd A.; Evans R. M. L.; Pusey P. N.; Robins M. M. *Faraday Discuss.* **1999**, *112*, 143-154.
- (22) Pine D. J.; Weitz D. A.; Chaikin P. M.; Herbolzheimer E. *Phys. Rev. Lett.* **1988**, *60*, 1134-1137.
- (23) Weitz D.A.; Pine D. J., in *Dynamic Light Scattering*, Brown W., Ed. Clarendon Press, Cambridge **1993**; Chapter 16.
- (24) Harden J. L.; Viasnoff V. *Curr. Op. Coll. Int. Sci.* **2001**, *6*, 438-445.
- (25) Hemar Y.; Hunter R. J.; Singh H.; Hébraud P.; Horne D. S. *J. Coll. Int. Sci.* **2003**, *264*, 502-508.
- (26) Krall A. H.; Weitz D. A. *Phys. Rev. Lett.* **1998**, *80*, 778-781.

- (27) Cardinaux F., Stradner A., Scheffold F., and Schurtenberger P. *Proceedings of the 3rd international symposium on food rheology and structure* Fischer, P., Marti, I., and Windhab, E. Eds, ETH, Zürich **2003**, 13-18.
- (28) Hébraud P.; Lequeux F.; Munch J. P.; Pine D. J. *Phys. Rev. Lett.* **1997**, *78*, 4657-4660.
- (29) Petekidis G.; Moussaïd A.; Pusey P. N. *Phys. Rev. E* **2002**, *66*, 051402.
- (30) Nicolas Y.; Paques M.; van den Ende D.; Dhondt J. K. G.; van Polanen R. C.; Knaebel A.; Munch J. P.; Blijdenstein T. B. J.; van Aken G. A. *Food Hydrocolloids* **2003**, *17*, 907-913.
- (31) Nicolas Y.; Paques M.; Knaebel A.; Steyer A.; Munch J. P.; Blijdenstein T. B. J.; van Aken G. A. *Rev. Sci. Instr.* **2003**, *74*, 3838-3844.
- (32) Blijdenstein, T. B. J., Nicolas, Y., van der Linden, E., van Vliet, T., Paques, M., van Aken, G. A., Knaebel, A., and Munch, J. P. *Proceedings of the 3rd international symposium on food rheology and structure* Fischer, P., Marti, I., and Windhab, E. Eds, ETH, Zürich **2003**, 343-346.
- (33) Mellema M.; van Opheusden J. H. J.; van Vliet T. *Journal of Rheology* **2002**, *46*, 11-29.
- (34) Kantor Y.; Webman I. *Phys. Rev. Lett.* **1984**, *21*, 1891-1894.
- (35) Stauffer D.; Coniglio A.; Adam M. *Adv. Polymer Sci.* **1982**, *44*, 103-158.
- (36) van der Linden E.; Sagis L. M. C. *Langmuir* **2001**, *17*, 5821-5824.
- (37) Mitescu C. D.; Musolf M. J. *J. Phys. Lett.* **1983**, *44*, L-679-L-683.
- (38) Feng S.; Sen P. N. *Phys. Rev. Lett.* **1984**, *52*, 216-219.
- (39) Segrè P. N.; Prasad V.; Schofield A. B.; Weitz D. A. *Phys. Rev. Lett.* **2001**, *86*, 6042-6045.
- (40) ten Grotenhuis E.; Paques M.; van Aken G. A. *J. Coll. Int. Sci.* **2000**, *227*, 495-504.
- (41) Romer S.; Scheffold F.; Schurtenberger P. *Phys. Rev. Lett.* **2000**, *85*, 4980-4983.
- (42) de Jongh H. H. J.; Gröneveld T.; de Groot J. *J. Dairy Sci.* **2001**, *84*, 562-571.
- (43) This thesis, chapter 2: Blijdenstein T. B. J.; van Vliet T.; van der Linden E.; van Aken G. A. *Food Hydrocolloids* **2003**, *17*, 661-669.
- (44) Kilfoil M. L.; Pashkovski E. E.; Masters J. A.; Weitz D. A. *Philosophical Transactions: Mathematical, Physical & Engineering Sciences* **2003**, *361*, 753.
- (45) Mellema M.; Heesakkers J. W. M.; van Opheusden J. H. J.; van Vliet T. *Langmuir* **2000**, *16*, 6847-6854.
- (46) Swenson J.; Smalley M. V.; Hatharasinghe H. L. M. *Phys. Rev. Lett.* **1998**, *81*, 5840-5843.
- (47) Cipelletti L.; Ramos L.; Manley S.; Pitard E.; Weitz D. A.; Pashkovski E.; Johansson M. *Faraday Disc. Chem. Soc.* **2003**, *123*, 237-251.
- (48) Whorlow R.W., in *Rheological techniques*, Grant E.H., Ed. Ellis Horwood Ltd., Chichester **1992**; Chapter 7.
- (49) Graessley W. W. *J. Chem. Phys.* **1967**, *47*, 1942-1953.
- (50) De Gennes P. G. *Macromolecules* **1976**, *9*, 594-598.
- (51) Vélez G.; Fernández M. A.; Muñoz J.; Williams P. A.; English R. J. *J. Agric. Food Chem.* **2003**, *51*, 265-269.

Summary - samenvatting

Summary

Oil-in-water emulsions are commonly encountered in the food industry. Emulsions are intrinsically unstable systems where one liquid is dispersed into another. As a consequence, emulsions tend to demix by processes as creaming, flocculation and coalescence. In this thesis, food-related model emulsions of sunflower oil in water are described that are stabilised by β -lactoglobulin (β -lg). This globular protein stabilises the emulsions against flocculation and coalescence, but not against creaming. In order to retard creaming and to control texture of emulsions, thickening agents such as polysaccharides are often used in the food industry. However, the role of polysaccharides in emulsions is more complex, because polysaccharides can induce flocculation of the emulsion droplets via mechanisms as depletion and bridging. In this thesis, the resulting changes are described in mechanical properties and macroscopic demixing behaviour of emulsions stabilised by protein.

Chapter 2 reports on creaming and flocculation in 10 wt % oil-in-water emulsions, flocculated by dextran. Dextran and an additional amount of β -lg were added at various concentrations after emulsion formation. A substantial effect of the β -lg concentration was observed. At higher β -lg concentrations, a larger dextran concentration was required to induce network formation. This effect was explained by a retardation of the flocculation process at larger β -lg concentrations, shown by diffusing wave spectroscopy (DWS). This retardation was caused by the unexpectedly high apparent viscosity at low shear-rates of mixed solutions of β -lg and dextran.

Chapter 3 discusses the change in phase behaviour and mechanical properties of oil-in-water emulsion gels brought about by variation of long- and short-range attractive interactions. A long-range depletion attraction was obtained by addition of dextran. At short distances, the interaction is dominated by electrostatic repulsion between the adsorbed layers of β -lg. This interaction was varied by addition of Ca^{2+} ions and by changing the NaCl concentration. Combination of long- and short-range attraction resulted into a substantial decrease in the rate of serum separation and an increase in the emulsion-gel modulus at small deformations, compared to depletion attraction alone. The flocculation process and the morphology of the flocs were investigated by Diffusing Wave Spectroscopy (DWS) and Confocal Scanning Laser Microscopy (CSLM). Above a

minimum concentration, dextran induced fast depletion flocculation, leading to a network of emulsion droplets. This network quickly collapsed due to gravity. Addition of Ca^{2+} ions above a minimum concentration induced slow flocculation and the flocs creamed before a network was formed. Addition of both dextran and Ca^{2+} ions resulted in a two-step mechanism of emulsion gel formation. A network is quickly formed by depletion-flocculation and subsequently the bonds between the emulsion droplets are reinforced by Ca^{2+} ions. Due to this reinforcement, rearrangements of this network were suppressed resulting in a smaller rate of serum separation.

In Chapter 4, the phase behaviour and mechanical properties oil-in-water emulsions, flocculated by the polysaccharide dextran were studied as a function of sucrose concentration. The sucrose concentration affected neither the polysaccharide concentration above which depletion flocculation occurred, nor the elastic modulus and maximum linear strain of the emulsion gels formed. Furthermore, only a minor change in size of dextran molecules was measured over the range of sucrose concentrations studied. From this we deduce that the depletion potential between the oil droplets was not significantly affected by addition of sucrose. However, the sucrose concentration did affect the rate of macroscopic phase separation, which could be attributed to a larger viscosity and density of the aqueous phase. Thus, in unheated systems sucrose has a kinetic effect on serum separation in depletion-flocculated emulsions but no significant effect on droplet-droplet interactions.

In chapter 5, stability against demixing, rheology and microstructure of emulsions flocculated by depletion or bridging were compared. Flocculation by depletion and bridging was induced by addition of the polysaccharide carboxy-methylcellulose (CMC) to β -lg-stabilised emulsions at pH of 6.7 and 3.0 respectively. Depletion-flocculated emulsions have a lower initial demixing rate than bridging-flocculated emulsions, but after long times they are compressed to a higher oil content by gravity. Differences in the initial demixing rate are shown to be caused by differences in porosity between the gels. In bridging-flocculated emulsions large irreversible flocs are formed by flow during mixing, inferring larger permeability than in depletion-flocculated emulsions. Rheological measurements showed that bridging-flocculated emulsions can withstand larger stresses than depletion-flocculated emulsions. Greater network strength and a lower probability of rearrangements explain why bridging flocculation systems can retain more water at longer times.

Finally, chapter 6 describes an experimental study of scaling behaviour of microstructure, rheology and demixing for bridging- and depletion-flocculated oil-in-water emulsions.

The elasticity of flocculated emulsions versus the emulsion volume fraction shows scaling behaviour with exponents of 2 and 5 for depletion- and bridging-flocculated emulsions, respectively. These exponents reflect a difference in bond type between the depletion- and the bridging mechanism. Depletion-flocculated emulsions exhibit a critical volume fraction for percolation in contrast to bridging-flocculated emulsions.

CSLM-imaging showed that bridging-flocculated emulsions were heterogeneous over larger length scales than depletion-flocculated emulsions. As a consequence, G' as determined from DWS corresponds well with G' as measured macroscopically for the depletion-flocculated emulsions, but this correspondence was not found for the bridging-flocculated emulsions. The heterogeneity of bridging-flocculated emulsions was confirmed by DWS-echo-measurements, indicating that their structure breaks up into large fragments upon oscillatory shear deformation larger than 1 %.

Gravity-induced demixing occurred in both emulsions, but the demixing processes differed. After preparation of bridging-flocculated emulsions, serum immediately started separating, whereas depletion-flocculated systems at polysaccharide concentrations in the overlap regime usually showed a delay time before demixing. The delay time was found to scale with the network permeability, B , the viscosity, η , of the aqueous phase and the density-difference between oil and water, $\Delta\rho$, as $t_{\text{delay}} \sim B^{-1} \cdot \eta \cdot \Delta\rho^{-1}$. The results are in line with a mechanism where erosion of the droplet network leads to widening of the channels within the droplet networks, enhancing drainage of liquid.

Samenvatting

Emulsies zijn dispersies van twee onderling niet mengbare vloeistoffen, waarin één vloeistof in de vorm van kleine druppeltjes is gedispergeerd in een andere vloeistof. Emulsies zijn instabiel en zullen na verloop van tijd ontmengen via processen als oproming, vlokking en coalescentie. In de levensmiddelenindustrie worden olie-in-water emulsies worden vaak toegepast om vetten en/of oliën in waterige systemen te brengen.

In dit proefschrift wordt een onderzoek naar de microstructuur, reologie en ontmenging van emulsies beschreven van zonnebloemolie in water. Deze emulsies staan model voor complexere emulsie systemen die in levensmiddelen voorkomen. De emulsies waren gestabiliseerd door het melkeiwit β -lactoglobuline (β -lg). Dit eiwit stabiliseerde de emulsies tegen vlokking en coalescentie, maar niet tegen oproming. Om oproming te vertragen en om de textuur van emulsies te sturen worden in de industrie vaak verdikkingsmiddelen zoals polysacchariden toegevoegd. De rol van polysacchariden in emulsies is echter ingewikkelder dan alleen het verhogen van de viscositeit. Polysacchariden kunnen immers vlokking van de emulsiedruppels teweeg brengen via mechanismen als depletie en brug-vorming. De resulterende veranderingen in de mechanische eigenschappen en het macroscopisch ontmenggedrag van eiwit-gestabiliseerde emulsies waren onderwerp van deze studie.

Hoofdstuk 2 rapporteert over oproming en vlokking van 10 wt % olie-in-water emulsies, onder invloed van dextraan. Dextraan en een additionele hoeveelheid eiwit waren toegevoegd in verschillende hoeveelheden na het maken van de emulsie. Een aanzienlijk effect van de concentratie β -lg werd waargenomen. Bij hogere concentraties β -lg was een hogere dextraanconcentratie nodig om de vorming van een netwerk van gevlokte druppels te induceren. Dit effect is verklaard door een vertraging van het vlokkingproces bij hogere concentraties β -lg, zoals aangetoond met behulp van diffuse golf spectroscopie (DWS). Deze vertraging werd veroorzaakt door de onverwacht hoge schijnbare viscositeit bij lage afschuifsnelheden in gemengde oplossingen van β -lg en dextran.

Hoofdstuk 3 bediscussieert de verandering in fasegedrag en mechanische eigenschappen van olie-in-water emulsies, die teweeggebracht werd door een variatie van attractieve lange- en korte-drachtsinteracties. Een lange-drachtsinteractie werd verkregen door toevoeging van dextran. Op korte afstanden werd de interactie gedomineerd door

electrostatistische repulsie tussen de geadsorbeerde lagen van β -lg. Deze interactie werd gevarieerd door toevoeging van Ca^{2+} ionen en door variatie van de concentratie NaCl. Combinatie van lange- en korte-drachtsinteracties resulteerde in een substantiële afname van de snelheid van serum-afscheiding en in een toename van de afschuifmodulus bij kleine vervormingen, vergeleken met de depletie-interactie alleen. Het vlokingsproces en de morfologie van de vlokken werden bestudeerd met behulp van diffuse golf spectroscopie (DWS) en confocale microscopie (CSLM). Dextran induceerde snelle depletievlokkings boven een minimum concentratie, hetgeen leidde tot de vorming van een netwerk van emulsiedruppels. Dit netwerk stortte snel ineen onder invloed van de zwaartekracht. Toevoeging van Ca^{2+} ionen boven een minimumconcentratie induceerde langzame vlokking en de vlokken roomden op voordat een druppelnetwerk was gevormd. Toevoeging van dextran en Ca^{2+} ionen resulteerde in een twee-stapsmechanisme van emulsie-gelvorming. Een netwerk wordt snel gevormd door depletie-vlokkings en vervolgens worden de bindingen tussen de emulsiedruppels versterkt door de Ca^{2+} ionen. Door deze versterking worden herrangschikkingen van het netwerk vertraagd, hetgeen resulteert in een lagere snelheid van serum-afscheiding.

In hoofdstuk 4 worden ontmenging en de mechanische eigenschappen van olie-in-water emulsies, gevlokt door dextran, bestudeerd als functie van de concentratie saccharose. De saccharoseconcentratie beïnvloedde noch de polysaccharide concentratie waarboven depletie-vlokkings optrad, noch de elasticiteitsmodulus en maximale lineaire afschuifvervorming van de gevormde emulsiegels. Daarnaast werd slechts een minimale verandering in de grootte van de dextraanmoleculen gemeten bij de bestudeerde saccharoseconcentraties. Hieruit wordt afgeleid dat de depletiepotentiaal tussen de emulsiedruppels niet significant beïnvloed werd door saccharose. De concentratie saccharose had echter wel invloed op de snelheid van macroscopische ontmenging, hetgeen veroorzaakt werd door een hogere viscositeit en dichtheid van de waterfase. Zo heeft sucrose effect op de kinetiek van serum-afscheiding in onverhitte depletie-gevlokte emulsies, maar geen significant effect op druppel-druppel interacties.

In hoofdstuk 5 worden de stabiliteit tegen ontmenging, de reologie en de microstructuur vergeleken van emulsies die gevlokt zijn door depletie of door brugvorming. Vlokkings door depletie of brugvorming werd geïnduceerd door toevoeging van het polysaccharide carboxy-methylcellulose (CMC) bij een pH van respectievelijk 6,7 of 3,0 aan emulsies die gestabiliseerd waren door β -lg. Depletie-gevlokte emulsies vertoonden een lagere initiële

ontmengingsnelheid dan emulsies die gevlokt waren door brugvorming, maar na een lange tijdsduur werden ze door de zwaartekracht gecompriëerd tot een hoger oliegehalte. Het werd aangetoond dat de verschillen in de initiële ontmengingsnelheid worden veroorzaakt door verschillen in porositeit tussen de gels. In emulsies die zijn gevlokt door brugvorming werden grote irreversibele vlokken gevormd als gevolg van stroming tijdens het mengen, hetgeen leidt tot een grotere permeabiliteit dan in depletie-gevlokte emulsies. Uit reologische metingen bleek dat emulsies gevormd door brugvorming grotere spanningen kunnen weerstaan dan depletie-gevlokte emulsies. Een grotere netwerksterkte en een lagere kans op herrangschikkingen verklaren waarom systemen die gevormd zijn door brugvorming meer water vasthouden over een langere tijdsduur genomen.

Tot slot wordt in hoofdstuk 6 een experimentele studie beschreven van het schalingsgedrag van de microstructuur, reologie en ontmenging voor olie-in-water emulsies die gevlokt waren door depletie en brugvorming.

De elasticiteitsmodulus van de gevlokte emulsies versus de volumefractie laat een schalingsgedrag zien met exponenten van respectievelijk 2 en 5 voor emulsies gevlokt door depletie en brugvorming. Deze exponenten weerspiegelen een verschil in bindingstype tussen het depletie- en het brugvormingsmechanisme. Depletie-gevlokte emulsies vertonen een ondergrens in de volumefractie aan oliedruppels voor percolatie in tegenstelling tot emulsies die gevlokt waren door brugvorming.

CSLM-opnames toonden aan dat emulsies die gevlokt waren door brugvorming heterogeen waren over grotere lengteschalen dan emulsies gevlokt door depletie. Voor de laatstgenoemde emulsies stemde G' zoals bepaald met DWS goed overeen met G' uit reologische metingen. Deze overeenstemming werd echter niet gevonden voor emulsies gevormd door brugvorming, waarschijnlijk vanwege te sterke heterogeniteit. De heterogeniteit van de emulsies gevlokt door brugvorming werd bevestigd door DWS-echo metingen. Deze metingen toonden aan dat hun structuur in grote fragmenten uiteenvalt boven een maximale oscillerende afchuiwing van 1 %.

Ontmenging als gevolg van de zwaartekracht vond plaats in beide emulsies, maar de ontmengingsprocessen verschilden. Na bereiding van emulsies gevlokt door brugvorming, begon zich direct serum af te scheiden, terwijl depletie-gevlokte emulsies bij polysaccharide-concentraties in het overlap-regime gewoonlijk een vertragingstijd vertoonden voordat ontmenging zichtbaar werd. De vertragingstijd bleek te schalen met de netwerk permeabiliteit, B , de viscositeit, η , en het dichtheidsverschil tussen olie en water,

$\Delta\rho$, volgens $t_{\text{vertraging}} \sim B^{-1} \cdot \eta^{-1} \cdot \Delta\rho^{-1}$. De resultaten sluiten aan bij een mechanisme, waarbij erosie van het druppelnetwerk leidt tot verwijding van de kanalen binnen het druppelnetwerk, hetgeen weer leidt tot een versterking van de drainage van serum.

Dankwoord

Na 4 jaar is het dan zover. De afronding van dit proefschrift is een feit. Ik kijk terug op een leuke tijd, waarin ik veel geleerd heb en met veel mensen heb samengewerkt. In deze tijd was ik werkzaam bij WCFS, maar in werkelijkheid was ik meestal te vinden in het Biotechnion en soms op het NIZO. Mede dankzij deze samenwerking is het boekje zo geworden als het geworden is. Een aantal mensen wil ik hierbij persoonlijk bedanken voor hun bijdrage.

Laat ik beginnen met mijn begeleiders. Erik, ik wil je bedanken voor het vertrouwen dat je me altijd gegeven hebt, vóór en tijdens mijn promotietijd en voor de daarop volgende periode. Je enthousiasme en generieke kijk op de emulsies waren goed voor me. George, vanaf onze eerste kennismaking heb ik het gevoel gehad dat we elkaar enthousiast konden maken over dit onderwerp en erover konden blijven praten. Ik heb je daarna leren kennen al een zeer gedreven en kritisch persoon en dit heeft in het bijzonder bijgedragen aan de leesbaarheid van de manuscripten. Ton, ik kan je het best omschrijven als het rustpunt van het geheel en ik ben jouw dankbaar voor je betrokkenheid.

Microstructural and microrheological characterisation of emulsions formed an important part of this thesis. I would like to thank Erik ten Grotenhuis, Alexandra Knaebel and Jean-Pierre Munch for introducing me to the interpretation of DWS-results. Later, the development of the Oscillatory Shear Cell was conducted by Yves Nicolas and Marcel Paques. I have enjoyed this cooperation between different projects and the discussions with both of you.

Harald Schuten, Ingrid Nijssen, Wouter Hendriks en Jony van Winden, jullie hebben middels jullie afstudeervakken duidelijk bijgedragen aan de inhoud van dit boekje. Het was mij een genoegen om met jullie samen te werken. De komst van Wouter en Jony was mogelijk dankzij samenwerking met respectievelijk Edward en Hein van de sectie zuivelkunde. Edward, studenten motiveren is jouw sterke kant. Als student was ik je daarvoor dankbaar en in mijn promotietijd wederom. Franklin, jou bedank ik voor je hulp op het lab aan mijn studenten en mezelf, je experimentele bijdragen aan dit boekje, de veele dropjes en... de smilestone.

Graag wil ik alle collega's van het WCFS-project SEF, Food Physics en PDQ bedanken voor de gezellige sfeer op de werkvloer, bij het koffieapparaat en tijdens de verschillende

uitjes. Voor DWS- en CSLM- metingen ben ik vaak bij NIZO food research geweest. De mensen van de Product Technologie groep van Kees de Kruif wil ik bedanken voor hun behulpzaamheid aldaar. Ook bedank ik alle deelnemers van het fasescheidingsgroepje voor de leerzame maandmiddagjes.

Het grootste deel van de tijd brengt een AIO door op kantoor en dan is het fijn om daar leuke collega's te hebben. Nou, dat zat wel snor op kippenhok 2.11A. Anneke en Natalie, mede SEF-AIO's, met jullie heb ik meer dan 3 jaar de kamer gedeeld. Ik heb het als erg gezellig ervaren, we konden al onze ervaringen met het virtuele instituut delen. Catriona, Jeannet en Hilde, jullie vulden de kamer daarna weer aan en de gezelligheid bleef. Ik hoop dat jullie snel een vervangende haan krijgen.

Anneke en Elke, op de organisatie en het verloop van het AIO-reisje naar Engeland kijk ik met veel genoegen terug. Anneke, ik ben blij dat je mijn paranimf wilt zijn.

Buurman Martin, rinkel rinkel..., koffietijd !, of dinsdag, speeltijd ! We begonnen op dezelfde dag en sindsdien ben je altijd een hele goede wekker geweest om even achter de PC weg te gaan. Echter meer dan dat hebben we 4 jaar veel muziek gespeuld en met veel plezier. Ik ben blij dat je mijn paranimf wilt zijn. Succes komende tijd met afschrijven van jouw boekje. Hierbij bedank ik ook alle Nozels voor de vele repetitieavonden en muziekweekendjes.

Vrienden van het goede leven, bedankt voor de gezelligheid tijdens weekendjes, etentjes en feestjes.

Papa, nu het zover is kun je er niet meer fysiek bij zijn, maar ik weet dat je trots zou zijn; je herinnering blijft altijd. Mama, er is veel veranderd in vier jaar, maar weekendjes thuis hebben me altijd weer rust gegeven om er weer tegenaan te kunnen. Ik ben jullie samen dankbaar voor alles wat ik van jullie heb meegekregen en de vrijheid die ik altijd heb mogen genieten in mijn keuzes.

Freek en Ella, dank voor de hartelijke ontvangst altijd en de ontspanning die ik bij jullie kon nemen.

Tot slot, lieve Cecile. Wat een vier jaartjes waren het. Dank je wel voor al je liefde, stimulans en afremming op de momenten dat het nodig was. Nu je zelf ook bijna klaar bent staan er al weer veel leuke en spannende dingen op ons te wachten, waar ik erg naar uitkijk.

Theo

Curriculum Vitae

Theodorus Berend Jan Blijdenstein werd op 18 september 1976 geboren te Oudenbosch. In 1994 behaalde hij het diploma gymnasium β aan het Norbertuscollege te Roosendaal. Aansluitend studeerde hij levensmiddelentechnologie aan de toenmalige Landbouwniversiteit Wageningen. Afstudeervakken werden uitgevoerd binnen de sectie levensmiddelen natuurkunde en bij ATO-DLO. Een stage werd uitgevoerd bij Unilever Research Laboratory Colworth House, UK. In 1999 ronde hij zijn studie af met als specialisatie levensmiddelen natuurkunde.

Van 1 oktober 1999 tot en met 31 oktober 2003 was hij als AIO in dienst van WCFS en gedetacheerd naar Wageningen Universiteit. In deze periode is het werk uitgevoerd dat staat beschreven in dit proefschrift.

Vanaf 17 november is hij als junior wetenschapper in dienst van WCFS binnen het project "Engineered textures of emulsions and foams".

Theo woont samen met Cecile Veerman en zij gaan trouwen op 16 april 2004. Beiden hebben een Talent-stipendium aangevraagd bij NWO voor een postdoc-positie aan the University of Delaware, USA.

List of Publications

Refereed Journals

- **T.B.J. Blijdenstein**, T. van Vliet, E. van der Linden, G.A. van Aken, **2003**, *Suppression of depletion flocculation in oil-in-water emulsions: A kinetic effect of β -lactoglobulin*, Food Hydrocolloids, 17, (5), 661-669.
- **Theo B.J. Blijdenstein**, Wouter P.G. Hendriks, Erik van der Linden, Ton van Vliet, George A. van Aken, **2003**, *Control of strength and stability of emulsion gels by a combination of long- and short-range interactions*. Langmuir, 19, (17), 6657-6663.
- Yves Nicolas, Marcel Paques, Alexandra Knaebel, Alain Steyer, Jean-Pierre Munch, **Theo B.J. Blijdenstein** and George A. van Aken, **2003**, *Microrheology: structural evolution under static and dynamic conditions by simultaneous analysis of confocal microscopy and diffusing wave spectroscopy*. Review of Scientific Instruments, 74, (8), 3838-3844.
- Yves Nicolas, Marcel Paques, Dirk van den Ende, Jan K. G. Dhont, Rob C. van Polanen, Alexandra Knaebel, Alain Steyer, Jean-Pierre Munch, **Theo B.J. Blijdenstein** and George A. van Aken, **2003**, *Microrheology: new methods to approach the functional properties of food*. Food Hydrocolloids, 17, (6), 907-913.
- George A. van Aken, **Theo B.J. Blijdenstein**, Natalie E. Hotrum, **2003**, *Colloidal destabilisation mechanisms in protein-stabilised emulsions*, Current Opinion in Colloid and Interface Science, 8, (4-5), 369-377.
- **T.B.J. Blijdenstein**, F.D. Zoet, T. van Vliet, E. van der Linden, G.A. van Aken, **2003**, *Dextran-induced depletion flocculation in oil-in-water emulsions in the presence of sucrose*, submitted.
- **T.B.J. Blijdenstein**, A.J.M. van Winden, T. van Vliet, E. van der Linden, G.A. van Aken, **2003**, *Phase behaviour and rheology of emulsion gels flocculated by a depletion- and a bridging mechanism*, submitted.
- **T.B.J. Blijdenstein**, C. Veerman, E. van der Linden, **2003**, *Depletion flocculation in oil-in-water emulsions induced by β -lactoglobulin fibrils*, submitted.
- **T.B.J. Blijdenstein**, E. van der Linden, T. van Vliet, G.A. van Aken, **2003**, *Scaling behaviour of delayed demixing, rheology and microstructure of emulsions flocculated by depletion and bridging*, in preparation.
- M.H. Vingerhoeds, **T.B.J. Blijdenstein**, F.D. Zoet, G.A. van Aken, **2003**, *Saliva- and mucin- induced emulsion flocculation*, in preparation.

Conference proceedings

- **T.B.J. Blijdenstein**, E. van der Linden, T. van Vliet, G.A. van Aken., **2002**, *Depletion flocculation of protein stabilised emulsions at high whey protein concentrations*, Proceedings of gums and stabilisers for the food industry 11, pp. 256-263.
- **T.B.J. Blijdenstein**, Y. Nicolas, E. van der Linden, T. van Vliet, M. Paques, A. Knaebel, J.P. Munch, **2003**, *Monitoring the structure of oil-in-water emulsion by a combination of DWS and CSLM*, Proceedings of the 3rd ISFRS, Zürich, Switzerland, pp. 343-347.

The study described in this thesis was part of the research programme ‘structure and functionality’ of the Wageningen Centre for Food Sciences. The work has been carried out at the Food Physics Group, Wageningen University and at the Department of Product Technology, NIZO food research, Ede, the Netherlands. Furthermore, the work was part of the research programme of the Graduate School VLAG (Food Technology, Nutrition & Health Sciences).

Cover: CSLM images of emulsion droplets, forming different microstructures.

Image taken by Wouter Hendriks and Yves Nicolas.